CONFIDENTIAL

JEF REPORT 5

ECN-176

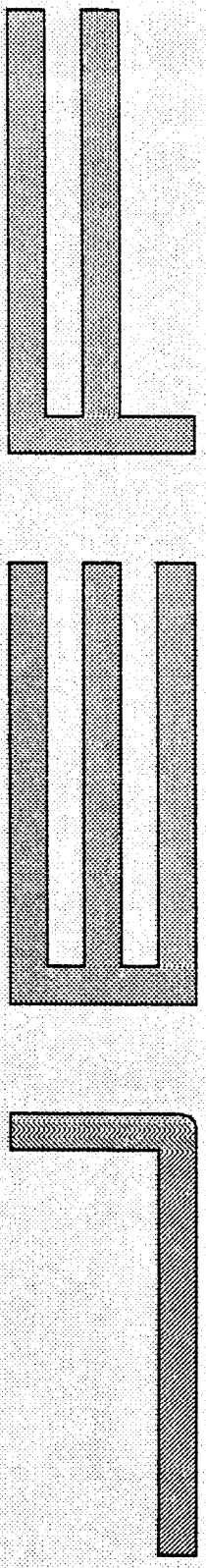

INTEGRAL-DATA TEST OF JEF-1 FISSION-PRODUCT CROSS SECTIONS

NOVEMBER 1985

A.J. JANSSEN, H. GUPPELAAR, R.J. HEIJBOER,
N. KAROUBY-COHEN, L. MARTIN-DEIDIER
G. RIMPAULT, M. SALVATORES

OECD

NEA DATA BANK
BANQUE DE DONNEES DE L'AEN

OCDE

ABSTRACT

This report describes an extensive integral-data test of the fission-product file of the JEF-1 data library (Joint Evaluated File). Integral data from STEK (5 cores), CFRMF, ZONA-1, RONA-3 and PHENIX were used to test the fast-capture cross section evaluations of 60 materials.
A table and a large number of figures are given with experimental and calculated capture reactivity worths in the five STEK cores for most of these nuclides. A correction for scattering was made based upon the original evaluation. There are indications that this correction is too small for some even-mass isotopes due to the neglect of direct-collective effects in the inelastic scattering evaluations. This also follows from comparison with activation and irradiation measurements performed in CFRMF, ZONA-1, RONA-3 and PHENIX, respectively. A survey of all the results, expressed by the ratio of experimental to calculated values as a function of the relative response above 1 keV in the various assemblies, is presented in a summary table. This material is discussed and conclusions about further improvements of the evaluations with respect to capture and inelastic scattering are presented.

KEYWORDS:

INTEGRAL CROSS SECTIONS
EVALUATED DATA
STEK REACTOR
FISSION PRODUCTS
NEUTRON REACTIONS
CAPTURE
INELASTIC SCATTERING

CONTENTS

1. INTRODUCTION

The Joint Evaluated File (JEF-1) is the result of a scientific collaboration between laboratories in Austria, France, F.R. Germany, Italy, Japan, Netherlands, Sweden, Switzerland and United Kingdom, and the NEA Data Bank [1]. The fission-product (fp) file has been selected from recent evaluations after a number of modifications and updatings. The bulk of the fp data is based upon ENDF/B-V, although replacements by other evaluations were made for about 50 nuclides.

In the frame-work of a French-Dutch cooperation concerning fission-product cross-section evaluations and tests, a comparison was made of calculated and measured integral data. All calculated data are based on the cross-section evaluations contained in the JEF-1 file. In this integral-data test use was made of STEK reactivity worths [2], ZONA-1 and RONA-3 activation data and PHENIX irradiation data [3], and CFRMF activation data [4]. The nuclides considered in this test are listed in Table 1. The results of the test mainly apply to the fast capture cross section. However, since reactivity worths contain a scattering component, the (inelastic) scattering cross section is also checked to a certain extent.

The calculated integral data were obtained by using the original data files of the evaluations adopted in JEF-1. The RCN-3 files were first translated into ENDF/B-V format using the KTOE-3 code [5]. The translated files contained the resolved and unresolved parameters together with a background function. Most of the group constants were processed with the 4-ACES code [6]. In a few cases the results were checked with the NJOY code [7].

In Chapters 2-4 some comments will be made on the way in which the integral data in the various facilities were calculated, and how they are presented in the tables. In Chapter 5 a short discussion is given for each nuclide, with notes regarding the need for further improvements of the evaluated cross sections *). Some conclusions are summarized in Chapter 6.

---

*) During the process of data testing several evaluations originally proposed for JEF-1 could already be improved or substituted by more recent evaluations. In this report we only consider those evaluations finally adopted in JEF-1.

2. STEK REACTIVITY WORTHS

Measurements have been conducted in five STEK cores with different neutron energy spectra, indicated by STEK-4000, -3000, -2000, -1000 and -500, respectively. For the evaluation of the reactivity worths 26-group constants were calculated using an "average" micro-flux weighting spectrum as given in ref. [8], table 40. The 26-group flux and adjoint spectra of the five cores are given in [9], table 14. Table 2 contains a straightforward E/C comparison of reactivity worths in STEK for all relevant samples. Measured and calculated values are normalized worths (ρ/ρ_o). Details of the measured and calculated normalization factor, ρ_o, can be found in [2] and [9], respectively.

The sample identifications in table 2 are in accordance with those given in ref. [4], where further details can be found concerning the physical and chemical compositions of the samples as well as their dimensions. The reactivity worths given in table 2 are the normalized worths of the fission products in the samples. The directly measured sample worths, given in ref. [2], have been corrected for the (separately measured) worths of non-fission-products (e.g. oxygen in Sm_2O_3).

Furthermore, table 2 shows capture reactivity worths, ρ_c/ρ_o. The experimental worths have been corrected for the calculated elastic and inelastic scattering effects of the fission products. Scattering effects are always positive in STEK, whereas capture effects are, of course, negative (for convenience, table 2 actually shows values of $-\rho_c/\rho_o$).

Finally, it should be mentioned that the values given in table 2 are fission-product capture reactivities per gram of sample material (including possible admixtures).

The error margins accompanying the experimental values in table 2 are the statistical measurement errors, also given in ref. [2], (1 σ values). For other, systematic, experimental errors we refer to [2] and [9].

Resonance self-shielding is an important feature for most of the STEK samples. Group-dependent and sample-dependent self-shielding factors of the fission-product capture cross-sections have been calculated with an improved version of the TRIX code [10], which uses the intermediate-resonance approximation [11] for individual Doppler-broadened resonances (in the unresolved resonance region TRIX generates resonances in accordance with average parameters and certain statistical distribution laws). In table 2 samples containing the same fission-product mixture are listed in order of increasing self-shielding effect. One might consider resonance shielding as a modification of the undisturbed neutron spectrum, resulting in a modification of the cross-section sensitivities: the energy-dependent relative contributions to the capture effect are shifted to higher energies where self-shielding is less prominent. A measure for this shift is given in table 2, viz. the relative contribution to ρ_c/ρ_o of neutrons with energies above 1 keV. Since this shift is frequently quite large, we would not, in general, recommend the extrapolation of experimental values to infinite dilution; the extrapolated value cannot be considered as a true measured value, and the uncertainties in the extrapolation are difficult to estimate. However, for completeness' sake we included in table 2 calculated worths of $-\rho_c/\rho_o$ in infinite dilution (under the "sample" name I.D.).

All experimental and calculated reactivity worths given in table 2 have been plotted in figures 1 to 51. Along the absciss in each of these figures is plotted the value of $\bar{\ell}$ x d, the product of the mean chord length and the density of the samples, as given in [2], which is a useful measure for the self-shielding effect.

The large amount of data in table 2 has been condensed in table 3. Samples with nearly equal energy-dependent responses (cf. column 3 in table 3) were taken together and average E/C ratios of ρ_c/ρ_o were determined for these groups of samples. In the averaging process the individual ratios were weighted with the inverses of their statistical variances. The statistical errors in the averages were determined likewise.

Under the heading "spectrum uncertainty" in table 3 relative uncertainties are given for the E/C ratios due to uncertainties in the calculated capture and scattering effects caused by spectrum (ψ and ψ^+) uncertainties as described in ref. [9].

Finally, table 3 gives the calculated correction for the scattering effect, ρ_{sc}/ρ_o, its absolute value as well as its value relative to the (average) calculated capture effect. (Thus, an uncertainty in the calculated scattering effect of, e.g., 30% leads to an uncertainty in the E/C ratios of table 3 equal to 0.3 times the relative scattering effect given in the table). The scattering corrections have been applied to all experimental data in tables 2 and 3, and in the figures.

3. FRENCH ACTIVATION AND TRANSMUTATION DATA

The calculation of the spectrum-averaged capture cross sections in PHENIX, RONA-3 and ZONA-1 was performed in 25 groups, using the standard CEA micro-flux weighting spectrum (CARNAVAL scheme). The calculated E/C-values are included in table 3, together with the "response above 1 keV". The error margins are experimental uncertainties (as usual, 2σ values are given for French experimental data).

4. CFRMF ACTIVATION DATA

For a number of the nuclides considered in this report there are CFRMF activation data available. To our knowledge, the most recent data are given by Harker and Anderl at the 1979-Bologna meeting [4]. These experimental data were used.

The calculated quantities have been obtained by averaging the JEF-1 evaluated cross sections over the energy range from 8.76 eV to 16.9 MeV using as a weighting function the calculated CFRMF flux spectrum. For this spectrum we have adopted the 69-group fluxes identified by "Version-V" in table 1 of ref. [12]. We have converted these group fluxes into a set of values for E (mid-energy of each group) and ψ (group flux divided by energy width of group). Assuming a log-log interpolation scheme, each point of this flux weighting spectrum is defined in the energy range given above. The integral over this spectrum equals 1.0012, close to the sum over all group fluxes that has been normalized to unity.

The average one-group cross sections were directly calculated with the 4-ACES code, using the above-mentioned flux-weighting function and the original data files (ENDF/B or KEDAK format). The results of the E/C values were checked with corresponding quantities given by Anderl at the 1982-Argonne meeting [13], for the nuclides for which ENDF/B-V was selected. The differences, which were always less than ±3%, are probably due to the use of slightly different neutron flux spectra. The E/C values are included in table 3; comparison of CFRMF data with data obtained for other neutron spectra is facilitated by considering the "response above 1 keV", also given in this table. The error margins are experimental uncertainties (1σ values).

5. DISCUSSION

For each nuclide a few comments will be made with respect to measured and calculated values, see tables 2 and 3 and Figs. 1 to 51.

5.1. Rb-87

There is only a single measurement in CFRMF available for this nuclide. The agreement between experimental and calculated capture rate is satisfactory.

Conclusion: no further action is needed.

5.2. Zr-90

Measurements in STEK were made with samples enriched in Zr-90. Contributions to ρ_c/ρ_o of other Zr isotopes are indicated in Fig. 1. The scattering corrections ρ_{sc}/ρ_o are very large; even in STEK-4000 ρ_{sc}/ρ_o is of the same order of magnitude as ρ_c/ρ_o. Moreover, ρ_{sc}/ρ_c contains an important contribution due to elastic scattering (from 40% in STEK-4000 to 50% in STEK-500). This calculated contribution is highly uncertain because of the coarse group structure used in the calculations. The usual (flux-weighted) down-elastic scattering cross section was used in these calculations. Within-group resonance scattering is thus neglected. In view of the shape of the importance function in STEK (nearly monotonically increasing with decreasing energy) this neglect will have caused an underestimation of ρ_{sc}/ρ_o. This observation applies to all even-mass Zr isotopes having strong scattering resonances.

Conclusion: Try to improve calculation of elastic-scattering reactivity effect and re-analyse the STEK-data. At present no conclusion on the quality of the evaluation can be made on the basis of integral data.

5.3. Zr-91

Measurements in STEK were made with highly-enriched samples. Contributions to ρ_c/ρ_o of other Zr isotopes are less than 5%. The scattering contribution is still high, but much less than for ^{90}Zr. Meaningful conclusions are only possible for the soft cores STEK-4000, -3000, and -2000. We observe an overestimation of about 10% in the four softer STEK spectra. In STEK-500 the discrepancy is larger, but rather uncertain, also due to the large scattering correction (with a calculated contribution of 40% due to elastic scattering).

Conclusion: Agreement within about 10±7% at low energies; no conclusion for fast range.

5.4. Zr-92

Highly enriched STEK samples were used. The contribution to ρ_c/ρ_o of the other Zr isotopes is less than 7%. Large scattering corrections had to be applied. The calculated contribution to ρ_{sc}/ρ_o due to elastic scattering is about 25%.

Conclusion: The high scattering correction permits no conclusion on the quality of the capture cross section. This situation could be improved by a better calculation of the elastic scattering reactivity contribution.

5.5. Zr-93

The STEK samples contain a Zr fission-product mixture prepared at ECN from nuclear waste. The exact isotopic composition (19.5% ^{93}Zr) is given in [2]. Recently, the samples have also been analysed at ORNL, where fairly large contaminations were found [14]. As far as possible we have corrected the measured reactivity worths for the reactivity effects of these admixtures. In Table 4 a survey is given of the detected admixtures, and Table 5 gives the resulting reactivity corrections.

The calculated contributions to ρ_c/ρ_o of the different Zr isotopes

are displayed in Fig. 4; at low energies the major contribution comes from Zr-93 (STEK-4000). There is a systematic difference between the measured worths of the L-sample and the two M-samples, which is quite significant in STEK-1000. The reason for this discrepancy is not clear. However, it should be stated here that oscillation measurements with radioactive samples were often not well reproducible because of enhanced reactor drift effects. Moisture contamination of the M-samples could also play a role: the drying and packing procedures for radioactive samples were very laborious and difficult.
The evaluation is mainly based upon theory; only one resonance is known at 110 eV; even the thermal cross section is very uncertain. Attempts are made to improve this situation by using the STEK sample for differential measurements [14].

There is a clear overestimation of ρ_c/ρ_o in all STEK spectra. An important part of this discrepancy is due to overestimation for the even-mass isotopes and for Zr-91. The magnitude of the remaining overestimation for Zr-93 is uncertain in view of the above-mentioned discrepant experimental worths. However, we may draw some conclusions from the soft-core measurements, where the main contributions come from the admixtures Zr-91 and Zr-96, that have no excessive scattering corrections. Using the values of E/C given in Table 3 for STEK-2000, -3000 and -4000 we find that the capture cross section of Zr-93 is 30% to 50% too high.

Conclusion: From the present analysis we find that the evaluated capture cross section of Zr-93 is at least 30% too high. A more refined analysis of the experimental data, using experimental corrections of the total reactivity worths of the other Zr isotopes, may be helpful to increase the accuracy of this estimate. Recent differential data [14] obtained with the STEK sample should be used to re-evaluate the capture cross section of Zr-93.

5.6. Zr-96

Measurements in STEK were made with samples enriched in Zr-96. The contribution to ρ_c/ρ_o of the other Zr isotopes is shown in Fig. 5. For the harder STEK spectra important scattering corrections had to be applied. In STEK-500 30% of ρ_{sc}/ρ_o is due to elastic scattering.

Conclusion: There is an overestimation of ρ_c/ρ_o, which strongly increases with increasing spectrum hardness. Evidently, the calculated scattering correction is significantly too small. In STEK-4000 the overprediction is about 13±7%. The thermal capture cross section should be decreased [15].

5.7. Zr-nat (isotopic files*)

Natural Zr foils have been measured in STEK. The contributions of the various isotopes to ρ_c/ρ_o are shown in Fig. 6.
The disagreement found for the individual isotopes can also be observed for natural Zr. The main reason for the discrepancy must be underestimation of the scattering-reactivity effect (elastic and inelastic).

We note that in JEF-1 a separate file has been selected for natural Zr. Here we have used the isotopic data from the fission-product file of JEF-1.

Conclusion: The large scattering correction prevents meaningful conclusions on the capture cross section. It would be interesting to test also the element file.

---

* Deviates from current JEF-1 file.

5.8. Mo-92

Measurements in STEK were made with samples enriched in Mo-92. Contributions to ρ_c/ρ_o of other Mo isotopes (mainly Mo-95) range from 8% (STEK-500) to 23% (STEK-4000). The scattering corrections are quite large. The experimental capture effects are rather inaccurate, but are generally lower than the calculated effects. This may be partly due to a too small scattering correction.

From a study [16] of inelastic scattering data we found that inelastic cross sections in JEF-1 have to be increased by a factor 1.3 to 2.0 at 1 MeV excitation energy for Mo-96, -98, -100. If this also holds for Mo-92 we may expect better agreement between experimental and calculated reactivity worths.

Conclusion: Consistency with integral data, except for STEK-500.

5.9. Mo-94

Measurements in STEK were made with samples enriched in Mo-94. There are important contributions to ρ_c/ρ_o of other Mo isotopes (mainly Mo-95), as shown in Fig. 8. The experimental capture effects are rather inaccurate, also because of large scattering corrections. Nevertheless, the calculated values seem to be too large (for nearly all even-mass nuclides the "experimental" data for STEK-500 are systematically below the evaluated data).

Since the discrepancies already occur in STEK-4000, the resolved-resonance part might need to be extended to about 20 keV.

Conclusion: Check evaluation in resolved-resonance range above 1 keV.

5.10. Mo-95

Highly-enriched STEK samples were used. There is a systematic overprediction of the capture effects in all STEK spectra of about 10%. This is consistent with PHENIX results, where the overprediction is 5%.

Conclusion: Some adjustment is needed to decrease the cross section by about 5%.

5.11. Mo-96

Measurements in STEK were made with samples enriched in Mo-96. Contributions of other Mo isotopes (mainly Mo-95) to ρ_c/ρ_o range from 10% (STEK-500) to 16% (STEK-4000). The calculated capture effects show a clear overestimation in all STEK spectra of 30-40%. Part of the discrepancy may be due to too small calculated scattering corrections. The PHENIX results also indicate that the capture cross section evaluation is too large (by 18%).

From the PHENIX data it seems clear that the capture cross section needs to be reduced in the unresolved-resonance range. Probably, the resolved-resonance range should be extended with available new data [15]. (indications from STEK). With respect to inelastic scattering the cross section for scattering to the first 2^+-state has to be increased by a factor of about 1.5 to 2.0 at 0.9 to 1.5 MeV to meet the experimental data [17]. This could be partly due to the choice of the optical model and partly due to direct (collective) excitations which have been neglected in the current fp evaluations. This indicates that systematic effects in the evaluation of inelastic-scattering cross sections might be a possible reason for the difficulties in the comparison of calculated and measured reactivity worths of STEK data for even-mass-nuclides [16].

Conclusion: Re-evaluation of capture and inelastic-scattering cross section needed.

5.12. Mo-97

Highly-enriched STEK samples were used. There is a systematic overprediction of the capture effects in all STEK spectra of about 10%, whereas the PHENIX measurement indicates an opposite effect of about -5%.

Probably the capture cross section is too high in the upper part of the resolved-resonance range.

Conclusion: Inspect energy range upto 10 keV.

5.13. Mo-98

The enrichment of the STEK samples was quite high; contributions to ρ_c/ρ_o of other Mo isotopes range from 4% (STEK-500) to 8% (STEK-4000). The calculated capture effects are clearly too large (from 20% in STEK-4000 to 55% in STEK-500). Part of this discrepancy can be ascribed to too small scattering corrections (the corrections are very important, in particular in STEK-500). Further support for this observation is supplied by the capture measurements in CFRMF (overprediction 22% ± 6%) and in RONA-3 and ZONA-1 (overprediction about 30%).
Indeed, the inelastic scattering cross section to the first-excited state is somewhat (~20%) too low as compared to the experimental data [16,17].

However, a significant reduction of the capture cross section is required in the first place.

Conclusion: Re-evaluation of capture and inelastic scattering cross section needed.

5.14. Mo-100

The enrichment of the STEK samples was quite high; contributions to ρ_c/ρ_o of other Mo isotopes range from 8% (STEK-500) to 15% (STEK-4000). The calculated capture effects are somewhat too large (from 12% in STEK-4000 to 26% in STEK-500), although there are large uncertainties. However, the average capture cross-section in CFRMF is underpredicted by 10%±17% and in ZONA-1 the underprediction is 7%.
A possible explanation for these discrepancies might be a too small scattering correction to the STEK measurements (the scattering effect in STEK-500 is very important indeed). In that case the high-energy capture cross-sections could be slightly too low.

The inelastic scattering data for excitation of the first 2^+ state need to be increased by about 20% according to experimental data [16,17]. This is a relatively small correction.

Conclusion: Inspect inelastic-scattering cross section.

5.15. Mo-nat. (isotopic files*)

Natural Mo platelets have been measured in STEK. The contributions of the various isotopes to ρ_c/ρ_o are shown in fig. 14. In the softer STEK spectra the discrepancy between calculation and measurement is somewhat less than what was found for the individual isotopes. This must be due to the larger dilution of the isotopes in the natural mixture and to the smaller dimensions of these samples, resulting in less self-shielding of the well-known resolved resonances (cf. responses above 1 keV in table 3). The results for STEK-500 again suggest a possible underprediction of the scattering reactivity effects.

We note that in JEF-1 the cross sections for natural Mo are different from those considered here.

General conclusion for Mo-isotopes:
For all isotopes, but in particular for the even-mass isotopes, the capture cross sections are overpredicted whereas the inelastic-scattering seems to be underpredicted at low energies.

5.16. Tc-99

Mono-isotopic STEK samples. There is a well-known discrepancy between STEK and CFRMF, but the CFRMF measurement is quite uncertain. A small underprediction of the high-energy response in STEK can be observed.

Conclusion: No re-evaluation of cross-sections needed.

5.17. Ru-101

Nearly mono-isotopic STEK-samples; very small contributions of Ru-102 and Ru-104. Inclusion of more recent resolved-resonance data would improve the E/C ratio for STEK-4000. Overprediction of the high-energy cross-sections, in accordance with PHENIX measurements.

---

*Deviates from current JEF-1 file.

Conclusion: Re-evaluation of cross-sections needed; at high energies the capture cross section should be decreased.

5.18. Ru-102

In the STEK samples there is a small contribution of Ru-101. The STEK values indicate a large overestimation of high-energy cross sections. However, there are also large uncertainties in the experimental STEK values, partly due to important scattering corrections. The tendency observed from CFRMF and RONA-3 is the same, but much less pronounced. Study of available experimental data for the inelastic scattering cross section for excitation of the first-excited 2^+-state [17] indicates that the evaluated cross section needs to be increased by almost a factor of 2, in agreement with the large values of the deformation parameter β (=0.264). A simple DWBA calculation already gives much improvement. A preliminary analysis yields that the C/E ratio of the capture effect becomes much closer to 1.0 after corrections of the inelastic-scattering effect by introducing direct-collective effects [16].

Conclusion: Re-evaluation of the inelastic-scattering cross sections is needed (direct effects); the fast-capture cross section should be decreased.

5.19 Ru-104

Nearly mono-isotopic STEK samples. There are large uncertainties in the experimental STEK values, partly due to important scattering corrections. Overestimation of STEK data, but the E/C values for RONA-3, ZONA-1, CFRMF are close to unity.
The inelastic-scattering cross section for excitation of the first-excited 2^+-state has been measured [17]. As for Ru-102, it follows that the evaluated cross section needs to be increased by a factor of about 2 [16]. The deformation parameter is β=0.288.

Conclusion: Re-evaluation of the inelastic-scattering cross section (direct effects) is needed.

5.20. Rh-103

The STEK samples numbered 1, 2 and 3 in tables 2 and 3 and figure 19 consist of Al-Rh alloy (4% Rh, see [2]). As an exception to the rule adopted in this report, the reactivity worths of Rh in these samples are given per gram of Rh and not per gram of Al-Rh alloy. There is excellent agreement with STEK measurements. The slight underestimation of the low-energy response may be associated with uncertainties in the neutron spectrum or in the calculated selfshielding effects at near-thermal energies.

Conclusion: No re-evaluation of cross sections needed.

5.21. Pd-104

In the adopted evaluation new resolved-resonance parameters (CBNM, Geel) have been used up to about 3 keV. At higher energies the evaluation is based upon model calculations, taking into account STEK data. The STEK measurements have a low accuracy. There is general consistency between evaluation and integral experiments for this rather unimportant nuclide. Note the quite large contribution of Pd-105 (up to 30%). The present inelastic-scattering cross section evaluation is far too low [17], due to the neglect of direct-collective effects [16].

Conclusion: No re-evaluation of capture cross-sections needed; the inelastic-scattering cross section needs to be re-evaluated (direct effects).

5.22. Pd-105

Nearly mono-isotopic samples were used in the STEK-measurements. The E/C ratios for the samples A1 and A2 are less reliable due to sample dimension uncertainties. Slight underprediction of measured values in all STEK cores. Discrepancy between STEK and PHENIX, where a much larger underprediction is observed. The results for sample T are still in

agreement with the PHENIX data (see fig. 21).

Conclusion: Upward adjustment needed; see also sect. 5.27 (natural Pd). The STEK data allow a "maximum" adjustment of about +10% (relying on sample T); it is also of interest to investigate the scattering correction.

5.23. Pd-106

In the adopted evaluation new resolved-resonance parameters (CBNM, Geel) have been used up to about 3 keV. At higher energies, the evaluation is based upon model calculations taking into account STEK data. There is a systematic underprediction of measurements in all STEK cores (~10%), although hardly significant in view of the rather large uncertainty margins. Note that there was a fairly large contribution of Pd-105 (10-15%) in the STEK samples. The underestimation of the PHENIX data is much more pronounced; also in this case there were sample problems (the PHENIX sample contained mainly Pd-105). New French measurements are underway. As for Pd-104 the inelastic-scattering cross section for Pd-104 is much too low [17].

Conclusion: Upward adjustment is needed; the scattering cross section needs to be corrected for direct-collective effects [16].

5.24. Pd-107

The adopted evaluation is based upon new resolved-resonance parameters (RPI) upto 650 eV [23] and model calculations, taking into account STEK data. The STEK samples contain a Pd fission-product mixutre with important contributions of other Pd isotopes, in particular Pd-105 (see fig. 23). There is a slight underestimation of the STEK data, especially in the softer STEK spectra, which may be due to too low Pd-105 cross-sections (also the cross-sections of the even-mass isotopes seem systematically too low).

Conclusion: Check again after adjustment of Pd-105 cross-sections. Include very recent differential data of Macklin [24].

5.25. Pd-108

In the adopted evaluation new resolved-resonance parameters (CBNM, Geel) have been used up to about 3 keV. At higher energies, the evaluation is based upon model calculations taking into account STEK data. The STEK measurements were performed with highly enriched samples. There is a general agreement between evaluation and STEK-data within the fairly large error margins. The RONA and CFRMF data do not conflict with the STEK data (see table 3).
The inelastic-scattering cross section for excitation of the first 2^+-state is far too low [17].

Conclusion: The inelastic-scattering cross section needs to be re-evaluated [16] (direct effects).

5.26. Pd-110

In the adopted evaluation new resolved-resonance parameters (CBNM, Geel) have been used up to about 3 keV. At higher energies, the evaluation is based upon model calculations taking into account STEK data. Agreement between evaluation and STEK data of poor accuracy.
The inelastic-scattering cross section for excitation of the first 2^+-state is much too low [16] as compared to the data [17].

Conclusion: Consistency with STEK data; upward adjustment perhaps needed. Re-evaluation of inelastic-scattering cross section required (direct effects).

5.27. Pd-nat

A natural isotopic mixture of Pd isotopes was used in the STEK measurements. There is an underprediction of integral data (~10%) in four STEK cores, but not in STEK-1000.
The main contribution comes from Pd-105. However, compared to the isotopic measurement (sect. 5.22) the applied scattering corrections (from even-mass isotopes) are much larger.

The contributions of different isotopes to ρ_c/ρ_o are indicated in fig. 26.

Conclusion: Increase cross-section of main component: Pd-105; re-evaluate inelastic scattering cross sections.

5.28. Ag-107

There is only a single CFRMF measurement available for this nuclide. Excellent agreement is found between experiment and calculation.

Conclusion: No action needed.

5.29. Ag-109

Highly enriched samples were used in the STEK measurements. The adopted evaluation has been adjusted to STEK and CFRMF data, resulting in good agreement for STEK measurements in the softer neutron spectra and a slight overestimation of the measurements in STEK-500.

Conclusion: Consistency with integral data; some increase of the high-energy cross sections is possible.

5.30. Sb-121

There is only a single CFRMF measurement available for this nuclide. Experiment and calculation show good consistency.

Conclusion: No action needed.

5.31. Sb-123

There is only a single CFRMF measurement available for this nuclide. Experiment and calculation show good consistency.

Conclusion: No action needed.

5.32. I-127

The samples measured in STEK contained PbI_2 (100% I-127) with a small admixture of $PbSO_4$. Measured reactivity worths of Pb and $PbSO_4$ were used to correct the experimental worths of the samples.
In the adopted evaluation an adjustment has been applied to the STEK measurements and the CFRMF activation data. There is a slight discrepancy between the STEK data and the CFRMF data. Therefore: small underestimation of the STEK data in the softer STEK spectra (~4%) and a slight overprediction of the CFRMF capture measurement (11%± 10%).

Conclusion: No action needed.

5.33. I-129

Recent resolved-resonance parameters were adopted [25].
The samples measured in STEK contained PbI_2 (86% I-129) with a small admixture of $PbSO_4$. Measured corrections for Pb and $PbSO_4$ were applied to the experimental reactivity worths. The contributions of I-127 and I-129 to ρ_c/ρ_o are shown in Fig. 29.
There is a small, but hardly significant, overprediction of σ_c, in agreement with the CFRMF result, where the E/C value is 0.94±0.06 (Table 3).

Conclusion: No action needed, agreement with recent differential capture data [25].

5.34. Xe-131

A sample containing a mixture of Xe isotopes has been measured in STEK. The sample contained only 41% of Xe-131 [2], but its reactivity effect is mainly due to this isotope. In Fig. 30 the contribution to ρ_c/ρ_o of the other isotopes (mainly Xe-132) is shown (a - very small - correction has been applied to the experimental reactivity worths for the 0.1 weight % admixture of CO_2).
Good agreement is found in the softer neutron spectra. At high energies there is an underprediction of ρ_c/ρ_o, but this discrepancy is hardly significant in view of the experimental uncertainties and the relatively large scattering corrections.

Conclusion: No action needed.

5.35. Xe-132

No separate STEK measurements are available for this nuclide. In CFRMF the E/C ratio of the capture rate is 0.91±0.07 (Table 3).

Conclusion: No action.

5.36. Xe-134

No separate STEK measurements are available for this nuclide. In CFRMF the E/C ratio of the capture rate is 0.57±0.04 (Table 3).

Conclusion: A decrease of about 40% of the capture cross section is needed.

5.37. Cs-133

The adopted evaluation has partly been adjusted to STEK integral data, CFRMF activation data and recent differential data.
The STEK measurements were performed with CsCl samples. Measured worths were corrected for Cl contributions, which were derived from the separately measured reactivities of $PbCl_2$ and Pb [2]. The dimensions of the samples A1, A2 and B are not known accurately. The self-shielding

calculations for these samples are therefore less reliable. There seems to be a general underestimation of the capture cross-section over the whole energy region of a few percent (for PHENIX and CFRMF excellent agreement is found).

Conclusion: A careful re-evaluation of the resolved-resonance range is recommended.

5.38. Cs-134

No separate STEK measurements are available for this nuclide. In PHENIX the E/C ratio of the capture rate is 1.135±0.064 (Table 3).

Conclusion: An increase of about 10% of the capture cross section is advisable.

5.39. La-139

Natural La_2O_3 (99.91% La-139) has been used in the STEK experiments. The experimental STEK data are highly uncertain due to very large corrections for the scattering reactivity effects (with significant contributions from elastic down-scattering).
In the adopted evaluation an adjustment has been applied to the CFRMF activation measurement. Therefore: good agreement between calculated and measured CFRMF data. The same applies to the capture data in ZONA-1. The measurement in RONA-3 indicates a somewhat (~10%) higher capture cross section (discrepancy?). From the STEK data one might conclude that the inelastic scattering cross-section has been evaluated reasonably well.

Conclusion: No action required.

5.40 Ce-140

Natural CeO_2 samples have been measured in STEK. The calculated contribution to ρ_c/ρ_o of Ce-142 (11.1 at.%) is indicated in Fig. 33 (the small contribution of other Ce isotopes, 0.4 at.%, has been neglected).

The originally adopted evaluation does not contain resolved-resonance parameters. However, in the new Brookhaven compilation these are available upto 240 keV [15]. Upto 20 keV there are very few gaps in the data. Therefore, we have inserted these data upto about 20 keV. However, with some additional evaluation effort this range could be extended to much higher energies.

The reactivity worths in STEK are strongly dominated by the inelastic scattering effect. There is a serious discrepancy between experiment and calculation, which increases with increasing spectrum hardness. At least a substantial part of this discrepancy must be due to too small scattering corrections. Experimental information from CFRMF (Table 3) suggests that σ_c at high energies has to be reduced by an order of magnitude.

Conclusion: No final conclusions can be drawn from the STEK data at present. From the CFRMF measurement it follows that the fast capture cross section is more than 10 times too large, which is not in contradiction with the STEK data.

5.41. Ce-142

Highly-enriched samples have been measured in STEK. Calculated contributions to ρ_c/ρ_o of other Ce isotopes are less than 4%. Large scattering corrections had to be applied to the measured reactivity worhts.

In the adopted evaluation four resolved resonances with uncertain parameters have been included.

The discrepancy between experiment and calculation increases with increasing spectrum hardness (Fig. 34). The main reason must be underestimation of the inelastic scattering effect. From the experimental CFRMF information one can conclude that σ_c at higher energies should be reduced (E/C = 0.63±0.05); see Table 3.

Conclusion: Reduce fast capture cross section by about 30 to 40%.

5.42. Pr-141

Mono-isotopic Pr_6O_{11} has been used in the STEK experiments. In the adopted evaluation a partial adjustment (only at high energies) has been applied to the STEK and CFRMF data. There is a small but insignificant overprediction of the capture data in CFRMF and RONA-3 (3-4%). The overprediction of the STEK data is larger (~10% in all neutron spectra). However, the STEK data suffer from important scattering corrections (also due to elastic down-scattering).

Conclusion: No action required.

5.43. Nd-142

Nd_2O_3 samples enriched in Nd-142 have been measured in STEK. Contributions to ρ_c/ρ_o of other isotopes (mainly Nd-143 of which σ_c is well known) range from 17% (STEK-500) to 35% (STEK-4000). There is a large overestimation of the capture effect; this overestimation increases with increasing spectrum hardness. Part of the discrepancy may well be due to an underestimation of the scattering correction.

With respect to inelastic scattering it is noted that deformation effects (observed in elastic and inelastic scattering; $\beta = 0.09$ [18, 19] enhance the inelastic scattering to the low-lying vibrational states, cf. Sect. 5.45 and [16].

Conclusion: Although this nuclide is not very important as a fission product, a significant reduction of σ_c is needed. The inelastic scattering needs to be enhanced with a direct component to vibrational states.

5.44. Nd-143

Highly-enriched samples have been measured in STEK. Calculated capture effects are a few per cent larger than the experimental values in all spectra, except in STEK-500. Here the deviation is larger, but the experimental value is more uncertain.

Conclusion: No actions required.

5.45 Nd-144

Samples enriched in Nd-144 have been measured in STEK. Contributions to ρ_c/ρ_o of other isotopes (mainly Nd-143 and Nd-145) range from 20% (STEK-500) to 38% (STEK-4000).
There is good agreement between calculated and measured capture reactivity effects in the softer neutron spectra, but also a clear tendency to an overestimation with increasing spectrum hardness. Part of this tendency may be due to a systematic underestimation of the scattering correction. This correction is very important in STEK-500.

For this nucleus the direct-collective excitation of the first 2^+-state has been studied quite well [18,19]. The value of β for this vibrational nucleus is β=0.12. There are also (n,n'γ) data measured at 2.75 MeV by Andreev et al. [20] showing large enhancements for the low-lying states, in particular for the 2^+- and 4^+-states at 0.697 and 1.315 MeV, respectively. The effect of these enhancements to the total inelastic cross sections is an increase of a factor 1.4. At lower incident energies (below 1.5 MeV) the increase could be more than a factor of 2. We note that if the total scattering reactivity effect would be increased by a factor of about 1.4 we would find consistency between calculations and measurements in all STEK-cores.

Conclusion: Re-evaluate inelastic-scattering cross section, using data of Andreev et al. [20].

5.46. Nd-145

Highly-enriched samples have been measured in STEK. Calculated capture effects are a few per cent smaller than the experimental values in all spectra, except in STEK-500. Here an overprediction of 16% is observed, however with a rather large uncertainty, also due to the scattering correction. Nevertheless, the STEK-500 result is in agreement with the 12% overprediction of the PHENIX measurement.

Conclusion: Reduce capture cross section with about 10% at high energies (above about 150 keV).

5.47. Nd-146

Samples enriched in Nd-146 have been measured in STEK. Contributions to ρ_c/ρ_o of other isotopes (mainly Nd-145) range from 15% (STEK-500) to 39% (STEK-4000). There is good agreement between calculated and measured capture reactivity effects in the softer neutron spectra, but also a tendency to an overestimation with increasing spectrum hardness. However, excellent agreement is found for the CFRMF activation data as well as for the RONA-3 and ZONA-1 measurements. The observed tendency for the STEK data may therefore be due to a systematic underprediction of the scattering reactivity effect (which is very important in STEK-500).

With respect to the inelastic-scattering the same remarks as given for Nd-144 (Sect. 5.45) apply. The deformation parameter is β=0.15 [18, 19] for this vibrational nucleus. It means that in particular the inelastic scattering cross sections to the low-lying 2^+, 4^+, 3^- states are enhanced. However, Coope et al. [21] have shown that there are depletions for higher-excited states, compared to statistical-model calculations. These compensating effects were not observed for Nd-144 [20]. Perhaps this has to do with the increased level density of Nd-146 as compared to Nd-144.

Conclusion: Relying upon the soft-core STEK data and the activation data there is no need to re-evaluate the capture cross section; add the direct 2^+-component to the inelastic-scattering cross section [16].

5.48 Nd-148

Samples enriched in Nd-148 have been measured in STEK. Contributions from other isotopes (mainly Nd-143 and Nd-145) to ρ_c/ρ_o range from 17% (STEK-500) to 23% (STEK-4000). The calculated reactivity worths are systematically too large in all STEK spectra (about 20%). The CFRMF capture measurement also suggests an overprediction (by 18%±14%). However, for the high-accuracy measurements in RONA-3 and ZONA-1 excellent agreement is found.

These results suggest that the cross section in the resolved-resonance

range should be decreased, in particular capture widths of the predominant resonances at 155 eV, 287 eV and 714 eV could be reduced by about 10%.

With respect to inelastic scattering similar remarks as given for Nd-146 apply (Sect. 5.47). The value of the deformation parameter is β=0.18 [18,19]. This should lead to a strong enhancement of the first 2^+-state. Possibly similar compensating effects as observed for Nd-146 [21] could play a role.

Conclusion: Reduce capture widths of strong resonances at low energies; add direct-component to inelastic-scattering cross section of the first 2^+-state [16].

5.49. Nd-150

Samples enriched in Nd-150 have been measured in STEK. Contributions to ρ_c/ρ_o of other isotopes (mainly Nd-143 and Nd-145) range from 10% (STEK-500) to 20% (STEK-4000). There is good agreement between calculated and measured capture reactivity worths in the softer STEK neutron spectra, but an overprediction in the hardest spectra of about 20%, although hardly significant in view of the rather large uncertainties in the experimental values.
However, this overprediction is in agreement with the CFRMF data (C/E ratio = 1.48±0.18) and the RONA-3 and ZONA-1 data (C/E ratio 1.21 and 1.47, respectively).

The deformation parameter for this transitional nucleus is quite large (β=0.21), suggesting that the inelastic scattering to the first 2^+-state should be enhanced. On the other hand, the level density of Nd-150 is relatively large such that collective excitations may be compensated or may be a small fraction of the total inelastic-scattering cross section, like for odd-mass nuclides.

Conclusion: Relying upon the activation data a reduction of about 20% in the fast-capture cross section is needed; direct inelastic scattering should be accounted for [16].

5.50 Nd-nat.

Two sets of samples have been measured in STEK, one with natural Nd powder and one with natural Nd_2O_3. In order to compare the results of the two sets we have given in the tables and Fig. 43 the reactivity effects of the Nd_2O_3 samples per gram Nd (and not, as usual, per gram Nd_2O_3).
The tendencies observed for the individual isotopes can also be found in the results for the natural mixture. Again, the results strongly suggest a systematic underprediction of the scattering reactivity effect.
In the sample-averaging process applied in Table 3 the sample N_I got by far the largest weight, which might be a bit risky. This large sample may have caused a flux depression. Since this depression has not been accounted for in our calculations, the calculated reactivity effects may be too large.

General conclusion for the Nd-isotopes

The best strategy seems to use the STEK data of cores 4000 and 3000 to fit the capture cross sections in the lower-energy range and to use the available activation and transmutation data for the adjustment of fast capture cross sections. The next step would be to correct the inelastic scattering cross section for direct-collective excitations to the first 2^+ state and possibly to higher-excited states as well. Finally, the results of STEK-2000, -1000, -500 should be used to check the evaluations of fast-capture and inelastic-scattering cross sections. This procedure should be followed in particular for the even-mass isotopes.

5.51. Pm-147

A mixture of Pm-147 and Sm-147 has been measured in STEK (see Sect. 5.52). Note that the atomic ratio varied during the STEK experiments [2]. The (calculated) contribution to ρ_c/ρ_o of Sm-147 is shown in Fig. 44. The adopted evaluation has been adjusted to (accurate) STEK measurements and a (less accurate) CFRMF measurement; therefore good agreement between calculated and measured STEK data. The CFRMF meas-

urement tends to lower cross-sections.

Conclusion: Consistency with STEK data; CFRMF indicates lower cross-sections.

5.52. Sm-147

Mono-isotopic Sm-147 STEK-samples. Excellent agreement with STEK measurements.

Conclusion: Consistency with STEK data.

5.53. Sm-148

Samples enriched in Sm-148 have been measured in STEK. Contributions to ρ_c/ρ_o of other isotopes (mainly Sm-149) are rather large, as shown in Fig. 46. We note that for Sm-149 reasonably good agreement with integral data is observed (Sect. 5.54). Good agreement between calculated and measured reactivity worths is found for the softer neutron spectra. The STEK results strongly suggest that a downward adjustment of the capture cross-section in the high-energy range is needed, although an underestimation of the scattering correction may have contributed to the observed discrepancy in the harder STEK spectra.

We note that the scattering reactivity effect gives a much smaller contribution to the total reactivity effect of the Sm-isotopes than for the Nd-isotopes (see Table 3). Still, the calculated scattering cross section should be increased, due to direct-collective contributions to rotational states. The deformation parameter is β=0.13 [19,22]. This means strong enhancements of the inelastic-scattering cross section to the first 2^+-state at 550 keV and also to higher-energy components of of the rotational band. Coope et al. [21] have measured a value of 504±40 mb at 2.47 MeV for the excitation of the first-excited state; the calculated value is about 470 mb. For some reason (optical model?) the adopted inelastic-scattering cross sections for the Sm-isotopes are already quite high, even without taking into account direct contributions.

On the other hand, we also know that the capture cross section is extremely high (unrealistically) at energies above 800 keV.

Conclusion: Reduce fast capture cross section at energies above 900 keV; the direct component to the inelastic scattering cross section should be accounted for [16].

5.54. Sm-149

Highly enriched samples have been measured in STEK. The calculated reactivity worths in STEK-4000 are rather uncertain, for the following reasons:

- Owing to the exceptionally high thermal cross section of Sm-149, more than 30% of the capture effect (in infinite dilution) stems from neutrons with energies below 1 eV. The low-energy tail of the STEK spectrum is not well known.
- The small level spacing of the (low-energy) resonances causes resonance overlap of the Doppler-broadened resonances. This overlap is not taken into account in the TRIX-code, which leads to an underestimation of the self-shielding effect and, hence, to too large calculated reactivity worths.
- The very strong thermal and near-thermal resonances cause flux depressions which, especially for the larger samples, cannot be calculated accurately with a simple self-shielding calculation based on the lumped absorber equivalence principle. It is quite probable that the flux depressions calculated by TRIX are too small, which again leads to too high calculated reactivity worths.

For the other STEK cores these difficulties play a minor role. Here we find a small underprediction of the measured values, which increases with increasing spectrum hardness, up to about 6% in STEK-500 (good agreement is found between calculated and measured PHENIX data).

Conclusion: Consistency with integral data.

5.55. Sm-150

Samples enriched in Sm-150 have been measured in STEK. Contributions to ρ_c/ρ_o of other isotopes (mainly Sm-149) range from 12% (STEK-500) to 30% (STEK-4000). Good agreement between calculated and measured reactivity worths is found for STEK-4000. In the harder spectra an underestimation of about 10% can be observed. This is in agreement with the transmutation measurement in PHENIX, where an underestimation of 13% was found.

With respect to inelastic scattering similar remarks as given for Sm-148 apply: β=0.17 [19,22]; $\sigma_{nn'}(2^+)$=491±30 mb at 2.47 MeV [21], adopted value: 427 mb.

However, in contrast to Sm-148, the capture cross section seems in reasonably good shape in the MeV range.

Conclusion: Increase fast capture cross section in smooth energy range by about 10%; the direct component to the inelastic scattering cross section should be accounted for [16].

5.56. Sm-151

A Sm isotopic mixture with only 6.13 at.% Sm-151 has been measured in STEK. The contributions of the various isotopes to ρ_c/ρ_o are shown in Fig. 49. Here the contribution denoted by "others" is mainly due to Sm-152. The results for the samples G, F and E are less reliable because of the uncertainties in the sample dimensions and possible contamination of the sample mixture. These results have not been used in the sample averaging process in Table 3.
A systematic overprediction of ρ_c/ρ_o of 4-9% can be observed for all STEK spectra. The reactivity effects of Sm-147 and Sm-152 are quite well predicted, whereas for Sm-149 and Sm-150 a slight underprediction has been observed. Therefore, the systematic overprediction must be ascribed to a too high (~30%) evaluated capture cross-section of Sm-151. The transmutation measurement in PHENIX, on the other hand, suggests that the evaluated cross-section is 16.5% too small. There is a serious discrepancy between STEK and PHENIX of almost a factor 2 with

respect to the capture effect of Sm-151. Since in both measurements there were sample problems, it is difficult to decide what to do when there is no further experimental information.

Conclusion: Wait for new PHENIX (Profile-2) data.

5.57. Sm-152

Highly-enriched samples have been measured in STEK. Fairly good agreement between calculated and measured STEK-reactivity worths can be observed, taking into account the error margins. The same applies to the capture data in CFRMF (overprediction 9%±6.4%). However, the capture data in RONA-1 and ZONA-3 are underpredicted by 15% and 33%, respectively.
From these results we conclude that the fast-capture cross section needs to be increased by at least 10%. This would lead to a worse agreement with the data in STEK-500. However, this could perhaps be compensated (at least partly) by an increase of the inelastic scattering cross section due to direct effects.

Inelastic-scattering experiments to the first 2^+ level of Sm-152 have been performed at 2.5 MeV (630 mb [21]), 2.75 MeV (890 mb [20]) and at 7 MeV (250 mb [22]). The adopted values are: 142, 100 and < 1 mb for these energies, respectively. This means that there are quite strong collective excitations (β=0.22) to the 2^+, 4^+, 6^+, 8^+ members of the ground-state rotational band (also observed in Refs. [20, 21]. Therefore we asume that a significant increase of the inelastic-scattering cross section is required.

Conclusion: Increase fast capture cross section by about 10%; increase inelastic-scattering cross section with direct-collective component.

5.58. Sm-154

Samples enriched in Sm-154 have been measured in STEK. Contributions to ρ_c/ρ_o of other isotopes (mainly Sm-149 and Sm-152) range from 5% (STEK-500) to 22% (STEK-4000). There is good agreement between calculated and measured reactivity worths in all STEK spectra.

The direct inelastic scattering to collective states (β=0.24 [19,22]) is quite important and these components should be accounted for [16]. However, the adopted inelastic scattering cross section for the Sm isotopes is already quite high, probably due to the use of the Moldauer potential.

Conclusion: Take into account direct-inelastic scattering component.

5.59. Eu-151

Natural Eu samples (48% Eu-151) have been measured in STEK, but the experimental data have not yet been analysed with respect to sample self-shielding. In CFRMF the E/C ratio is 1.05±0.06 (Table 3).

Conclusion: Evaluation is probably correct; wait for analysis of STEK data.

5.60. Eu-153

Highly-enriched samples have been measured in STEK, but the experimental data have not yet been analysed with respect to sample self-shielding. In CFRMF the E/C ratio is 1.02±0.07 (Table 3).

Conclusion: Evaluation is probably correct; wait for analysis of STEK data.

6. CONCLUSIONS

A short paper with the most important conclusions has recently been presented at a conference [26]. The conclusions are also given in this chapter.

First we mention the results of the STEK measurements in the "soft" STEK-4000 core, where the maximum sensitivity is generally below 1 keV and the major contribution is due to resolved resonances, see Table 3. Here the results for the Zr and Mo isotopes are unsatisfactory, but for most of the other nuclides reasonably good agreement was found without systematic trends. Some noteworthy exceptions are: Ru-104, La-139, Ce-140, Nd-142, Nd-148. However, in these cases the uncertainty due to the scattering correction is rather large. The absence of systematic trends suggests that our analysis is reasonably good, including the treatment of self-shielding. For most of the Zr and Mo isotopes new evaluations are needed.

Next, we shortly summarize the results from the fast-spectrum measurements, also given in Table 3. Here the major contribution comes from a region well-above 1 keV. A first observation is that the results of the US and French measurements are generally quite consistent. For most of the important odd-mass nuclides the STEK data are also consistent with the US and French data. However, puzzling discrepancies are found between some STEK and PHENIX data for Pd-105, Sm-151 and Mo-97. As long as the reason for these discrepancies is unknown, we may compare the evaluated quantities with some "average" over the experimental integral data. This leads to the conclusion that e.g. the capture cross sections of Pd-105, Sm-151, Pd-106 need to be increased and e.g. those of Mo-98, Zr-93, Xe-134 to be decreased. These changes will be made for JEF-2. Moreover, the results of forthcoming PHENIX irradiation measurements will be usedto try to resolve some remaining discrepancies.

From the integral-data test summarized in Table 3 it is also seen that the E/C values from STEK-1000 and STEK-500 are systematically lower than those from other experiments for many even-mass nuclides. A possible explanation is that the inelastic-scattering correction

is systematically too low for these nuclides. We have investigated several possible reasons for systematical underprediction of inelastic scattering cross sections and we have concluded that the neglect of direct-collective excitations in the present fp evaluations is the most important one. To our knowledge the inelastic-scattering cross sections in the current fp evaluations are mainly based upon Hauser-Feshbach calculations with width-fluctuation corrections, but without competition of direct comments. However, this is not justified, since already at quite low incident energies large collective effects have been observed, in particular for the excitation of the first-excited 2^+ vibrational state of Mo-, Ru-, Pd-, Nd-, and Sm-isotopes [17-22]. We have checked that indeed the cross sections from all present evaluations including JEF-1 and ENDF/B-V need to be increased by factors up to 2.0 to meet the data quoted in Ref. [17]. As an example we have studied the data for Ru-102. A simple Distorted Wave Born Approximation (DWBA) calculation with β_2=0.264 already gives significant improvements. We have checked that by using the experimental scattering cross sections the E/C ratio for Ru-102 improves considerably. A more extensive review on the status of inelastic-scattering data will be given elsewhere [16].

7. REFERENCES

[1] Rowlands, J. and Tubbs, N.; in Proc. Int. Conf. on Nuclear Data for Basic and Applied Science, Santa Fe, NM, May 13-17. 1985.

[2] Veenema, J.J. and Janssen, A.J.
Small-sample reactivity worths of fission product isotopes and some other materials measured in STEK; ECN-10 (1976).

[3] Martin-Deidier, L.; Mesure intégrale de la capture des produits de fission dans les réacteurs à neutrons rapides.
CEA-R-5023 (1979).

[4] Harker, Y.D. and Anderl, R.A.
Integral cross-section measurements on fission products in fast neutron fields; Proc. Specialists' Meeting on Neutron cross sections of fission product nuclei, Bologna 1979, NEANDC(E) 209 "L" (1980).

[5] Panini, G.C. and Nordborg, C.
KTOE-3, A programme to translate KEDAK into ENDF/B format; private communication (1983).

[6] Panini, G.C.
Four Aces, a programme for producing group averaged cross sections from different files; RT/FI (73)6 and private communication (1982).

[7] MacFarlane, R.E., Muir, D.W. and Bolcourt, R.M.
The NJOY Nuclear Data Processing System, Vol. 1: Users' Manual; La-9303-M, Vol. 1 (1982); code received from NEA Data Bank.

[8] Dekker, J.W.M.
Tables and figures of adjusted and unadjusted capture group cross sections based on the RCN-2 evaluation and integral measurements in STEK, Vol. 1, ECN-14 (1977).

[9] Dekker, J.W.M. et al.
Adjusted neutron spectra of STEK cores for reactivity calculations, ECN-35 (1978).

[10] Otter, J.M.
The TRIX-1 code, an improved analytic calculation of resonance integrals; NAA-SR-Memo-11538, Atomics International (1965).

[11] Goldstein, R.
Intermediate resonance absorption for multi-nuclide systems; Nucl. Sci. Eng. 30, 304 (1967).

[12] Anderl, R.A. et al.
Addendum to integral data-testing report for ENDF/B-V dosimeter cross sections; EGG-PHYS-5668 (1982).

[13] Anderl, R.A.
Integral measurements and tests of fission-product neutron capture cross sections; Proc. NEANDC/NEACRP specialists' meeting on Fast neutron capture cross sections, Argonne, 1982, NEANDC(US)-214/L (1983), p. 518.

[14] Macklin, R.L., Oak Ridge National Laboratory, Neutron capture measurements on radioactive ^{93}Zr, to be publ. in Astrophysics and Space Science (1985).

[15] Mughabghab, S.F., Divadeenam, M. and Holden, N.E.
Neutron Cross Sections, Vol. 1A, Acad. Press (1981) and S.F. Mughabghab, Vol. 1B (Acad. Press, 1984).

[16] Gruppelaar, H. Invited paper NEANDC Mtg. on the Optical Model, Paris, Nov. 1985.

[17] Konobeevskii, E.S. and Popov, V.I.
Excitation of collective states in inelastic scattering of low-energy neutrons in the 3p-resonance region; Sov. J. of Nucl. Phys. 33 (1981), p.7.

[18] Houat, G., et al.
Optical potential and nuclear deformation for even Nd isotopes from fast neutron scattering; Phys. Rev. C20 (1979), p.78.

[19] Shamu, R.E., Bernstein, E.M. and Ramirez, J.J.
Effects of deformation on neutron total cross sections of even-A Nd and Sm isotopes; Phys. Rev. C22 (1980), p.1857.

[20] Andreev, E.A., Basenko, V.K. and Sit'ko, S.P.
Excitation of Nd-144 by dd neutrons; Sov. J. Nucl. Phys. 23 (1976) p.6.

[21] Coope, D.F. et al.
Strong collective excitations in low-energy neutron scattering from transitional nuclei; Phys. Rev. C16 (1977) p.2223.

[22] McEllistrem, M.T., et al.
Deformation effects in neutron scattering from the Sm isotopes; Phys. Rev. C15 (1977) p.927.

[23] Singh, U.N., Block, R.C., and Nakagome, Y.
Neutron capture and transmission measurements on fission product Palladium-107, Nucl. Science and Eng. 67 (1978), p.54.

[24] Macklin, R.L.
Neutron capture measurements on fission product ^{107}Pd, Nucl. Science and Eng. 89 (1985), p.79.

[25] Macklin, R.L.
Neutron capture cross sections and resonances of Iodine-127 and Iodine-129, Nucl. Science and Eng. 85 (1983), p.350.

[26] Gruppelaar, H., Heijboer, R.J., Janssen, A.J., Van der Kamp, H.A.J., Karouby-Cohen, N., Martin-Deidier, L., Rimpault, G. and Salvatores, M.; Integral test of fission-product cross sections, Contr. to the Int. Conf. on Nuclear Data for Basic and Applied Science, Santa Fe, NM, May 13-17, 1985.

Table 1. Nuclides considered in the integral-data test.

Rb-87	Pd-104	Ce-140
Zr-90	Pd-105	Ce-142
Zr-91	Pd-106	Pr-141
Zr-92	Pd-107	Nd-142
Zr-93	Pd-108	Nd-143
Zr-94[1])	Pd-110	Nd-144
Zr-96	Pd-nat.	Nd-145
Zr-nat.[2])	Ag-107	Nd-146
Mo-92	Ag-109	Nd-148
Mo-94	Sb-121	Nd-150
Mo-95	Sb-123	Nd-nat.
Mo-96	I-127	Pm-147
Mo-97	I-129	Sm-147
Mo-98	Xe-131	Sm-148
Mo-100	Xe-132	Sm-149
Mo-nat.[2])	Xe-134	Sm-150
Tc-99	Xe-136[1])	Sm-151
Ru-101	Cs-133	Sm-152
Ru-102	Cs-134	Sm-154
Ru-104	La-139	Eu-151
Rh-103		Eu-153

1) Only present as admixture in STEK samples.

2) Isotopic evaluations used in integral-data test; different from JEF-1 evaluation for natural mixture.

Table 2. Comparison of experimental and calculated capture reactivity worths of fission products in samples measured in STEK. See chapter 2 for explanation of symbols.

Isotope	Core	Sample	Exp. $-\rho_c/\rho_o$	Calc. $-\rho_c/\rho_o$	E/C	Response above 1 keV (rel.)
Zr-90	4000	I.D.		.0142		.90
		K	-.016 ±.011	.0116	-1.34±.95	.89
		M	.0004±.0020	.0106	.04±.19	.88
	3000	I.D.		.0183		.93
		K	.009 ±.012	.0150	.58±.80	.92
		M	.0017±.0020	.0136	.13±.15	.91
	2000	I.D.		.0206		.95
		K	-.004 ±.011	.0169	-.24±.65	.94
		M	.003 ±.002	.0154	.19±.13	.93
	1000	I.D.		.0227		.97
		K	-.005 ±.021	.0189	-.26±1.11	.97
		M	-.002 ±.004	.0172	-.12±.23	.96
	500	I.D.		.0213		.99
		M	.0003±.0060	.0170	.02±.35	.99
Zr-91	4000	I.D.		.141		.34
		K	.076 ±.019	.098	.78±.19	.44
		O	.072 ±.015	.096	.75±.16	.44
		L	.081 ±.008	.090	.90±.09	.46
	3000	I.D.		.151		.41
		K	.089 ±.022	.107	.83±.21	.52
		O	.095 ±.018	.105	.90±.17	.52
		L	.097 ±.008	.099	.98±.08	.54
	2000	I.D.		.147		.47
		K	.126 ±.019	.107	1.18±.18	.58
		O	.079 ±.021	.105	.75±.20	.59
		L	.086 ±.007	.100	.86±.07	.60
	1000	I.D.		.123		.60
		K	.056 ±.070	.095	.59±.74	.71
		O	.074 ±.027	.094	.79±.29	.71
		L	.083 ±.014	.089	.93±.16	.73
	500	I.D.		.077		.81
		L	.043 ±.016	.064	.67±.25	.89

Table 2 (continued)

Isotope	Core	Sample	Exp.	Calc.	E/C	Response above 1 keV (rel.)
Zr-92	4000	I.D.		.034		.96
		O	.028 ±.014	.028	1.00±.50	.95
		M	.004 ±.005	.026	.16±.20	.95
	3000	I.D.		.044		.97
		O	.015 ±.015	.036	.42±.42	.97
		M	.0040±.0035	.033	.12±.11	.96
	2000	I.D.		.050		.98
		O	-.018 ±.019	.041	-.44±.46	.98
		M	.002 ±.005	.037	.05±.13	.97
	1000	I.D.		.054		.99
		O	.027 ±.022	.045	.60±.49	.99
		M	-.002 ±.006	.042	-.05±.14	.99
	500	I.D.		.049		1.00
		M	-.007 ±.010	.039	-.18±.26	1.00
Zr-93	4000	I.D.		.168		.22
		L	.094 ±.010	.125	.75±.08	.28
		M1	.079 ±.009	.127	.62±.07	.28
		M2	.082 ±.009	.127	.65±.07	.28
	3000	I.D.		.162		.29
		L	.093 ±.018	.124	.75±.15	.37
		M1	.075 ±.010	.126	.60±.08	.36
		M2	.077 ±.009	.126	.61±.07	.36
	2000	I.D.		.146		.37
		L	.079 ±.017	.116	.68±.15	.45
		M1	.067 ±.012	.117	.57±.10	.44
		M2	.065 ±.012	.117	.56±.10	.44
	1000	I.D.		.108		.54
		L	.118 ±.020	.091	1.30±.22	.62
		M1	.052 ±.017	.092	.57±.18	.61
		M2	.037 ±.016	.092	.40±.17	.61
	500	I.D.		.063		.82
		L	.031 ±.028	.059	.53±.47	.86
		M1	.011 ±.024	.059	.19±.41	.85
		M2	.017 ±.022	.059	.29±.37	.85

Table 2 (continued)

Isotope	Core	Sample	Exp.	Calc.	E/C	Response above 1 keV (rel.)
Zr-96	4000	I.D.		.091		.24
		K	.029 ±.009	.046	.63±.20	.40
		L	.037 ±.003	.041	.90±.07	.43
	3000	I.D.		.095		.31
		K	.020 ±.010	.050	.40±.20	.48
		L	.031 ±.004	.045	.69±.09	.51
	2000	I.D.		.090		.37
		K	.032 ±.009	.050	.64±.18	.55
		L	.022 ±.004	.045	.49±.09	.58
	1000	I.D.		.070		.52
		K	.026 ±.016	.044	.59±.36	.69
		L	.008 ±.006	.041	.20±.15	.72
	500	I.D.		.042		.80
		L	-.012 ±.008	.031	-.39±.26	.90
Zr-nat.	4000	I.D.		.049		.59
		3 foils	.028 ±.004	.041	.68±.10	.62
		6 foils	.026 ±.002	.038	.68±.05	.63
	3000	I.D.		.057		.66
		1 foil	.018 ±.015	.053	.34±.28	.68
		3 foils	.029 ±.004	.048	.60±.08	.69
		6 foils	.024 ±.0026	.045	.54±.06	.71
	2000	I.D.		.060		.72
		1 foil	.014 ±.017	.055	.25±.31	.73
		3 foils	.029 ±.005	.051	.57±.10	.75
		6 foils	.0256±.0027	.0474	.54±.06	.76
	1000	I.D.		.058		.82
		3 foils	.022 ±.008	.051	.43±.16	.84
	500	I.D.		.0470		.94
		6 foils	.0010±.0055	.0404	.02±.14	.95

Table 2 (continued)

Isotope	Core	Sample	Exp.	Calc.	E/C	Response above 1 keV (rel.)
Mo-97	2000	I.D.		.631		.65
		K	.500±.046	.541	.924±.085	.73
		O	.494±.013	.527	.937±.025	.74
		L	.455±.008	.513	.887±.016	.75
	1000	I.D.		.589		.76
		K	.471±.025	.525	.897±.048	.82
		O	.460±.016	.515	.893±.031	.83
		L	.442±.007	.504	.877±.014	.84
	500	I.D.		.446		.90
		K	.369±.036	.419	.881±.086	.93
		O	.353±.022	.414	.853±.053	.93
		L	.379±.016	.409	.927±.039	.94
Mo-98	4000	I.D		.233		.33
		T	.082±.010	.117	.701±.085	.50
		O	.082±.003	.102	.804±.029	.53
	3000	I.D		.257		.40
		T	.104±.012	.132	.788±.091	.59
		O	.086±.003	.117	.735±.026	.62
	2000	I.D		.259		.45
		T	.113±.013	.138	.819±.094	.66
		O	.085±.004	.123	.691±.033	.68
	1000	I.D.		.232		.57
		T	.077±.014	.137	.562±.102	.77
		O	.067±.004	.124	.540±.032	.79
	500	I.D.		.163		.78
		O	.047±.008	.109	.431±.073	.92
Mo-100	4000	I.D.		.172		.50
		T	.063±.030	.105	.60±.29	.62
		K	.094±.011	.100	.94±.11	.62
		L	.080±.005	.092	.870±.054	.63
	3000	I.D.		.189		.58
		T	.085±.029	.120	.71±.24	.71
		K	.097±.013	.114	.85±.11	.71
		L	.088±.006	.105	.838±.057	.72
	2000	I.D.		.189		.65
		T	.079±.029	.125	.63±.23	.77
		K	.105±.014	.120	.88±.12	.77
		L	.098±.006	.110	.891±.055	.78

Table 2 (continued)

Isotope	Core	Sample	Exp.	Calc.	E/C	Response above 1 keV (rel.)
Mo-100	1000	I.D.		.169		.77
		T	.073±.030	.123	.59±.24	.86
		K	.091±.018	.118	.77±.15	.86
		L	.088±.007	.110	.800±.064	.87
	500	I.D.		.123		.91
		L	.069±.010	.093	.74±.11	.95
Mo-nat.	4000	I.D.		.465		.26
		1 mm	.320±.011	.347	.922±.032	.34
		2 mm	.293±.007	.311	.942±.023	.38
		3 mm	.272±.004	.291	.935±.014	.40
		4 mm	.263±.003	.276	.953±.011	.42
	3000	I.D.		.402		.39
		1 mm	.319±.010	.327	.976±.031	.48
		2 mm	.271±.006	.302	.897±.020	.51
		3 mm	.268±.004	.288	.931±.014	.53
		4 mm	.257±.003	.278	.924±.011	.55
	2000	I.D.		.357		.51
		1 mm	.278±.010	.308	.903±.032	.58
		2 mm	.274±.005	.291	.942±.017	.61
		3 mm	.258±.005	.280	.921±.018	.62
		4 mm	.251±.004	.272	.923±.015	.64
	1000	I.D.		.290		.69
		1 mm	.254±.012	.269	.944±.045	.74
		2 mm	.232±.011	.260	.892±.042	.76
		3 mm	.237±.008	.255	.929±.031	.77
	500	I.D.		.212		.89
		1 mm	.185±.026	.206	.898±.126	.90
		2 mm	.169±.014	.204	.828±.069	.91
		4 mm	.154±.006	.200	.770±.030	.92

Table 2 (continued)

Isotope	Core	Sample	Exp.	Calc.	E/C	Response above 1 keV (rel.)
Tc-99	4000	I.D.		1.970		.24
		P	1.126±.12	1.292	.872±.093	.36
		G	1.166±.04	1.135	1.027±.035	.41
		H	1.076±.03	1.091	.986±.027	.42
		F	1.056±.02	1.049	1.007±.019	.43
		E	1.026±.03	1.027	.999±.029	.44
		K	1.006±.01	1.013	.993±.010	.45
	3000	I.D.		1.503		.42
		P	1.13±.09	1.191	.949±.076	.52
		G	1.12±.07	1.091	1.027±.064	.56
		H	1.09±.03	1.062	1.026±.028	.57
		F	1.08±.03	1.032	1.047±.029	.58
		E	1.06±.02	1.016	1.043±.020	.59
		K	1.01±.01	1.006	1.004±.010	.59
	2000	I.D.		1.324		.54
		P	1.17±.11	1.140	1.026±.096	.62
		G	1.20±.06	1.067	1.125±.056	.65
		H	1.11±.03	1.044	1.063±.029	.66
		F	1.08±.03	1.021	1.058±.029	.67
		E	1.05±.02	1.008	1.042±.020	.68
		K	1.042±.014	1.000	1.042±.014	.68
	1000	I.D.		1.103		.72
		P	1.30±.13	1.024	1.27±.13	.77
		G	1.03±.07	.983	1.048±.071	.79
		H	1.00±.04	.969	1.032±.041	.79
		F	.99±.03	.955	1.037±.031	.80
		E	.97±.02	.947	1.024±.021	.80
		K	1.02±.02	.942	1.083±.021	.81
	500	I.D.		.817		.90
		P	.776±.29	.794	.98±.37	.92
		H	.876±.06	.774	1.132±.078	.93
		K	.812±.028	.763	1.064±.037	.93

Table 2 (continued)

Isotope	Core	Sample	Exp.	Calc.	E/C	Response above 1 keV (rel.)
Ru-101	4000	I.D.		1.445		.37
		P	.937±.03	.907	1.033±.033	.56
		H	.857±.01	.807	1.062±.012	.61
	3000	I.D.		1.338		.53
		P	.986±.025	.983	1.003±.025	.69
		H	.916±.012	.901	1.017±.013	.72
	2000	I.D.		1.272		.64
		P	1.056±.034	1.018	1.037±.033	.76
		H	.939±.013	.949	.989±.014	.79
	1000	I.D.		1.149		.80
		P	1.05±.07	1.016	1.033±.069	.86
		H	.91±.02	.968	.940±.021	.88
	500	I.D.		.930		.93
		P	.744±.08	.881	.844±.091	.95
		H	.784±.02	.857	.915±.023	.96
Ru-102	4000	I.D.		.185		.82
		S	.156±.024	.161	.969±.149	.83
		H	.141±.015	.157	.898±.096	.83
	3000	I.D.		.225		.88
		S	.191±.028	.198	.965±.141	.89
		H	.126±.017	.192	.656±.089	.89
	2000	I.D.		.247		.91
		S	.185±.038	.219	.85±.17	.92
		H	.170±.014	.212	.802±.066	.92
	1000	I.D.		.262		.95
		S	.167±.058	.236	.71±.25	.96
		H	.152±.019	.230	.661±.083	.96
	500	I.D.		.238		.98
		H	.112±.032	.218	.514±.147	.99

Table 2 (continued)

Isotope	Core	Sample	Exp.	Calc.	E/C	Response above 1 keV (rel.)
Ru-104	4000	I.D.		.239		.49
		P	.142±.040	.147	.97±.27	.67
		H	.109±.010	.127	.86±.08	.72
	3000	I.D.		.274		.56
		P	.137±.030	.177	.77±.17	.74
		H	.113±.016	.156	.72±.10	.78
	2000	I.D.		.282		.62
		P	.127±.034	.191	.67±.18	.78
		H	.120±.013	.170	.706±.076	.82
	1000	I.D.		.261		.73
		P	.120±.063	.194	.62±.32	.86
		H	.114±.020	.177	.64±.11	.89
	500	I.D.		.197		.89
		H	.113±.024	.158	.72±.15	.96
Rh-103	4000	I.D.		2.535		.18
		1	2.309±.103	2.197	1.051±.047	.21
		2	2.216±.072	2.105	1.053±.034	.22
		3	2.107±.049	1.972	1.068±.025	.23
		4	1.687±.019	1.633	1.033±.012	.28
		5	1.432±.009	1.386	1.033±.006	.32
		6	1.189±.005	1.162	1.023±.004	.37
		7	1.058±.004	1.049	1.009±.004	.41
		8	.980±.0025	.972	1.008±.003	.43
	3000	I.D.		1.496		.40
		5	1.092±.011	1.099	.994±.010	.54
		6	1.002±.0055	.991	1.011±.006	.58
		7	.938±.0034	.930	1.009±.004	.61
		8	.883±.0028	.886	.997±.003	.63

Table 2 (continued)

Isotope	Core	Sample	Exp.	Calc.	E/C	Response above 1 keV (rel.)
Rh-103	2000	I.D.		1.254		.55
		2	1.233±.083	1.196	1.031±.069	.58
		3	1.166±.064	1.176	.991±.054	.59
		4	1.127±.023	1.109	1.016±.021	.62
		5	1.078±.010	1.046	1.031±.010	.65
		6	.985±.006	.972	1.013±.006	.68
		7	.935±.004	.927	1.009±.004	.71
		8	.897±.004	.893	1.004±.004	.72
	1000	I.D.		1.082		.72
		2	1.205±.120	1.058	1.139±.113	.74
		3	.903±.081	1.048	.862±.077	.74
		4	1.018±.032	1.014	1.004±.032	.76
		5	1.010±.015	.980	1.031±.015	.78
		6	.946±.008	.935	1.012±.009	.81
		7	.914±.0054	.905	1.010±.006	.82
		8	.887±.004	.882	1.006±.005	.83
	500	I.D.		.835		.90
		2	.887±.180	.827	1.07±.22	.90
		3	.907±.140	.824	1.10±.17	.90
		4	.900±.044	.812	1.108±.054	.91
		5	.798±.024	.800	.998±.030	.92
		6	.784±.013	.783	1.001±.017	.93
Pd-104	4000	I.D.		.535		.32
		S1	.301±.086	.373	.81±.23	.44
		S2	.303±.082	.373	.81±.22	.44
	3000	I.D.		.536		.43
		S1	.400±.093	.397	1.01±.23	.54
		S2	.407±.090	.397	1.03±.23	.54
	2000	I.D.		.509		.51
		S1	.52±.09	.397	1.31±.23	.62
		S2	.27±.10	.397	.68±.25	.62
	1000	I.D.		.428		.69
		S1	.284±.16	.366	.78±.44	.76
		S2	.414±.06	.366	1.13±.16	.76
	500	I.D.		.313		.89
		S1	.196±.18	.295	.66±.61	.92
		S2	.256±.16	.295	.87±.54	.92

Table 2 (continued)

Isotope	Core	Sample	Exp.	Calc.	E/C	Response above 1 keV (rel.)
Pd-105	4000	I.D.		1.516		.39
		A1	1.394±.031	1.367	1.020±.023	.43
		A2	1.306±.018	1.286	1.016±.014	.45
		K	1.224±.019	1.199	1.021±.016	.48
		T	1.225±.025	1.196	1.024±.021	.48
	3000	I.D.		1.523		.52
		A1	1.541±.045	1.412	1.091±.032	.55
		A2	1.389±.022	1.350	1.029±.016	.57
		K	1.294±.015	1.282	1.009±.012	.60
		T	1.305±.025	1.279	1.020±.020	.60
	2000	I.D.		1.490		.61
		A1	1.44 ±.03	1.405	1.025±.021	.64
		A2	1.37 ±.02	1.356	1.010±.015	.66
		K	1.31 ±.02	1.302	1.006±.015	.68
		T	1.34 ±.03	1.300	1.031±.023	.68
	1000	I.D.		1.357		.75
		A1	1.347±.051	1.310	1.028±.039	.77
		A2	1.308±.022	1.281	1.021±.017	.79
		K	1.262±.026	1.249	1.010±.021	.80
		T	1.325±.040	1.248	1.062±.032	.80
	500	I.D.		1.084		.91
		K	1.018±.038	1.047	.972±.036	.93
		T	1.141±.053	1.046	1.091±.051	.93
Pd-106	4000	I.D.		.276		.53
		H	.209±.016	.191	1.094±.084	.68
	3000	I.D.		.313		.61
		H	.242±.017	.227	1.066±.075	.76
	2000	I.D.		.325		.68
		H	.278±.016	.245	1.135±.065	.81
	1000	I.D.		.313		.79
		H	.265±.027	.254	1.043±.106	.88
	500	I.D.		.257		.92
		H	.250±.036	.230	1.087±.157	.96

Table 2 (continued)

Isotope	Core	Sample	Exp.	Calc.	E/C	Response above 1 keV (rel.)
Pd-107	4000	I.D.		1.294		.35
		T	1.021±.015	.986	1.035±.015	.45
		K	.988±.012	.951	1.039±.013	.46
		O	.948±.004	.912	1.039±.004	.48
	3000	I.D.		1.234		.49
		T	1.062±.016	1.021	1.040±.016	.58
		K	1.010±.011	.993	1.017±.011	.59
		O	.975±.0065	.963	1.012±.007	.60
	2000	I.D.		1.170		.59
		T	1.046±.015	1.017	1.029±.015	.66
		K	1.029±.009	.996	1.033±.009	.67
		O	1.001±.007	.972	1.030±.007	.69
	1000	I.D.		1.032		.75
		T	.948±.023	.955	.993±.024	.79
		K	.959±.012	.942	1.018±.013	.80
		O	.947±.007	.928	1.020±.008	.81
	500	I.D.		.808		.91
		T	.775±.030	.784	.989±.038	.93
		K	.773±.016	.779	.992±.021	.93
		O	.774±.010	.774	1.000±.013	.93
Pd-108	4000	I.D.		1.594		.07
		H	.389±.030	.359	1.084±.084	.28
		T	.343±.035	.341	1.006±.103	.29
	3000	I.D.		1.008		.15
		H	.360±.041	.298	1.21±.14	.46
		T	.312±.030	.286	1.09±.11	.47
	2000	I.D.		.687		.25
		H	.310±.040	.264	1.17±.15	.59
		T	.287±.025	.256	1.12±.10	.61
	1000	I.D.		.366		.53
		H	.176±.058	.227	.78±.26	.80
		T	.232±.030	.222	1.05±.14	.80
	500	I.D.		.221		.86
		T	.164±.047	.191	.86±.25	.94

Table 2 (continued)

Isotope	Core	Sample	Exp.	Calc.	E/C	Response above 1 keV (rel.)
Pd-110	4000	I.D.		.143		.51
		S1	.099±.078	.129	.77±.60	.54
		S2	.119±.067	.129	.92±.52	.54
	3000	I.D.		.151		.64
		S1	-.026±.086	.139	-.19±.62	.66
		S2	.066±.104	.139	.47±.75	.66
	2000	I.D.		.153		.72
		S1	.016±.09	.143	1.12±.63	.74
		S2	-.034±.084	.143	-.24±.59	.74
	1000	I.D.		.148		.83
		S1	.26±.14	.141	1.84±.99	.84
		S2	.19±.07	.141	1.35±.50	.84
	500	I.D.		.125		.94
		S1	.18±.20	.121	1.49±1.65	.94
		S2	.10±.16	.121	.83±1.32	.94
Pd-nat	4000	I.D.		.913		.25
		1	.594±.036	.576	1.031±.063	.39
		2	.620±.023	.576	1.076±.040	.39
		3	.620±.009	.576	1.076±.016	.39
	3000	I.D.		.767		.39
		1	.586±.054	.565	1.037±.096	.52
		2	.611±.013	.565	1.081±.023	.52
	2000	I.D.		.673		.51
		1	.636±.046	.546	1.165±.084	.62
		2	.603±.010	.546	1.104±.018	.62
	1000	I.D.		.542		.71
		1	.539±.024	.495	1.089±.048	.77
		2	.503±.015	.495	1.016±.030	.77
		3	.494±.010	.495	.998±.020	.77
	500	I.D.		.410		.90
		1	.537±.119	.399	1.35±.30	.92
		2	.459±.022	.399	1.150±.055	.92

Table 2 (continued)

Isotope	Core	Sample	Exp.	Calc.	E/C	Response above 1 keV (rel.)
Ag-109	4000	I.D.		4.161		.12
		P	1.427±.06	1.422	1.004±.042	.33
		H	1.197±.02	1.215	.985±.016	.38
	3000	I.D.		2.284		.29
		P	1.22 ±.06	1.209	1.009±.050	.52
		H	1.08 ±.027	1.083	.997±.025	.57
	2000	I.D.		1.675		.45
		P	1.20 ±.07	1.137	1.055±.062	.64
		H	1.06 ±.02	1.047	1.012±.019	.68
	1000	I.D.		1.220		.69
		P	1.20 ±.11	1.040	1.154±.106	.79
		H	.96 ±.03	.990	.970±.030	.81
	500	I.D.		.915		.90
		P	1.05 ±.16	.869	1.21 ±.18	.93
		H	.77 ±.05	.849	.907±.059	.94
I-127	4000	I.D.		.915		.21
		S	.601±.047	.587	1.023±.080	.32
		T	.567±.022	.538	1.054±.041	.34
		O	.503±.008	.479	1.050±.017	.38
	3000	I.D.		.742		.33
		S	.526±.040	.543	.969±.074	.45
		T	.551±.020	.509	1.083±.039	.47
		O	.479±.008	.466	1.028±.017	.51
	2000	I.D.		.629		.45
		S	.502±.053	.503	.998±.105	.55
		T	.501±.022	.479	1.046±.046	.57
		O	.465±.009	.447	1.040±.020	.60
	1000	I.D.		.475		.66
		S	.414±.093	.426	.972±.22	.72
		T	.477±.035	.414	1.152±.085	.73
		O	.414±.011	.397	1.043±.028	.76
	500	I.D.		.328		.87
		S	.453±.109	.316	1.43 ±.34	.90
		T	.345±.049	.313	1.102±.157	.90
		O	.301±.014	.307	.980±.046	.91

Table 2 (continued)

Isotope	Core	Sample	Exp.	Calc.	E/C	Response above 1 keV (rel.)
I-129	4000	I.D.		.358		.34
		T	.268±.026	.305	.88±.09	.38
		K	.271±.011	.290	.94±.04	.40
	3000	I.D.		.344		.46
		T	.273±.030	.303	.90±.10	.51
		K	.282±.014	.291	.97±.05	.52
	2000	I.D.		.324		.55
		T	.300±.030	.292	1.03±.10	.60
		K	.293±.032	.283	1.04±.11	.61
	1000	I.D.		.277		.72
		T	.266±.042	.260	1.02±.16	.75
		K	.242±.022	.254	.95±.09	.76
	500	I.D.		.205		.90
		T	.168±.065	.200	.84±.33	.91
		K	.198±.025	.198	1.00±.13	.91
Xe-131	4000	I.D.		1.327		.05
		RB	.609±.013	.624	.976±.021	.11
	3000	I.D.		.656		.14
		RB	.362±.009	.379	.955±.024	.25
	2000	I.D.		.408		.27
		RB	.276±.010	.282	.978±.035	.38
	1000	I.D.		.222		.55
		RB	.218±.013	.195	1.11 ±.07	.62
	500	I.D.		.139		.84
		RB	.159±.020	.135	1.17 ±.15	.86

Table 2 (continued)

Isotope	Core	Sample	Exp.	Calc.	E/C	Response above 1 keV (rel.)
Cs-133	4000	I.D.		1.287		.17
		A1	.938±.018	.867	1.082±.021	.24
		A2	.737±.007	.686	1.074±.010	.30
		H	.713±.024	.663	1.075±.036	.31
		K	.622±.009	.598	1.107±.015	.34
		L	.544±.004	.537	1.013±.007	.36
		B	.563±.003	.535	1.052±.006	.36
		M	.487±.002	.489	.996±.004	.39
	3000	I.D.		.952		.30
		A1	.755±.021	.736	1.026±.029	.38
		A2	.640±.009	.618	1.036±.015	.43
		H	.620±.024	.604	1.026±.040	.44
		K	.557±.013	.556	1.002±.023	.47
		L	.511±.004	.510	1.002±.008	.50
		B	.521±.002	.507	1.028±.004	.50
		M	.465±.002	.471	.987±.004	.53
	2000	I.D.		.795		.40
		A1	.710±.022	.659	1.077±.033	.48
		A2	.607±.008	.574	1.057±.014	.53
		H	.584±.026	.563	1.037±.046	.54
		K	.550±.011	.526	1.046±.021	.57
		L	.500±.0046	.489	1.022±.009	.60
		B	.512±.003	.487	1.051±.006	.59
		M	.466±.0026	.458	1.017±.006	.62
	1000	I.D.		.591		.60
		A1	.528±.040	.530	.996±.075	.65
		A2	.509±.014	.485	1.049±.029	.69
		H	.484±.030	.479	1.010±.063	.70
		K	.494±.016	.458	1.079±.035	.72
		L	.458±.005	.435	1.053±.011	.74
		B	.464±.005	.433	1.072±.012	.74
		M	.434±.003	.414	1.048±.007	.76
	500	I.D.		.382		.84
		A1	.383±.053	.365	1.049±.145	.86
		A2	.375±.018	.351	1.068±.051	.88
		H	.479±.049	.350	1.369±.140	.89
		K	.361±.020	.342	1.056±.058	.90
		L	.349±.0084	.333	1.048±.025	.90

Table 2 (continued)

Isotope	Core	Sample	Exp.	Calc.	E/C	Response above 1 keV (rel.)
La-139	4000	I.D.		.095		.18
		M	.047±.003	.042	1.12±.07	.34
		L	.044±.003	.041	1.07±.07	.35
		N	.046±.001	.038	1.21±.03	.37
	3000	I.D.		.075		.30
		M	.042±.003	.038	1.11±.08	.50
		L	.042±.004	.037	1.14±.11	.50
		N	.041±.001	.035	1.17±.03	.52
	2000	I.D.		.061		.41
		M	.0450±.0038	.036	1.25±.11	.61
		L	.0372±.0036	.035	1.06±.10	.61
		N	.0376±.0008	.034	1.11±.02	.63
	1000	I.D.		.042		.65
		M	.0409±.0040	.031	1.32±.13	.77
		L	.0321±.0067	.031	1.04±.22	.77
		N	.0324±.0014	.030	1.08±.05	.78
	500	I.D.		.027		.89
		L	.0056±.0090	.024	.16±.38	.92
		N	.0184±.0022	.023	.80±.10	.92

Table 2 (continued)

Isotope	Core	Sample	Exp.	Calc.	E/C	Response above 1 keV (rel.)
Ce-140	4000	I.D.		.0076		.95
		M	.0053±.0020	.0068	.78±.29	.95
		N	.0043±.0010	.0067	.64±.15	.95
	3000	I.D.		.0101		.99
		M	.0033±.0014	.0091	.36±.15	.98
		N	.0040±.0006	.0089	.45±.07	.98
	2000	I.D.		.0118		.99
		M	-.0006±.0017	.0107	-.06±.16	.99
		N	+.0017±.0006	.0106	.16±.06	.99
	1000	I.D.		.0143		1.00
		M	-.0011±.0040	.0131	-.08±.31	1.00
		N	-.0011±.0014	.0129	-.09±.11	1.00
	500	I.D.		.0164		1.00
		N	-.0064±.0014	.0153	-.42±.09	1.00
Ce-142	4000	I.D.		.0206		.96
		O	.010 ±.006	.0171	.58±.35	.95
		L	.014 ±.003	.0167	.84±.18	.95
	3000	I.D.		.0264		.98
		O	.0125±.0065	.0222	.56±.29	.98
		L	.0119±.0032	.0217	.55±.15	.98
	2000	I.D.		.0299		.99
		O	.010±.007	.0254	.39±.28	.99
		L	.016±.004	.0248	.65±.16	.99
	1000	I.D		.0334		.99
		O	-.013±.011	.0290	-.45±.38	.99
		L	-.001±.006	.0284	-.04±.21	.99
	500	I.D.		.0328		1.00
		L	-.010±.008	.0294	-.34±.27	1.00

Table 2 (continued)

Isotope	Core	Sample	Exp.	Calc.	E/C	Response above 1 keV (rel.)
Pr-141	4000	I.D.		.251		.21
		L	.117±.004	.124	.944±.032	.35
		M1	.112±.003	.118	.949±.025	.36
		M2	.110±.002	.119	.924±.017	.36
		N	.105±.001	.113	.929±.009	.37
	3000	I.D.		.254		.27
		L	.119±.0044	.129	.922±.034	.44
		M1	.117±.002	.123	.951±.016	.45
		M2	.115±.002	.124	.927±.016	.45
		N	.106±.001	.119	.891±.008	.46
	2000	I.D.		.237		.33
		L	.122±.004	.127	.961±.031	.51
		M1	.117±.003	.121	.967±.025	.53
		M2	.110±.0037	.122	.902±.030	.52
		N	.103±.001	.117	.880±.009	.54
	1000	I.D.		.183		.46
		L	.105±.004	.110	.955±.036	.66
		M1	.096±.005	.106	.906±.047	.67
		M2	.091±.003	.107	.850±.028	.66
		N	.095±.002	.103	.922±.019	.68
	500	I.D.		.103		.72
		L	.075±.011	.077	.974±.143	.86
		M1	.067±.006	.076	.882±.079	.86
		M2	.0654±.0065	.076	.861±.086	.86
		N	.0654±.0020	.074	.884±.027	.87
Nd-142	4000	I.D.		.0640		.38
		O	.024±.014	.0623	.38±.22	.37
		L	.046±.012	.0620	.73±.19	.37
		M	.036±.007	.0615	.58±.11	.37
	3000	I.D.		.0593		.54
		O	.045±.019	.0574	.79±.33	.53
		L	.022±.015	.0570	.39±.26	.53
		M	.026±.006	.0565	.46±.11	.53
	2000	I.D.		.0573		.64
		O	.012±.017	.0554	.22±.31	.64
		L	.024±.014	.0550	.44±.25	.64
		M	.016±.007	.0545	.29±.13	.63
	1000	I.D.		.0526		.79
		O	-.033±.034	.0508	-.64±.67	.79
		L	-.004±.015	.0505	-.07±.30	.79
		M	+.017±.010	.0500	+.34±.20	.79
	500	I.D.		.0443		.94
		M	.015±.014	.0425	.35±.33	.93

Table 2 (continued)

Isotope	Core	Sample	Exp.	Calc.	E/C	Response above 1 keV (rel.)
Nd-143	4000	I.D.		.804		.17
		H	.467±.039	.472	.989±.083	.25
		L	.375±.005	.387	.969±.013	.28
	3000	I.D.		.687		.25
		H	.424±.039	.413	1.027±.094	.38
		L	.319±.004	.337	.947±.012	.43
	2000	I.D.		.590		.33
		H	.365±.039	.375	.973±.104	.47
		L	.305±.006	.312	.978±.019	.53
	1000	I.D.		.414		.51
		H	.245±.057	.301	.81±.19	.65
		L	.261±.010	.262	.996±.038	.70
	500	I.D.		.240		.81
		H	.223±.094	.210	1.06±.45	.88
		L	.157±.012	.195	.805±.062	.90
Nd-144	4000	I.D.		.103		.34
		O	.105±.016	.086	1.22±.19	.36
		L	.094±.009	.084	1.12±.11	.37
		M	.079±.005	.081	.975±.06	.37
	3000	I.D.		.105		.44
		O	.086±.016	.087	.99±.18	.47
		L	.075±.009	.085	.88±.11	.48
		M	.076±.004	.082	.93±.05	.48
	2000	I.D.		.102		.52
		O	.069±.021	.085	.81±.25	.56
		L	.083±.010	.083	1.00±.12	.56
		M	.071±.005	.080	.89±.06	.57
	1000	I.D.		.090		.66
		O	.071±.023	.076	.93±.30	.71
		L	.059±.021	.075	.79±.28	.71
		M	.064±.008	.072	.89±.11	.72
	500	I.D.		.067		.86
		M	.033±.009	.059	.56±.15	.90

Table 2 (continued)

Isotope	Core	Sample	Exp.	Calc.	E/C	Response above 1 keV (rel.)
Nd-145	4000	I.D.		1.104		.21
		S	.781±.066	.669	1.167±.099	.32
		K	.611±.014	.576	1.061±.024	.35
		O	.571±.009	.551	1.036±.016	.36
	3000	I.D.		.873		.34
		S	.588±.076	.609	.966±.125	.45
		K	.573±.016	.540	1.061±.030	.48
		O	.543±.009	.520	1.044±.017	.49
	2000	I.D.		.749		.44
		S	.624±.071	.568	1.10 ±.13	.54
		K	.537±.019	.512	1.049±.037	.58
		O	.512±.011	.495	1.034±.022	.59
	1000	I.D.		.574		.62
		S	.502±.094	.482	1.04 ±.20	.70
		K	.479±.030	.446	1.074±.067	.73
		O	.441±.015	.435	1.014±.034	.73
	500	I.D.		.375		.84
		S	.427±.100	.345	1.24 ±.29	.88
		K	.292±.030	.330	.885±.091	.89
		O	.258±.022	.325	.794±.068	.90
Nd-146	4000	I.D.		.099		.43
		K	.078±.013	.080	.98 ±.16	.46
		L	.074±.006	.076	.974±.079	.47
	3000	I.D.		.106		.53
		K	.085±.015	.086	.99 ±.17	.58
		L	.074±.006	.082	.902±.073	.59
	2000	I.D.		.106		.61
		K	.070±.014	.088	.80 ±.16	.66
		L	.072±.006	.084	.857±.071	.67
	1000	I.D.		.099		.74
		K	.040±.036	.085	.47 ±.42	.79
		L	.061±.010	.082	.74 ±.12	.80
	500	I.D.		.081		.90
		L	.055±.013	.072	.76 ±.18	.93

Table 2 (continued)

Isotope	Core	Sample	Exp.	Calc.	E/C	Response above 1 keV (rel.)
Nd-148	4000	I.D.		.311		.19
		T	.120±.042	.189	.63 ±.22	.27
		K	.161±.017	.179	.889±.095	.28
		L	.129±.006	.164	.787±.037	.30
	3000	I.D.		.293		.26
		T	.133±.036	.184	.72 ±.20	.37
		K	.135±.018	.175	.77 ±.10	.38
		L	.134±.006	.161	.832±.037	.40
	2000	I.D.		.261		.34
		T	.156±.037	.172	.91 ±.22	.46
		K	.120±.018	.163	.74 ±.11	.47
		L	.118±.007	.152	.776±.046	.49
	1000	I.D.		.191		.51
		T	.129±.072	.140	.92 ±.51	.64
		K	.093±.034	.135	.69 ±.25	.65
		L	.107±.009	.127	.843±.071	.67
	500	I.D.		.116		.81
		L	.092±.014	.096	.96 ±.15	.89
Nd-150	4000	I.D.		.241		.28
		S	.181±.055	.147	1.23 ±.37	.40
		T	.124±.025	.130	.95 ±.19	.42
		K	.115±.012	.123	.935±.098	.43
		O	.127±.007	.118	1.076±.059	.44
	3000	I.D.		.232		.39
		S	.148±.069	.150	.99 ±.46	.51
		T	.120±.020	.135	.89 ±.15	.54
		K	.129±.011	.129	1.000±.085	.55
		O	.120±.007	.124	.968±.056	.56
	2000	I.D.		.215		.47
		S	.266±.051	.146	1.82 ±.35	.60
		T	.117±.023	.133	.88 ±.17	.63
		K	.138±.013	.128	1.08 ±.10	.64
		O	.126±.010	.124	1.016±.081	.65
	1000	I.D.		.176		.63
		S	.174±.080	.132	1.32 ±.61	.75
		T	.106±.040	.123	.86 ±.33	.77
		K	.095±.016	.120	.79 ±.13	.77
		O	.097±.008	.117	.829±.068	.78
	500	I.D.		.122		.85
		T	.119±.040	.101	1.18 ±.40	.92
		K	.109±.020	.100	1.09 ±.20	.92
		O	.063±.014	.098	.64 ±.14	.92

Table 2 (continued)

Isotope	Core	Sample	Exp.	Calc.	E/C	Response above 1 keV (rel.)
Nd-nat.*)	4000	I.D.		.324		.23
		H	.259±.033	.280	.925±.118	.26
		L1	.270±.008	.265	1.019±.030	.27
		M1	.250±.005	.260	.962±.019	.28
		L	.259±.007	.258	1.004±.027	.28
		N1	.225±.001	.239	.941±.005	.29
	3000	I.D.		.284		.34
		H	.267±.048	.252	1.06 ±.19	.38
		L	.215±.007	.235	.915±.030	.40
		N1	.201±.001	.221	.910±.005	.42
	2000	I.D.		.254		.44
		H	.190±.040	.230	.83 ±.17	.47
		L1	.209±.008	.221	.946±.036	.49
		M1	.202±.006	.218	.927±.028	.49
		L	.201±.009	.217	.926±.041	.49
		N1	.188±.001	.205	.917±.005	.51
	1000	I.D.		.199		.61
		H	.188±.093	.186	1.01 ±.50	.64
		L1	.160±.013	.181	.884±.072	.66
		M1	.160±.006	.180	.889±.033	.66
		L	.150±.012	.179	.838±.067	.66
		N1	.156±.003	.172	.907±.017	.68
	500	I.D.		.134		.85
		L1	.113±.021	.129	.876±.163	.87
		M1	.079±.010	.128	.617±.078	.87
		N1	.095±.003	.126	.754±.024	.88

*) The subscripted sample identifications L1, M1 and N1 refer to samples containing natural Nd_2O_3; the nonsubscripted identifications H and L refer to samples containing natural Nd. The reactivity worths of L1, M1 and N1 are given per gram Nd.

Table 2 (continued)

Isotope	Core	Sample	Exp.	Calc.	E/C	Response above 1 keV (rel.)
Pm-147	4000	I.D.		4.596		.13
		T	2.505±.04	2.520	.994±.016	.23
		K	2.335±.02	2.371	.985±.008	.25
		O	2.225±.01	2.227	.999±.004	.26
	3000	I.D.		3.034		.26
		T	2.142±.04	2.078	1.031±.019	.37
		K	1.962±.022	1.989	.986±.011	.38
		O	1.922±.013	1.900	1.012±.007	.40
	2000	I.D.		2.352		.37
		T	1.868±.04	1.845	1.012±.022	.47
		K	1.818±.025	1.784	1.019±.014	.48
		O	1.794±.017	1.721	1.042±.010	.49
	1000	I.D.		1.635		.58
		T	1.41±.06	1.457	.968±.041	.63
		K	1.42±.04	1.428	.994±.028	.64
		O	1.401±.016	1.396	1.004±.011	.65
	500	I.D.		1.008		.82
		T	.896±.08	.967	.927±.083	.84
		K	.946±.05	.958	.987±.052	.85
Sm-147	4000	I.D.		4.041		.14
		H	2.076±.04	2.083	.997±.019	.26
		T	1.926±.03	1.984	.971±.015	.27
		K	1.846±.02	1.864	.990±.011	.28
	3000	I.D.		2.913		.25
		H	1.801±.055	1.823	.988±.030	.38
		T	1.764±.037	1.755	1.005±.021	.40
		K	1.648±.022	1.671	.986±.013	.41
	2000	I.D.		2.324		.35
		H	1.60±.05	1.642	.974±.030	.48
		T	1.60±.04	1.591	1.006±.025	.49
		K	1.55±.026	1.528	1.014±.017	.51
	1000	I.D.		1.601		.56
		H	1.242±.06	1.321	.940±.045	.65
		T	1.202±.055	1.294	.929±.043	.66
		K	1.302±.027	1.259	1.034±.021	.67

Table 2 (continued)

Isotope	Core	Sample	Exp.	Calc.	E/C	Response above 1 keV (rel.)
Sm-148	4000	I.D.		.638		.25
		S	.456±.050	.401	1.14±.12	.36
		H	.396±.020	.381	1.04±.05	.37
		T	.356±.030	.378	.94±.08	.37
	3000	I.D.		.553		.39
		S	.375±.053	.363	1.03±.15	.53
		H	.305±.028	.347	.88±.08	.55
		T	.341±.019	.344	.99±.055	.55
	2000	I.D.		.505		.49
		S	.377±.049	.352	1.07±.14	.64
		H	.278±.027	.338	.82±.08	.65
		T	.242±.024	.335	.72±.07	.66
	1000	I.D.		.419		.67
		S	.245±.069	.330	.74±.21	.79
		H	.231±.034	.320	.72±.11	.80
		T	.230±.027	.318	.72±.085	.81
	500	I.D.		.324		.89
		S	.076±.110	.294	.26±.37	.94
		H	.146±.045	.290	.50±.16	.94
		T	.206±.040	.289	.71±.14	.94
Sm-149	4000	I.D.		9.382		.11
		P	4.144±.07	4.215	.983±.017	.23
		S	3.844±.04	3.895	.987±.010	.25
		H	3.554±.02	3.660	.971±.005	.26
		K	3.056±.006	3.277	.933±.002	.29
	3000	I.D.		5.370		.24
		P	3.505±.073	3.427	1.023±.021	.37
		S	3.330±.052	3.233	1.030±.016	.39
		H	3.123±.024	3.084	1.013±.008	.41
		K	2.797±.010	2.831	.988±.004	.43
	2000	I.D.		4.159		.35
		P	3.233±.072	3.047	1.061±.024	.47
		S	3.026±.047	2.911	1.040±.016	.49
		H	2.902±.030	2.803	1.035±.011	.50
		K	2.665±.011	2.615	1.019±.004	.53
	1000	I.D.		2.840		.56
		P	2.714±.13	2.414	1.124±.054	.64
		S	2.464±.06	2.346	1.050±.026	.66
		H	2.394±.03	2.290	1.045±.013	.67
		K	2.274±.01	2.187	1.040±.005	.69
	500	I.D.		1.697		.82
		P	1.82 ±.16	1.605	1.134±.100	.85
		S	1.58 ±.07	1.585	.997±.044	.86
		H	1.69 ±.05	1.567	1.078±.032	.86
		K	1.642±.020	1.533	1.071±.013	.87

Table 2 (continued)

Isotope	Core	Sample	Exp.	Calc.	E/C	Response above 1 keV (rel.)
Sm-150	4000	I.D.		1.669		.11
		S	.740±.091	.775	.955±.117	.22
		T	.701±.066	.716	.979±.092	.23
		H	.694±.044	.711	.976±.062	.23
		K	.687±.020	.654	1.050±.031	.25
		O	.620±.016	.625	.992±.026	.25
	3000	I.D.		1.016		.24
		S	.642±.089	.588	1.09 ±.15	.38
		T	.537±.047	.552	.973±.085	.40
		H	.603±.055	.549	1.10 ±.10	.40
		K	.560±.022	.513	1.092±.043	.42
		O	.532±.015	.494	1.077±.030	.43
	2000	I.D.		.760		.36
		S	.61 ±.12	.513	1.19 ±.23	.50
		T	.53 ±.055	.486	1.09 ±.11	.52
		H	.54 ±.06	.485	1.11 ±.12	.52
		K	.53 ±.025	.458	1.157±.055	.54
		O	.50 ±.02	.444	1.126±.045	.55
	1000	I.D.		.519		.59
		S	.354±.160	.420	.84 ±.38	.69
		T	.433±.080	.405	1.07 ±.20	.70
		H	.450±.080	.404	1.11 ±.20	.70
		K	.422±.025	.388	1.088±.064	.72
		O	.450±.023	.380	1.184±.061	.73
	500	I.D.		.351		.84
		T	.32 ±.11	.317	1.01 ±.35	.90
		K	.33 ±.05	.310	1.06 ±.16	.90
		O	.337±.032	.307	1.10 ±.10	.91
Sm-151	4000	I.D.		3.744		.12
		S	2.124±.050	2.334	.910±.021	.19
		T	2.004±.030	2.209	.907±.014	.20
		O	1.804±.010	1.977	.912±.005	.22
		G	2.054±.030	2.180	.942±.014	.20
		F	1.974±.030	2.062	.957±.015	.21
		E	1.754±.010	1.957	.896±.005	.22
	3000	I.D.		2.371		.24
		S	1.631±.050	1.751	.931±.029	.32
		T	1.581±.030	1.684	.939±.018	.33
		O	1.441±.010	1.552	.928±.006	.36
		G	1.631±.040	1.667	.978±.024	.34
		F	1.551±.030	1.601	.969±.019	.35
		E	1.401±.010	1.540	.910±.006	.36

Table 2 (continued)

Isotope	Core	Sample	Exp.	Calc.	E/C	Response above 1 keV (rel.)
Sm-151	2000	I.D.		1.817		.36
		S	1.352±.060	1.483	.912±.040	.43
		T	1.307±.030	1.439	.908±.021	.44
		O	1.281±.010	1.350	.949±.007	.46
		G	1.322±.040	1.428	.926±.028	.44
		F	1.307±.030	1.384	.944±.022	.45
		E	1.247±.010	1.342	.929±.007	.46
	1000	I.D.		1.239		.57
		S	1.051±.076	1.124	.935±.068	.61
		T	1.113±.045	1.104	1.008±.041	.62
		O	1.021±.013	1.061	.962±.012	.64
		G	1.019±.050	1.099	.927±.045	.62
		F	.949±.041	1.078	.880±.038	.63
		E	.941±.014	1.057	.890±.013	.64
	500	I.D.		.765		.82
		S	.883±.130	.738	1.20 ±.18	.84
		T	.593±.055	.733	.809±.075	.85
		O	.678±.034	.719	.943±.047	.85
Sm-152	4000	I.D.		4.574		.04
		P	.985±.090	.962	1.024±.094	.17
		S	.845±.040	.851	.993±.047	.19
		T	.725±.040	.747	.971±.054	.20
		K	.675±.010	.667	1.012±.015	.22
	3000	I.D.		1.897		.12
		P	.702±.100	.621	1.13 ±.16	.35
		S	.602±.060	.563	1.07 ±.11	.37
		T	.519±.025	.507	1.024±.049	.40
		K	.474±.010	.462	1.026±.022	.43
	2000	I.D.		1.082		.25
		P	.628±.080	.509	1.23 ±.16	.48
		S	.558±.056	.471	1.18 ±.12	.51
		T	.478±.020	.432	1.106±.046	.54
		K	.438±.010	.400	1.095±.025	.57
	1000	I.D.		.569		.52
		P	.59 ±.17	.406	1.45 ±.42	.69
		S	.411±.060	.386	1.06 ±.16	.71
		T	.392±.023	.364	1.077±.063	.73
		K	.374±.014	.345	1.084±.041	.75
	500	I.D.		.347		.82
		P	.31 ±.22	.308	1.01 ±.71	.89
		S	.36 ±.12	.300	1.20 ±.40	.90
		T	.246±.040	.291	.85 ±.14	.91
		K	.261±.024	.283	.922±.085	.92

Table 2 (continued)

Isotope	Core	Sample	Exp.	Calc.	E/C	Response above 1 keV (rel.)
Sm-154	4000	I.D.		.494		.20
		H	.239±.026	.230	1.04 ±.11	.36
		T	.222±.021	.228	.974±.092	.36
	3000	I.D.		.414		.31
		H	.206±.028	.214	.96 ±.13	.51
		T	.208±.018	.212	.981±.085	.51
	2000	I.D.		.355		.41
		H	.148±.030	.204	.73±.15	.61
		T	.213±.024	.202	1.05±.12	.61
	1000	I.D.		.262		.61
		H	.162±.034	.182	.89 ±.19	.76
		T	.188±.034	.181	1.04 ±.19	.76
	500	I.D.		.173		.85
		H	.192±.050	.147	1.31 ±.34	.92
		T	.162±.050	.146	1.11 ±.34	.92

Table 3. Survey of E/C values of integral capture data.

Isotope	Core	Sample aver.*)	Response above 1 keV (rel.)	E/C	Spectrum uncertainty (rel.)	Scattering effect rel.	Scattering effect abs.
Rb-87	CFRMF			.86 ±.09			
Zr-90	4000	all	.88	-.01 ±.19	.09	.8	.008
	3000	all	.92	.15 ±.15	.11	.9	.012
	2000	all	.94	.17 ±.13	.12	1.0	.015
	1000	all	.96	-.13 ±.23	.16	1.1	.020
	500	M	.99	.02 ±.35	.29	1.4	.024
Zr-91	4000	all	.45	.85 ±.07	.025	.13	.012
	3000	all	.53	.95 ±.07	.025	.17	.018
	2000	all	.59	.89 ±.06	.035	.22	.023
	1000	all	.72	.89 ±.14	.055	.32	.029
	500	L	.89	.67 ±.25	.12	.54	.035
Zr-92	4000	all	.95	.28 ±.19	.07	.6	.016
	3000	all	.97	.14 ±.11	.08	.7	.024
	2000	all	.97	.01 ±.13	.10	.8	.030
	1000	all	.99	-.00 ±.13	.13	.9	.038
	500	M	1.00	-.18 ±.26	.24	1.2	.047
Zr-93	4000	all	.28	.67 ±.04	.03	.11	.013
	3000	all	.36	.62 ±.05	.035	.16	.020
	2000	all	.44	.59 ±.06	.045	.22	.025
	1000	all	.61	.68 ±.11	.07	.35	.032
	500	all	.85	.32 ±.24	.15	.67	.039
Zr-96	4000	all	.42	.87 ±.07	.03	.27	.011
	3000	all	.50	.64 ±.08	.045	.36	.017
	2000	all	.57	.52 ±.08	.06	.46	.021
	1000	all	.71	.26 ±.14	.11	.65	.027
	500	L	.90	-.39 ±.26	.24	1.1	.032
Zr-nat.	4000	all	.63	.68 ±.04	.04	.4	.015
	3000	all	.70	.56 ±.05	.05	.5	.023
	2000	all	.75	.54 ±.05	.07	.6	.029
	1000	all	.84	.43 ±.16	.11	.7	.037
	500	all	.95	.02 ±.14	.23	1.1	.045

*) Average over samples with about the same response, cf. text.

Table 3 (continued)

Isotope	Core	Sample aver.*)	Response above 1 keV (rel.)	E/C	Spectrum uncertainty (rel.)	Scattering effect rel.	Scattering effect abs.
Mo-92	4000	all	.71	.86 ±.24	.03	.27	.017
	3000	all	.80	.86 ±.24	.035	.34	.025
	2000	all	.86	.83 ±.27	.045	.39	.032
	1000	all	.93	1.11 ±.21	.065	.45	.040
	500	K	.98	.38 ±.45	.12	.53	.047
Mo-94	4000	all	.64	.50 ±.20	.02	.17	.016
	3000	all	.79	.94 ±.21	.02	.23	.024
	2000	all	.86	.83 ±.18	.025	.28	.031
	1000	all	.94	.69 ±.17	.04	.34	.040
	500	T	.98	1.18 ±.42	.075	.42	.049
Mo-95	4000	all	.44	.909±.009	.03	.05	.028
	3000	all	.60	.897±.013	.03	.08	.042
	2000	all	.70	.892±.016	.03	.11	.055
	1000	all	.83	.893±.014	.035	.15	.072
	500	H,K	.94	.952±.080	.065	.23	.092
	PHENIX		.89	.956±.024			
Mo-96	4000	all	.42	.71 ±.09	.025	.12	.016
	3000	P,H	.56	.55 ±.12	.025	.18	.025
	2000	all	.66	.75 ±.10	.03	.23	.032
	1000	all	.82	.47 ±.15	.04	.31	.040
	500	S,H	.96	.66 ±.24	.08	.43	.049
	PHENIX		.92	.848±.16			
Mo-97	4000	all	.60	.925±.013	.03	.065	.029
	3000	all	.68	.887±.013	.025	.09	.044
	2000	all	.74	.902±.013	.025	.11	.057
	1000	all	.83	.881±.012	.04	.14	.074
	500	all	.93	.899±.030	.07	.23	.094
	PHENIX		.90	1.057±.034			
Mo-98	4000	all	.52	.79 ±.03	.025	.22	.024
	3000	all	.61	.74 ±.025	.035	.30	.036
	2000	all	.67	.71 ±.03	.045	.36	.046
	1000	all	.78	.54 ±.03	.075	.48	.062
	500	O	.92	.43 ±.07	.16	.74	.080
	CFRMF		.74	.82 ±.05			
	RONA		.73	.731±.035			
	ZONA		.81	.812±.039			
Mo-100	4000	all	.62	.88 ±.05	.025	.30	.029
	3000	all	.71	.84 ±.05	.04	.39	.044
	2000	all	.77	.88 ±.05	.055	.48	.056
	1000	all	.86	.78 ±.06	.09	.64	.073
	500	L	.95	.74 ±.11	.21	1.00	.093
	CFRMF		.85	1.12 ±.19			
	ZONA		.89	1.076±.057			

*) Average over samples with about the same response, cf. text.

Table 3 (continued)

Isotope	Core	Sample aver.*)	Response above 1 keV (rel.)	E/C	Spectrum uncertainty(rel.)	Scattering effect rel.	Scattering effect abs.
Mo-nat.	4000	1 mm	.34	.922±.032	.03	.065	.023
	4000	2,3,4 mm	.40	.946±.008	.025	.08	.023
	3000	1 mm	.48	.976±.031	.03	.10	.034
	3000	2,3,4 mm	.53	.922±.008	.025	.12	.034
	2000	all	.61	.926±.009	.03	.15	.044
	1000	all	.76	.923±.022	.045	.22	.057
	500	all	.91	.785±.027	.085	.35	.071
Tc-99	4000	all	.42	.996±.008	.03	.025	.026
	3000	all	.57	1.015±.008	.03	.04	.040
	2000	all	.66	1.049±.010	.03	.05	.052
	1000	all	.79	1.051±.012	.035	.07	.068
	500	all	.93	1.076±.033	.05	.11	.086
	CFRMF		.82	.80 ±.12			
Ru-101	4000	all	.59	1.059±.011	.03	.03	.027
	3000	all	.71	1.014±.012	.03	.045	.042
	2000	all	.78	.996±.013	.025	.055	.054
	1000	all	.87	.948±.020	.03	.075	.072
	500	all	.96	.911±.022	.05	.11	.094
	PHENIX		.93	.885±.030			
Ru-102	4000	all	.83	.92 ±.08	.03	.11	.017
	3000	all	.89	.74 ±.08	.025	.13	.026
	2000	all	.92	.81 ±.06	.025	.16	.034
	1000	all	.96	.67 ±.08	.03	.19	.044
	500	all	.99	.51 ±.15	.055	.25	.055
	CFRMF		.98	.89 ±.06			
	RONA		.97	.942±.043			
Ru-104	4000	all	.70	.87 ±.08	.03	.095	.013
	3000	all	.76	.74 ±.09	.025	.12	.020
	2000	all	.80	.70 ±.07	.025	.14	.026
	1000	all	.88	.64 ±.11	.03	.18	.034
	500	all	.96	.72 ±.15	.06	.27	.042
	CFRMF		.84	.96 ±.06			
	RONA		.85	1.050±.046			
	ZONA		.90	1.089±.048			

*) Average over samples with about the same response, cf. text.

Table 3 (continued)

Isotope	Core	Sample aver.*)	Response above 1 keV (rel.)	E/C	Spectrum uncertainty(rel.)	Scattering effect rel.	Scattering effect abs.
Rh-103	4000	1,2,3	.22	1.061±.019	.08	.015	.028
	4000	4,5	.30	1.033±.005	.065	.02	.028
	4000	6,7,8	.41	1.012±.002	.055	.025	.028
	3000	5	.54	.994±.010	.045	.04	.042
	3000	6,7,8	.61	1.003±.002	.035	.045	.042
	2000	2,3	.58	1.006±.043	.04	.045	.055
	2000	4,5	.64	1.028±.009	.035	.05	.055
	2000	6,7,8	.71	1.008±.003	.03	.06	.055
	1000	all	.80	1.009±.003	.035	.075	.072
	500	all	.92	1.009±.014	.05	.11	.092
Pd-104	4000	all	.44	.81 ±.16	.025	.06	.022
	3000	all	.54	1.02 ±.16	.025	.08	.033
	2000	all	.62	1.03 ±.17	.03	.10	.042
	1000	all	.76	1.09 ±.15	.035	.15	.054
	500	all	.92	.78 ±.41	.06	.22	.066
Pd-105	4000	all	.46	1.019±.009	.03	.025	.033
	3000	all	.58	1.022±.008	.03	.035	.050
	2000	all	.67	1.014±.009	.03	.050	.064
	1000	all	.79	1.024±.012	.035	.065	.086
	500	K,T	.93	1.012±.029	.045	.11	.111
	PHENIX		.91	1.167±.039			
Pd-106	4000	H	.68	1.09 ±.08	.025	.11	.021
	3000	H	.76	1.07 ±.08	.02	.14	.031
	2000	H	.81	1.14 ±.07	.02	.16	.040
	1000	H	.88	1.04 ±.11	.03	.20	.051
	500	H	.96	1.09 ±.16	.065	.27	.063
	PHENIX		.91	1.65 ±.11			
Pd-107	4000	all	.46	1.039±.004	.03	.03	.027
	3000	all	.59	1.017±.006	.03	.04	.041
	2000	all	.67	1.031±.005	.03	.05	.053
	1000	all	.80	1.017±.007	.035	.075	.069
	500	all	.93	.997±.011	.05	.11	.089
Pd-108	4000	all	.29	1.05 ±.07	.04	.065	.023
	3000	all	.46	1.13 ±.08	.04	.12	.034
	2000	all	.60	1.14 ±.08	.04	.17	.043
	1000	all	.80	.99 ±.12	.04	.25	.056
	500	all	.94	.86 ±.25	.08	.36	.070
	CFRMF		.66	1.10 ±.07			
	RONA		.83	1.115±.070			
	ZONA		.90	.959±.050			

*) Average over samples with about the same response, cf. text.

Table 3 (continued)

Isotope	Core	Sample aver.*)	Response above 1 keV (rel.)	E/C	Spectrum uncertainty(rel.)	Scattering effect rel.	Scattering effect abs.
Pd-110	4000	all	.54	.86 ±.39	.02	.18	.024
	3000	all	.66	.08 ±.48	.025	.26	.036
	2000	all	.74	.40 ±.43	.035	.32	.046
	1000	all	.84	1.45 ±.45	.06	.42	.059
	500	all	.94	1.09 ±1.03	.13	.61	.074
Pd-nat.	4000	all	.39	1.074±.014	.03	.04	.024
	3000	all	.52	1.079±.022	.03	.065	.036
	2000	all	.62	1.107±.018	.03	.085	.046
	1000	all	.77	1.013±.016	.035	.12	.059
	500	all	.92	1.156±.054	.055	.19	.075
Ag-107	CFRMF			1.00 ±.19			
Ag-109	4000	all	.36	.987±.015	.035	.02	.027
	3000	all	.54	.999±.022	.035	.035	.041
	2000	all	.66	1.016±.018	.03	.05	.052
	1000	all	.80	.984±.029	.03	.065	.068
	500	all	.93	.935±.056	.04	.10	.087
	CFRMF		.82	1.10 ±.11			
Sb-121	CFRMF			.93 ±.08			
Sb-123	CFRMF			1.08 ±.08			
I-127	4000	S,T,O	.36	1.050±.015	.035	.02	.010
	3000	S,T,O	.49	1.034±.015	.035	.03	.015
	2000	S,T,O	.58	1.040±.018	.04	.04	.020
	1000	S,T,O	.74	1.052±.026	.04	.06	.026
	500	S,T,O	.90	.997±.044	.06	.10	.032
	CFRMF		.75	.90 ±.09			
I-129	4000	all	.39	.926±.035	.03	.035	.010
	3000	all	.52	.958±.043	.03	.05	.014
	2000	all	.61	1.03 ±.08	.035	.065	.018
	1000	all	.76	.97 ±.08	.04	.09	.024
	500	all	.91	.98 ±.12	.06	.15	.029
	CFRMF		.83	.94 ±.06			
Xe-131	4000	RB	.11	.976±.021	.085	.03	.019
	3000	RB	.25	.955±.024	.085	.075	.028
	2000	RB	.38	.978±.035	.08	.13	.036
	1000	RB	.62	1.11 ±.07	.065	.23	.045
	500	RB	.86	1.17 ±.15	.10	.41	.055
Xe-132	CFRMF		.88	.91 ±.07			
Xe-134	CFRMF		.98	.57 ±.04			

*) Average over samples with about the same response, cf. text.

Table 3 (continued)

Isotope	Core	Sample aver.*)	Response above 1 keV (rel.)	E/C	Spectrum uncertainty(rel.)	Scattering effect rel.	Scattering effect abs.
Cs-133	4000	A1	.24	1.082±.021	.035	.02	.016
	4000	A2,H,K	.32	1.084±.008	.03	.025	.016
	4000	L,B,M	.37	1.013±.003	.03	.03	.016
	3000	A1	.38	1.026±.029	.04	.03	.024
	3000	A2,H,K	.45	1.026±.012	.035	.04	.024
	3000	L,B,M	.51	1.007±.003	.03	.05	.024
	2000	A1	.48	1.077±.033	.045	.045	.030
	2000	A2,H,K	.55	1.053±.011	.04	.055	.030
	2000	L,B,M	.60	1.032±.004	.035	.065	.030
	1000	A1	.65	.996±.075	.05	.075	.039
	1000	A2,H,K	.70	1.055±.021	.045	.08	.039
	1000	L,B,M	.75	1.054±.005	.04	.09	.039
	500	all	.89	1.059±.020	.06	.14	.049
	CFRMF		.71	.988±.065			
	PHENIX		.85	1.006±.030			
Cs-134	PHENIX		.83	1.135±.064			
La-139	4000	all	.35	1.18 ±.03	.035	.34	.013
	3000	all	.51	1.16 ±.03	.07	.55	.020
	2000	all	.62	1.11 ±.02	.10	.74	.025
	1000	all	.77	1.11 ±.05	.17	1.06	.031
	500	all	.92	.76 ±.10	.37	1.63	.038
	CFRMF		.73	.96 ±.05			
Ce-140	4000	all	.95	.67 ±.13	.15	1.1	.007
	3000	all	.98	.43 ±.06	.17	1.2	.011
	2000	all	.99	.13 ±.06	.19	1.3	.013
	1000	all	1.00	-.09 ±.10	.22	1.3	.017
	500	N	1.00	-.42 ±.09	.32	1.3	.020
	CFRMF		1.00	.061±.004			
Ce-142	4000	all	.95	.79 ±.16	.10	.8	.013
	3000	all	.98	.55 ±.13	.12	.9	.020
	2000	all	.99	.59 ±.14	.13	1.0	.025
	1000	all	.99	-.14 ±.18	.18	1.1	.032
	500	L	1.00	-.34 ±.27	.30	1.3	.039
	CFRMF		1.00	.63 ±.05			
Pr-141	4000	all	.36	.931±.007	.025	.13	.015
	3000	all	.45	.908±.006	.03	.16	.020
	2000	all	.53	.895±.008	.035	.20	.025
	1000	all	.67	.908±.014	.06	.30	.031
	500	all	.86	.885±.024	.13	.50	.038
	CFRMF		.59	.97 ±.15			
	RONA		.70	.964±.050			

*) Average over samples with about the same response, cf. text.

Table 3 (continued)

Isotope	Core	Sample aver.*)	Response above 1 keV (rel.)	E/C	Spectrum uncertainty (rel.)	Scattering effect rel.	Scattering effect abs
Nd-142	4000	all	.37	.58 ±.09	.025	.12	.008
	3000	all	.53	.48 ±.10	.03	.19	.011
	2000	all	.64	.31 ±.11	.035	.25	.014
	1000	all	.79	.16 ±.16	.055	.34	.017
	500	M	.93	.35 ±.33	.12	.47	.020
Nd-143	4000	all	.27	.969±.013	.035	.035	.015
	3000	all	.41	.948±.012	.035	.06	.021
	2000	all	.50	.978±.019	.04	.08	.027
	1000	all	.68	.989±.037	.045	.12	.033
	500	all	.89	.810±.061	.065	.19	.039
Nd-144	4000	all	.37	1.02±.05	.02	.17	.014
	3000	all	.48	.93±.05	.03	.25	.021
	2000	all	.56	.91±.05	.045	.32	.027
	1000	all	.71	.88±.10	.07	.46	.034
	500	M	.90	.56±.15	.16	.71	.041
Nd-145	4000	all	.35	1.046±.013	.03	.035	.021
	3000	all	.48	1.047±.015	.035	.06	.031
	2000	all	.58	1.039±.019	.035	.08	.039
	1000	all	.73	1.027±.030	.045	.11	.049
	500	all	.89	.841±.054	.065	.18	.058
	PHENIX		.84	.892±.029			
Nd-146	4000	all	.47	.98 ±.07	.02	.22	.017
	3000	all	.59	.92 ±.07	.03	.30	.025
	2000	all	.67	.85 ±.07	.045	.38	.032
	1000	all	.80	.72 ±.12	.07	.50	.041
	500	L	.93	.76 ±.18	.15	.71	.051
	CFRMF		.89	.97 ±.06			
	RONA		.85	.971±.047			
	ZONA		.90	1.000±.048			
Nd-148	4000	all	.29	.796±.034	.025	.12	.020
	3000	all	.39	.821±.034	.03	.18	.030
	2000	all	.48	.776±.042	.04	.24	.038
	1000	all	.66	.833±.068	.06	.38	.049
	500	L	.89	.96 ±.15	.13	.63	.061
	CFRMF		.67	.85 ±.12			
	RONA		.73	1.017±.051			
	ZONA		.83	1.000±.048			

*) Average over samples with about the same response, cf. text.

Table 3 (continued)

Isotope	Core	Sample aver.*)	Response above 1 keV (rel.)	E/C	Spectrum uncertainty (rel.)	Scattering effect rel.	Scattering effect abs.
Nd-150	4000	all	.43	1.036±.048	.02	.15	.018
	3000	all	.55	.970±.044	.025	.21	.027
	2000	all	.64	1.044±.058	.035	.27	.035
	1000	all	.77	.827±.059	.06	.37	.044
	500	T,K,O	.92	.82 ±.11	.12	.54	.054
	CFRMF		.67	.68 ±.08			
	RONA		.80	.823±.042			
	ZONA		.86	.681±.036			
Nd-nat.	4000	all	.28	.946±.005	.03	.065	.016
	3000	H,L,N_1	.40	.910±.005	.035	.11	.024
	2000	all	.49	.918±.005	.04	.15	.031
	1000	all	.66	.900±.014	.05	.22	.039
	500	L_1,M_1,N_1	.87	.745±.023	.095	.37	.047
Pm-147	4000	all	.25	.996±.003	.04	.01	.022
	3000	all	.38	1.007±.006	.045	.015	.032
	2000	all	.48	1.032±.008	.045	.02	.041
	1000	all	.64	1.001±.010	.05	.04	.054
	500	all	.85	.970±.044	.07	.07	.068
	CFRMF		.70	.81 ±.10			
Sm-147	4000	all	.27	.986±.008	.04	.01	.023
	3000	all	.40	.991±.010	.04	.02	.034
	2000	all	.49	1.005±.013	.045	.025	.043
	1000	all	.66	1.003±.017	.05	.045	.055
Sm-148	4000	all	.37	1.026±.040	.035	.035	.013
	3000	all	.55	.961±.043	.03	.055	.019
	2000	all	.65	.801±.049	.025	.07	.024
	1000	all	.80	.722±.064	.025	.10	.031
	500	all	.94	.59 ±.10	.03	.13	.038
Sm-149	4000	all	.26	.940±.002	.04	.01	.028
	3000	all	.40	.996±.003	.04	.015	.042
	2000	all	.50	1.023±.004	.045	.02	.054
	1000	all	.67	1.042±.004	.05	.03	.070
	500	all	.86	1.068±.012	.065	.055	.088
	PHENIX		.82	.998±.019			
Sm-150	4000	all	.24	1.009±.018	.045	.025	.017
	3000	all	.41	1.075±.023	.04	.05	.026
	2000	all	.53	1.133±.032	.04	.07	.033
	1000	all	.71	1.130±.042	.035	.11	.043
	500	T,K,O	.90	1.084±.082	.045	.17	.054
	PHENIX		.85	1.154±.032			

*) Average over samples with about the same response, cf. text.

Table 3 (continued)

Isotope	Core	Sample aver.*)	Response above 1 keV (rel.)	E/C	Spectrum uncertainty (rel.)	Scattering effect rel.	Scattering effect abs.
Sm-151	4000	S,T,O	.21	.911±.005	.045	.01	.021
	3000	S,T,O	.34	.929±.006	.05	.02	.032
	2000	S,T,O	.45	.944±.007	.05	.03	.041
	1000	S,T,O	.63	.965±.011	.055	.05	.053
	500	S,T,O	.85	.919±.039	.065	.09	.066
	PHENIX		.81	1.20 ±.06			
Sm-152	4000	all	.20	1.008±.014	.055	.03	.022
	3000	all	.40	1.029±.020	.045	.065	.033
	2000	all	.54	1.103±.021	.04	.10	.042
	1000	all	.73	1.083±.033	.035	.15	.055
	500	all	.91	.913±.071	.055	.24	.069
	CFRMF		.70	.92 ±.06			
	RONA		.79	1.17 ±.06			
	ZONA		.86	1.50 ±.08			
Sm-154	4000	all	.36	1.00±.07	.03	.055	.012
	3000	all	.51	.97±.07	.03	.085	.018
	2000	all	.61	.93±.09	.03	.12	.023
	1000	all	.76	.96±.13	.035	.16	.030
	500	all	.92	1.21±.24	.06	.25	.036
Eu-151	CFRMF			1.05 ±.06			
Eu-153	CFRMF			1.02 ±.07			

*) Average over samples with about the same response, cf. text.

Table 4. Admixtures in $^{93}ZrO_2$ samples.

Element	Weight (µg per gram Zr) 3)	Reactivity correction 1)
Pb	300	+
Au	400	+
W	400	+
Ta	≤ 400	-
Hf	2000	+
La	20	+
Ba	700	-
Cs	7	-
Pd	≤ 100	-
Mo-95	2000 ±2000 2)	+
Sr	50	-
Rb	20	-
Ga	30	-
Zn	200	-
Cu	1000	-
Ni	≤ 100	-
Co	10	-
Fe	30000	+

Element	Weight (µg per gram Zr)	Reactivity correction 1)
Mn	80	+
Cr	400	+
V	20	-
Ca	1000	-
K	5000	-
Cl	200	+
S	300	-
Si	20000	+
Al	5000	+
Mg	700	-
Na	2000	-
B	50	+
U-235	2000	+
U-236	500	+
Np-237	300	-
U-238	800	+
Pu-239	600	+
Pu-240	70	+

1) +: correction is applied
-: no correction applied

2) measured mass 95: < 0.4 at.%

3) sum: (0.076±0.002) gram per gram Zr

Table 5. Reactivity corrections for $^{93}ZrO_2$ samples (per gram sample mixture)

Element	Weight (g)	Reactivity effect (ρ/ρ_o)	STEK-4000	STEK-3000	STEK-2000	STEK-1000	STEK-500
O_2	.2421±.0060	total	+.0223±.0010	+.0337±.0013	+.0458±.0016	+.0639±.0026	+.0828±.0037
Admixtures	.0535±.0014	total	-.0050±.0021	-.0018±.0014	-.0002±.0012	+.0020±.0009	+.0044±.0006
Zr	.7044	scattering	+.0134	+.0200	+.0253	+.0323	+.0393

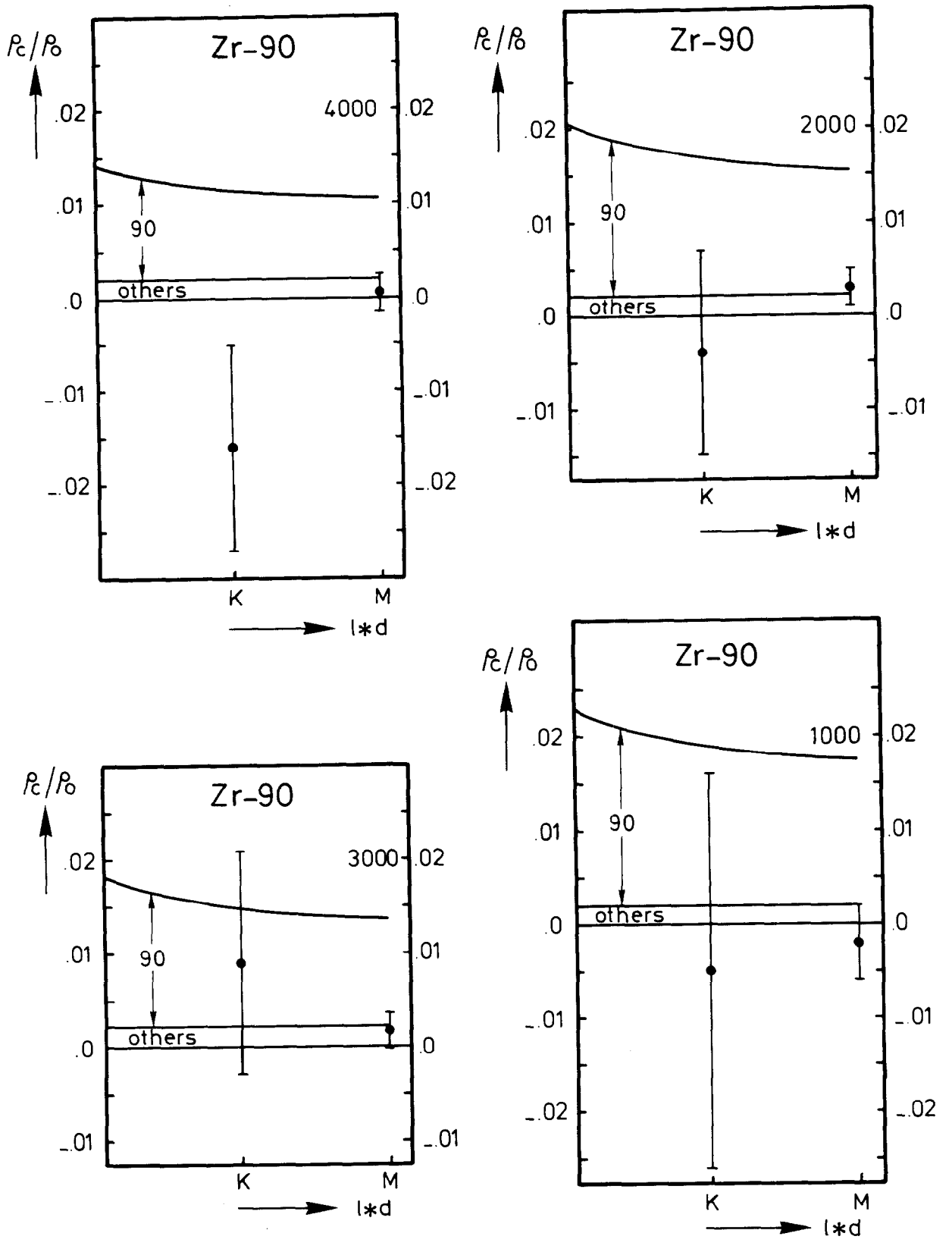

Fig. 1a
(Note to all figures: symbols are explained in Chapter 2)

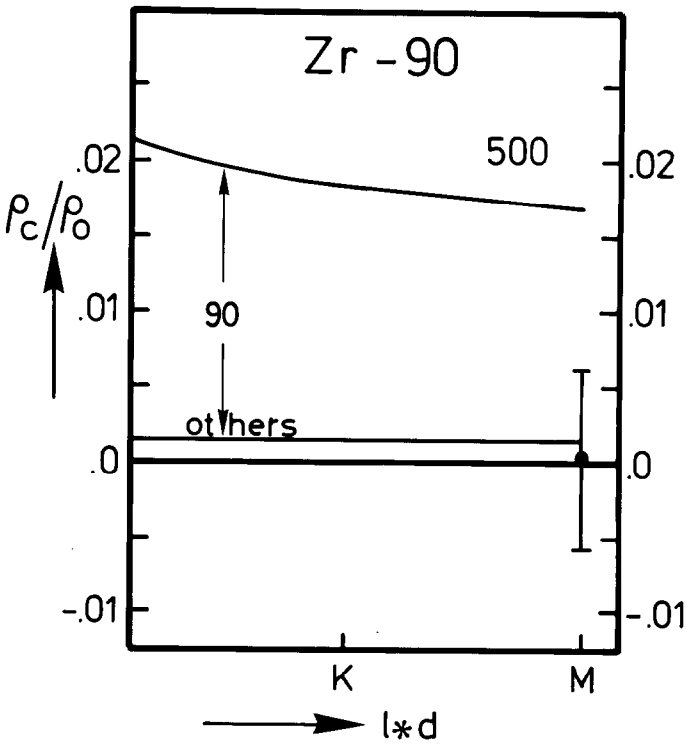

Fig. 1b

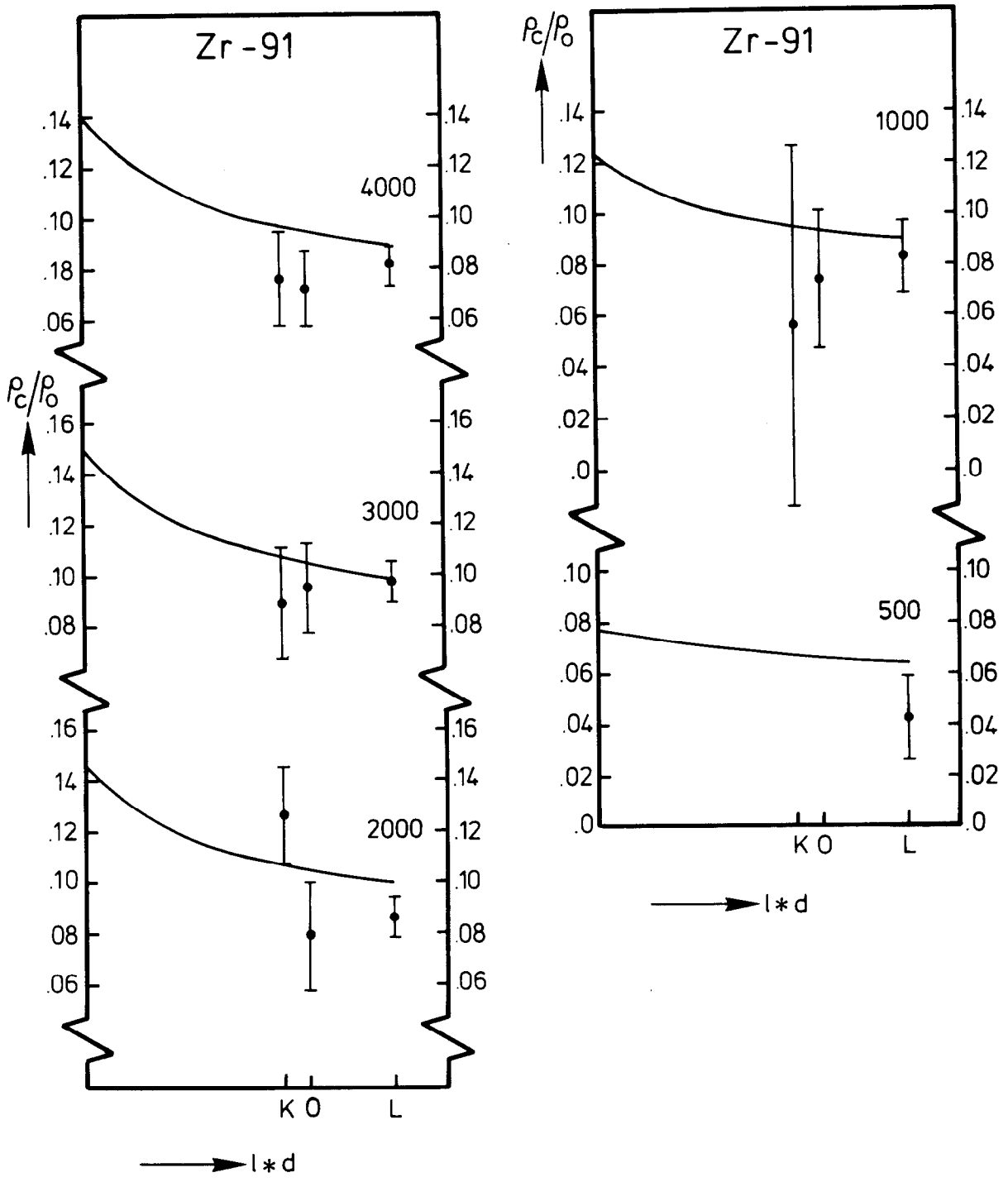
Zr-91
4000
3000
2000
ρ_c/ρ_o
K O L
l * d
Zr-91
1000
500
ρ_c/ρ_o
K O L
l * d

Fig. 2.

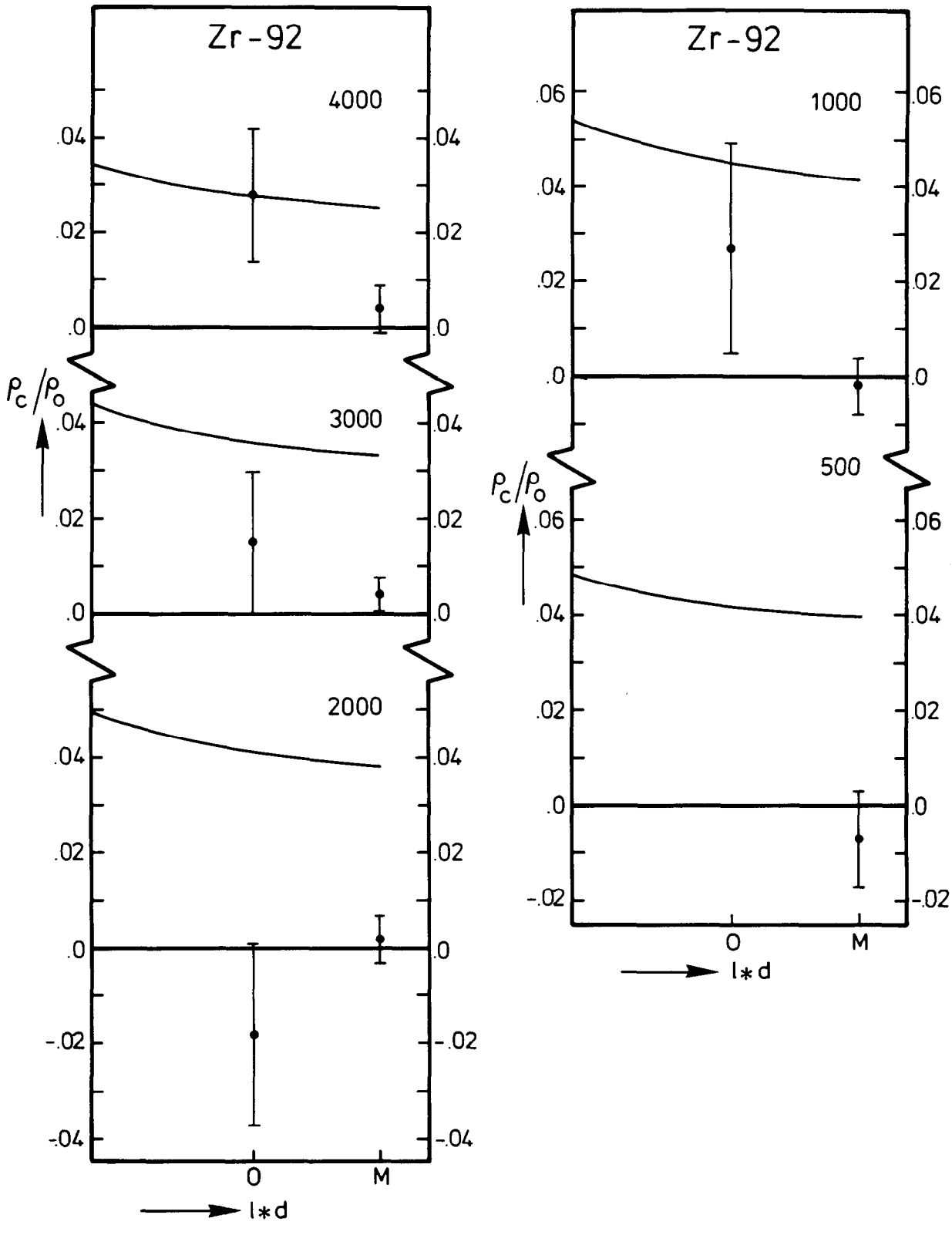
Zr-92
4000
3000
2000
ρ_c/ρ_o
.04
.02
.0
-.02
-.04
O
M
l*d
Zr-92
1000
500
ρ_c/ρ_o
.06
.04
.02
.0
-.02
O
M
l*d

Fig. 3.

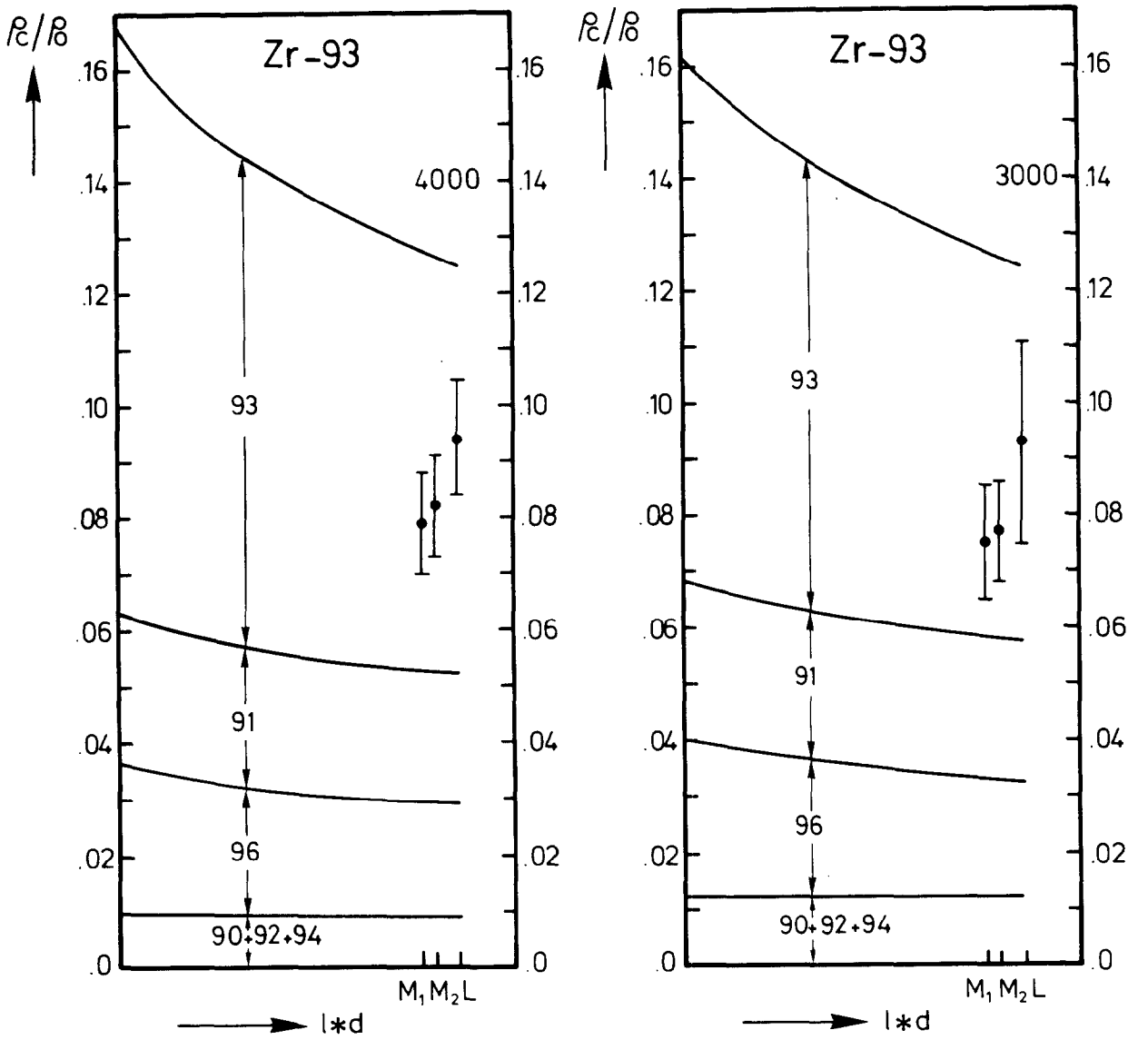
Pc/Pb
Zr-93
4000
93
91
96
90+92+94
M1 M2 L
l*d
Pc/Pb
Zr-93
3000
93
91
96
90+92+94
M1 M2 L
l*d

Fig. 4a.

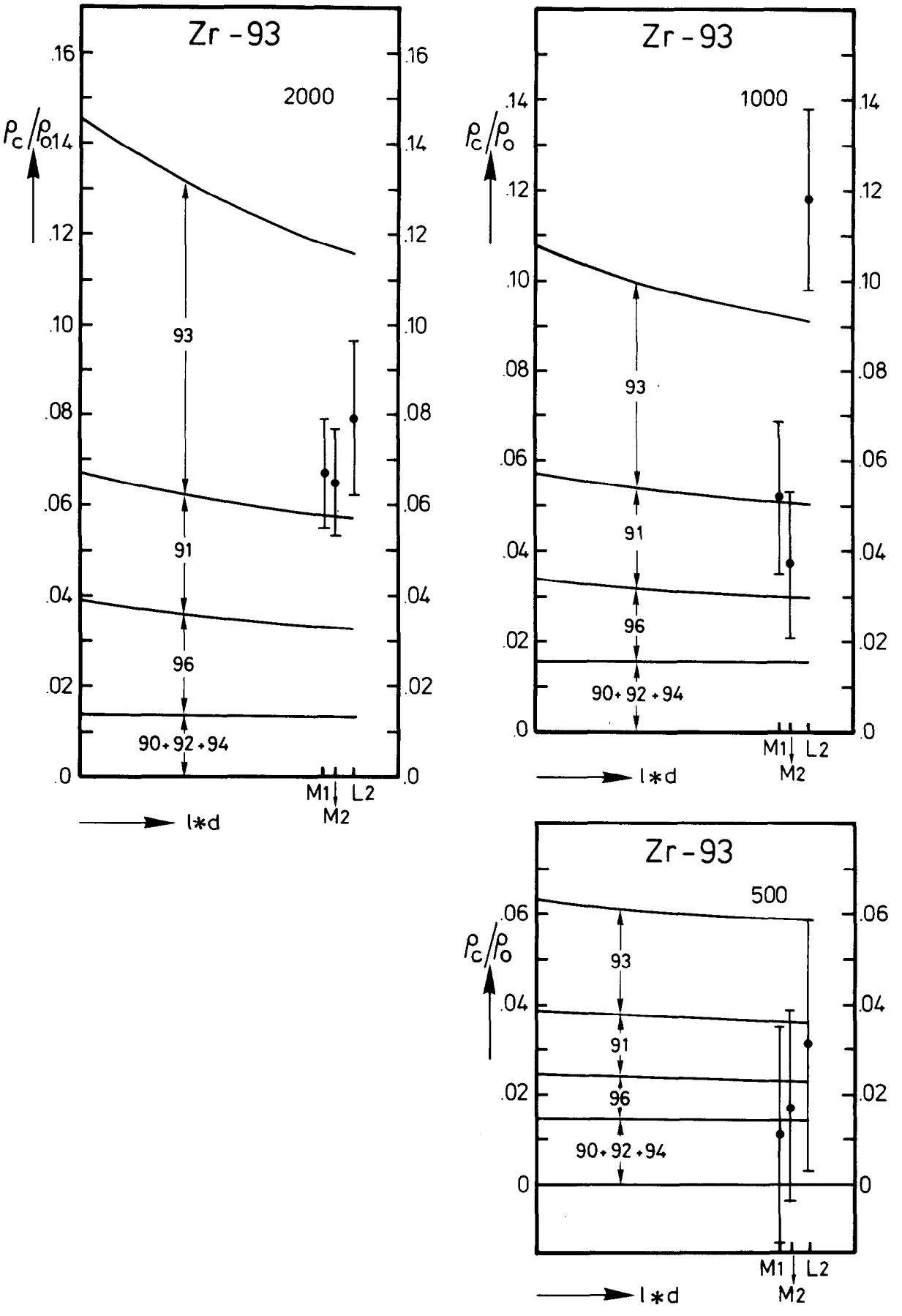
Zr -93
2000
ρ_c/ρ_o
93
91
96
90+92+94
M1
M2
L2
l*d
Zr -93
1000
ρ_c/ρ_o
93
91
96
90+92+94
M1
M2
L2
l*d
Zr -93
500
ρ_c/ρ_o
93
91
96
90+92+94
M1
M2
L2
l*d

Fig. 4b.

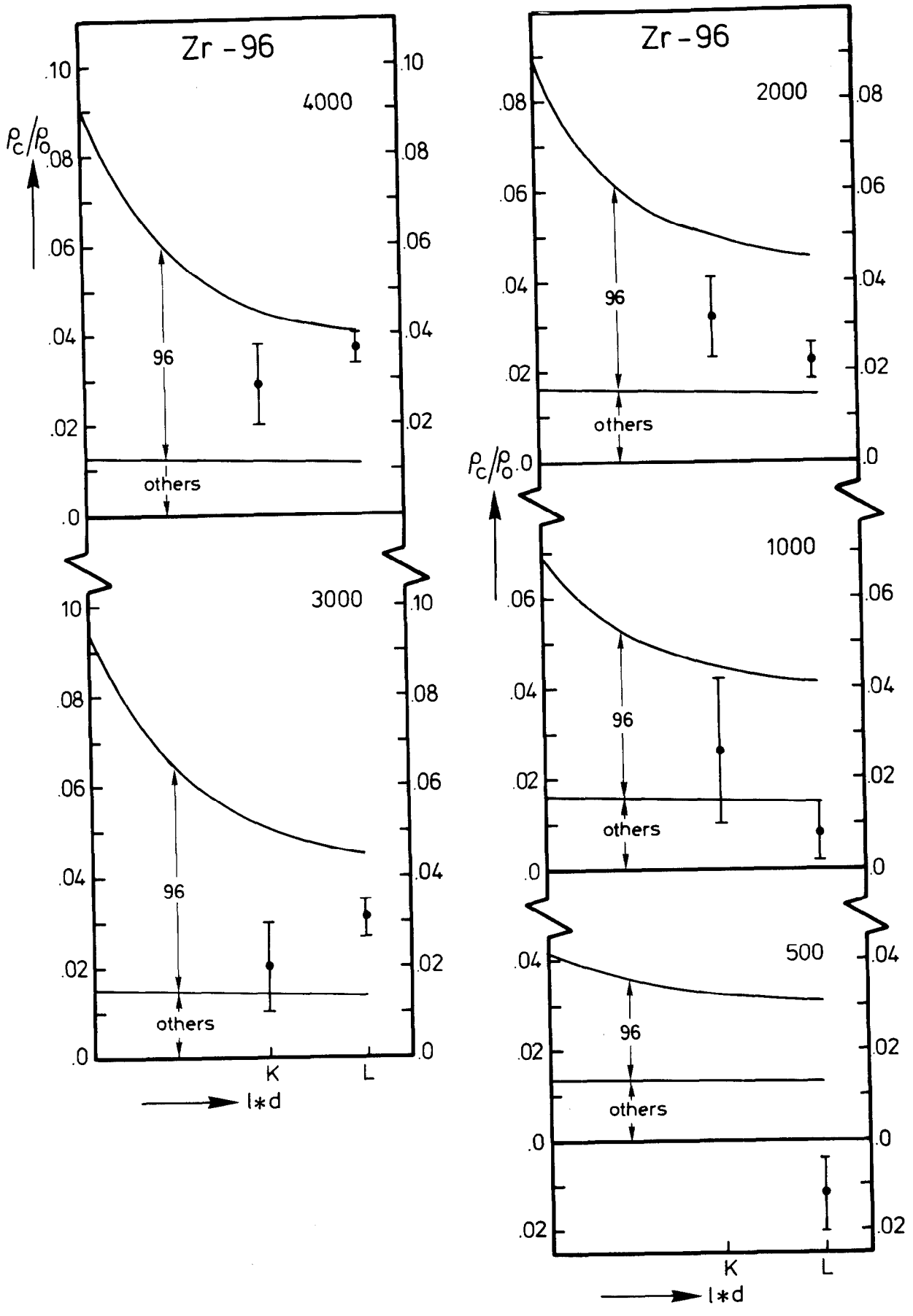

Fig. 5.

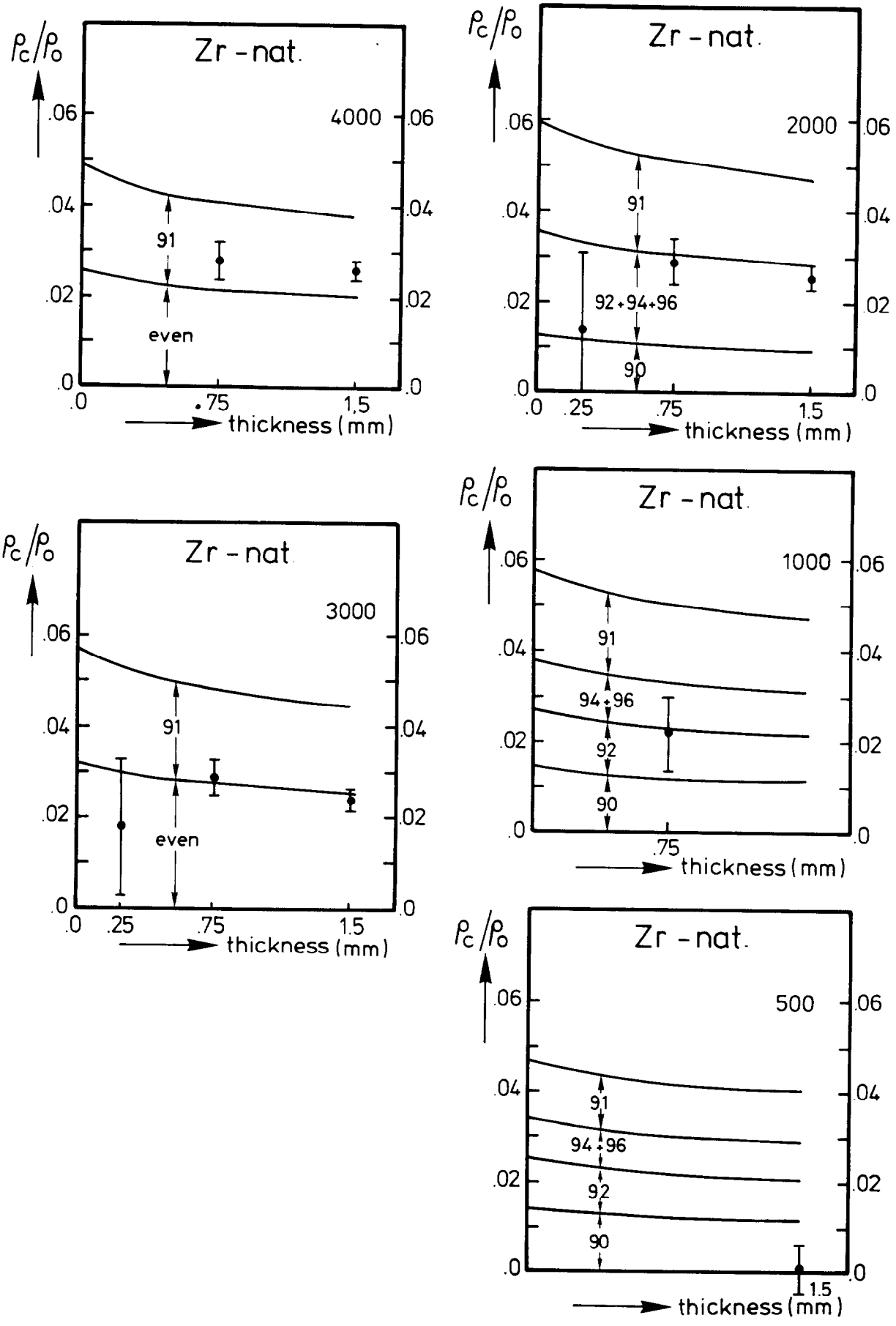
Zr - nat.
4000
91
even
thickness (mm)
Zr - nat.
2000
91
92+94+96
90
thickness (mm)
Zr - nat
3000
91
even
thickness (mm)
Zr - nat.
1000
91
94+96
92
90
thickness (mm)
Zr - nat.
500
91
94+96
92
90
1.5
thickness (mm)

Fig. 6.

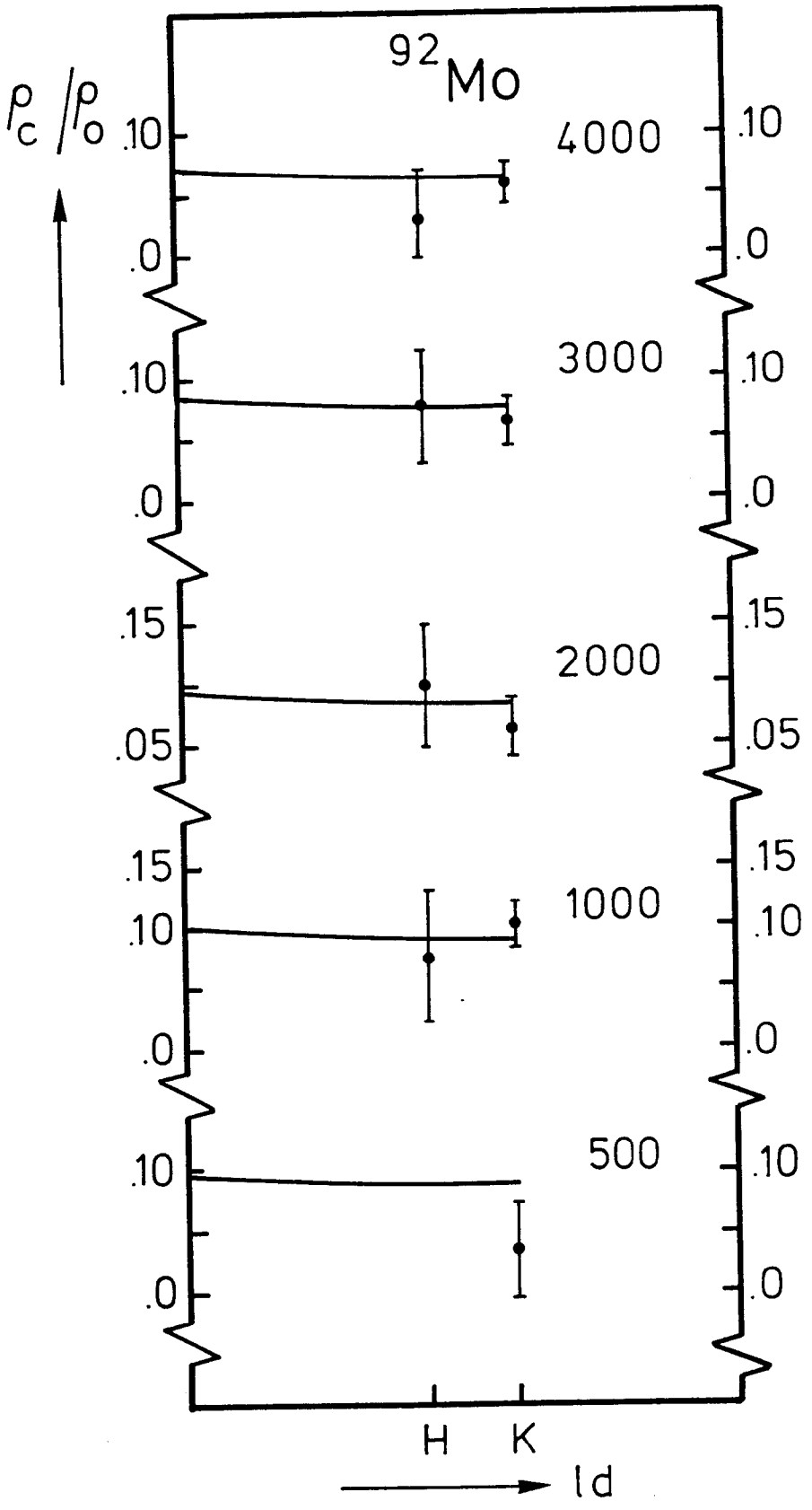

Fig. 7.

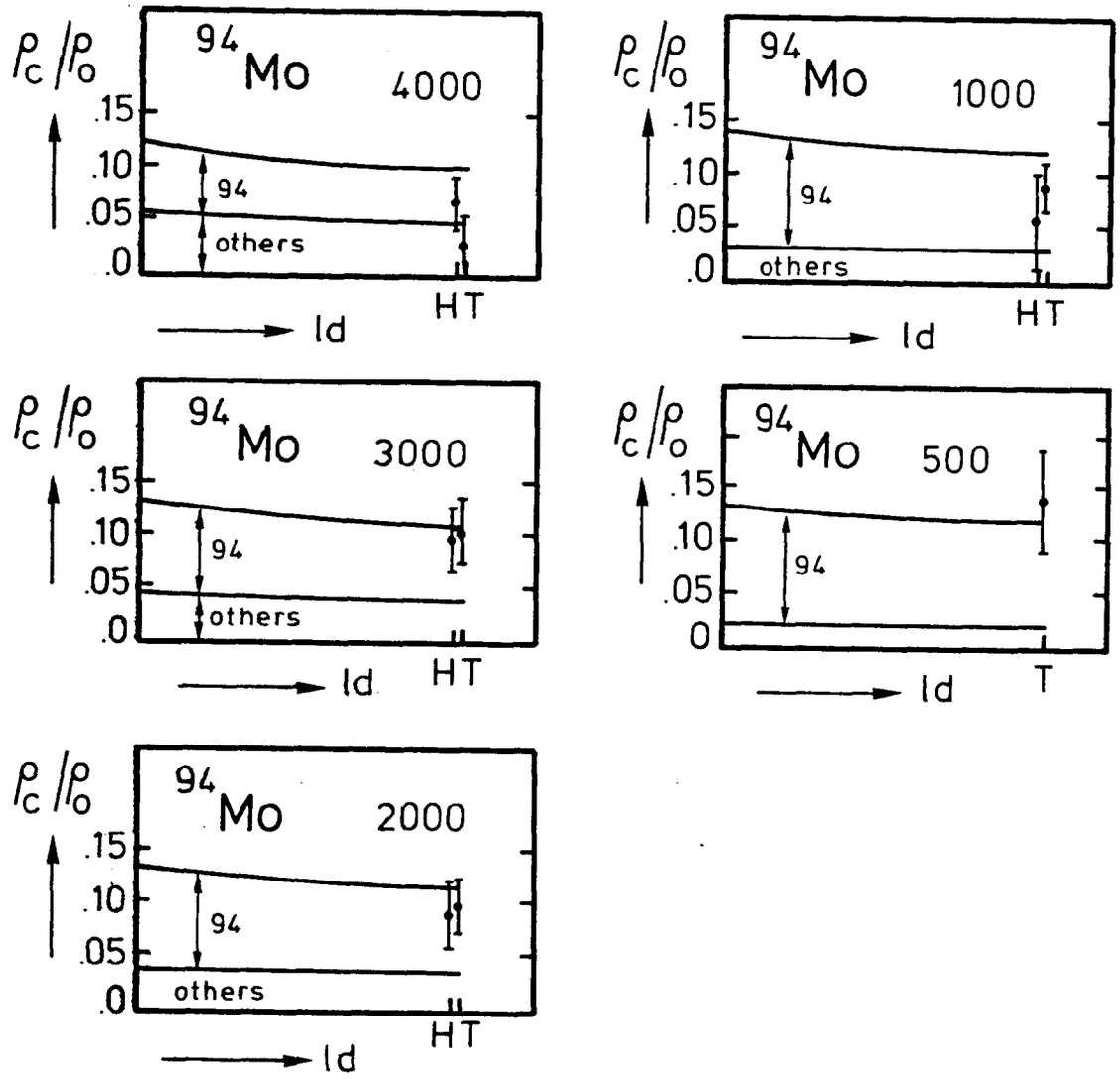
ρ_c/ρ_o
^{94}Mo
4000
.15
.10
.05
.0
94
others
HT
Id
ρ_c/ρ_o
^{94}Mo
1000
.15
.10
.05
.0
94
others
HT
Id
ρ_c/ρ_o
^{94}Mo
3000
.15
.10
.05
.0
94
others
HT
Id
ρ_c/ρ_o
^{94}Mo
500
.15
.10
.05
0
94
T
Id
ρ_c/ρ_o
^{94}Mo
2000
.15
.10
.05
.0
94
others
HT
Id

Fig. 8.

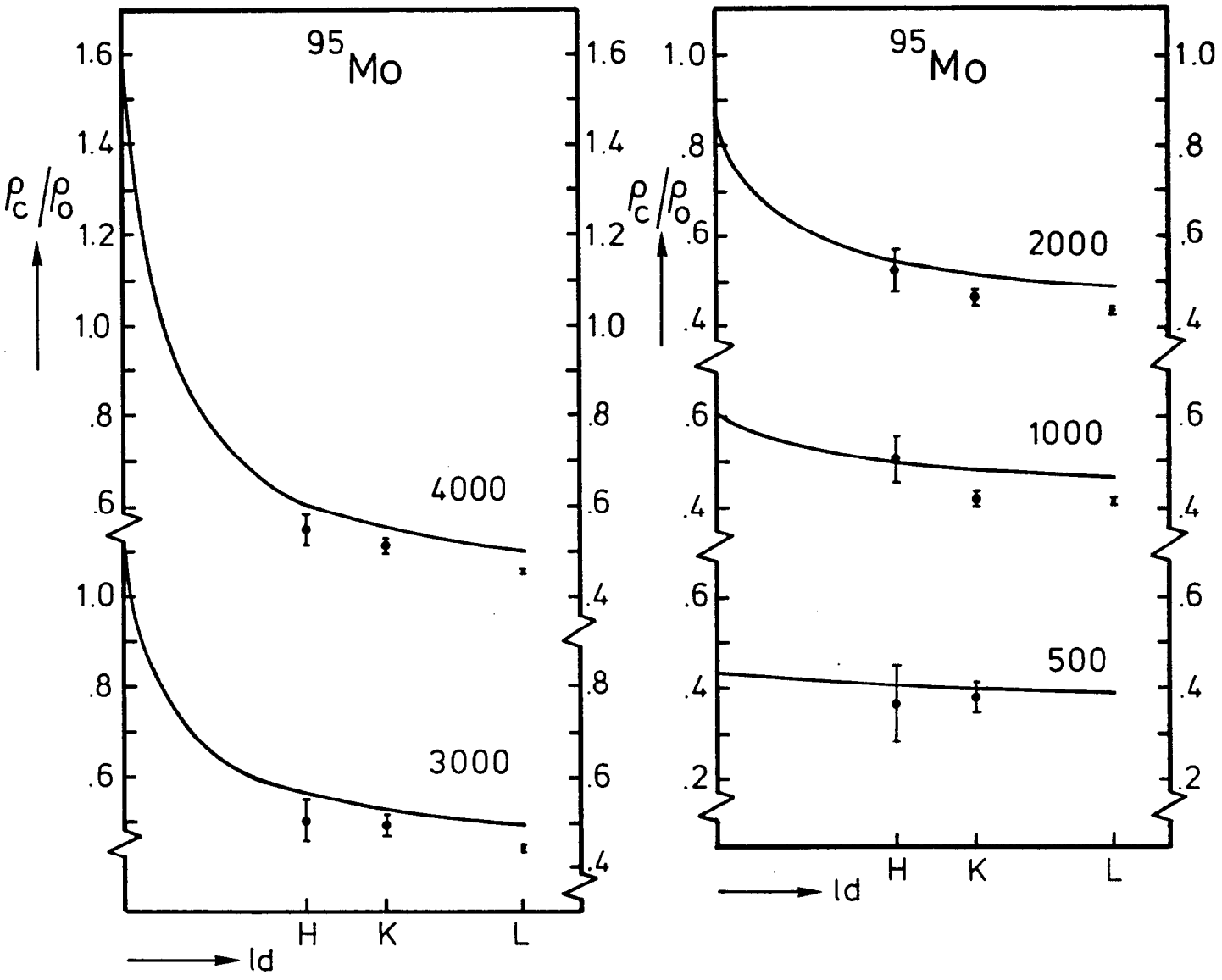

Fig. 9.

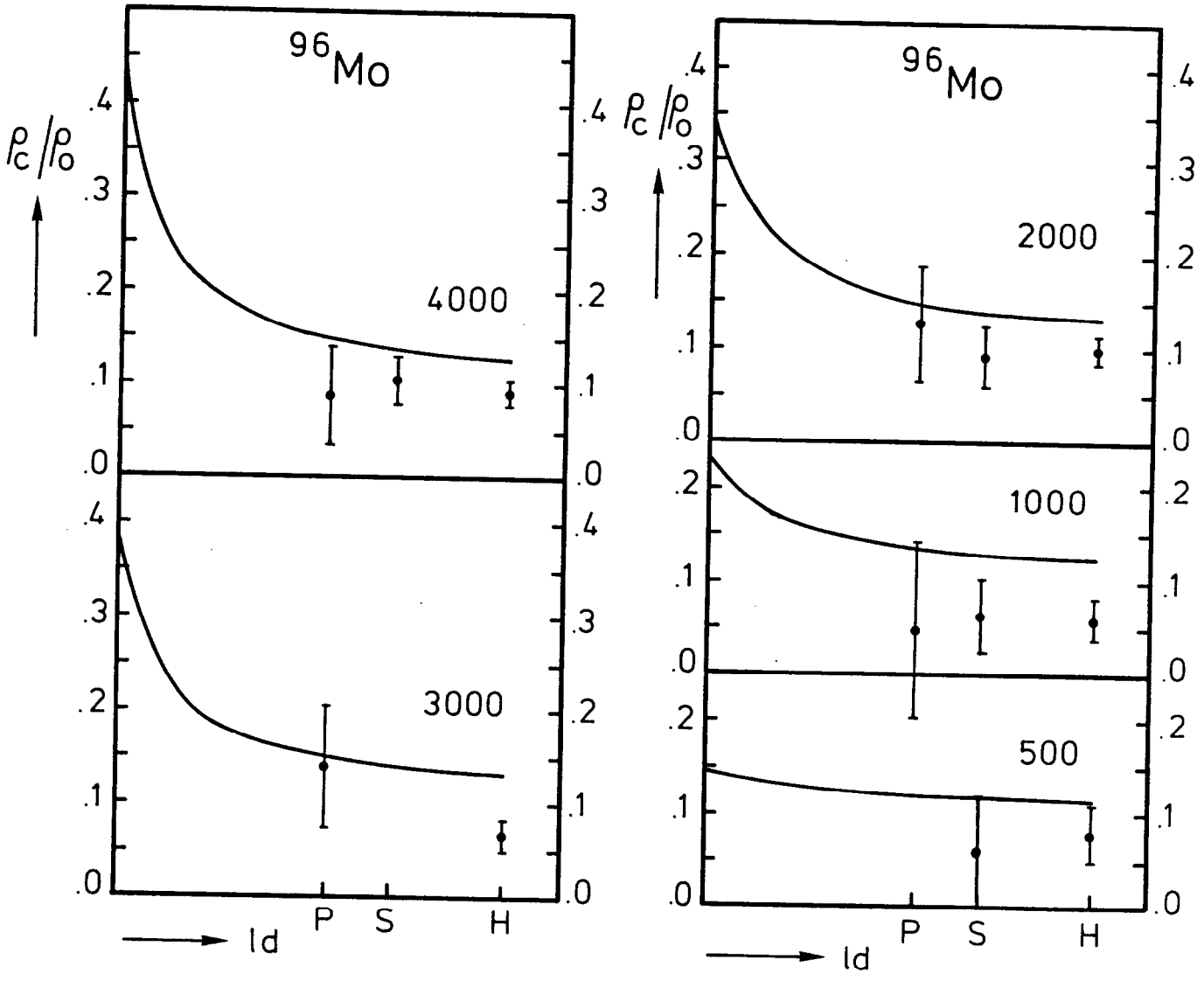

Fig. 10.

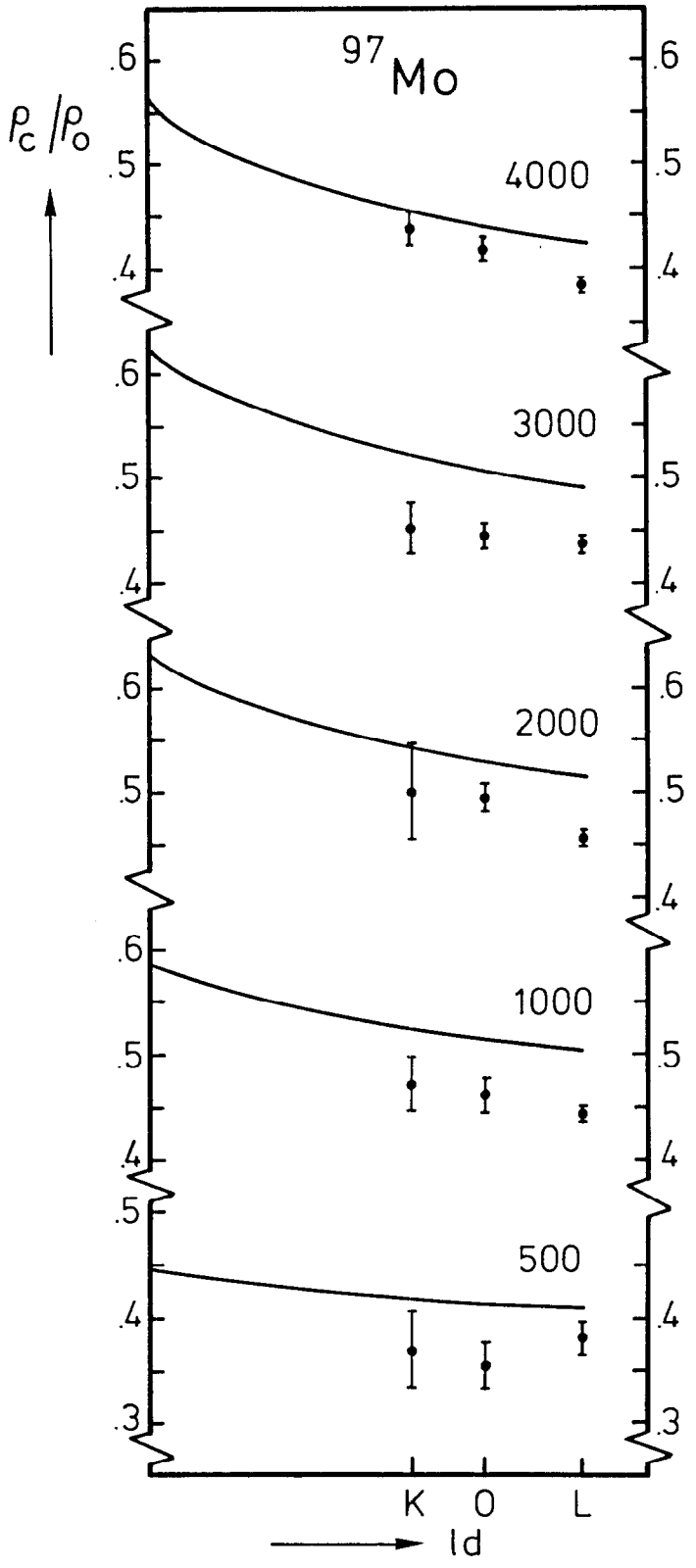

Fig. 11.

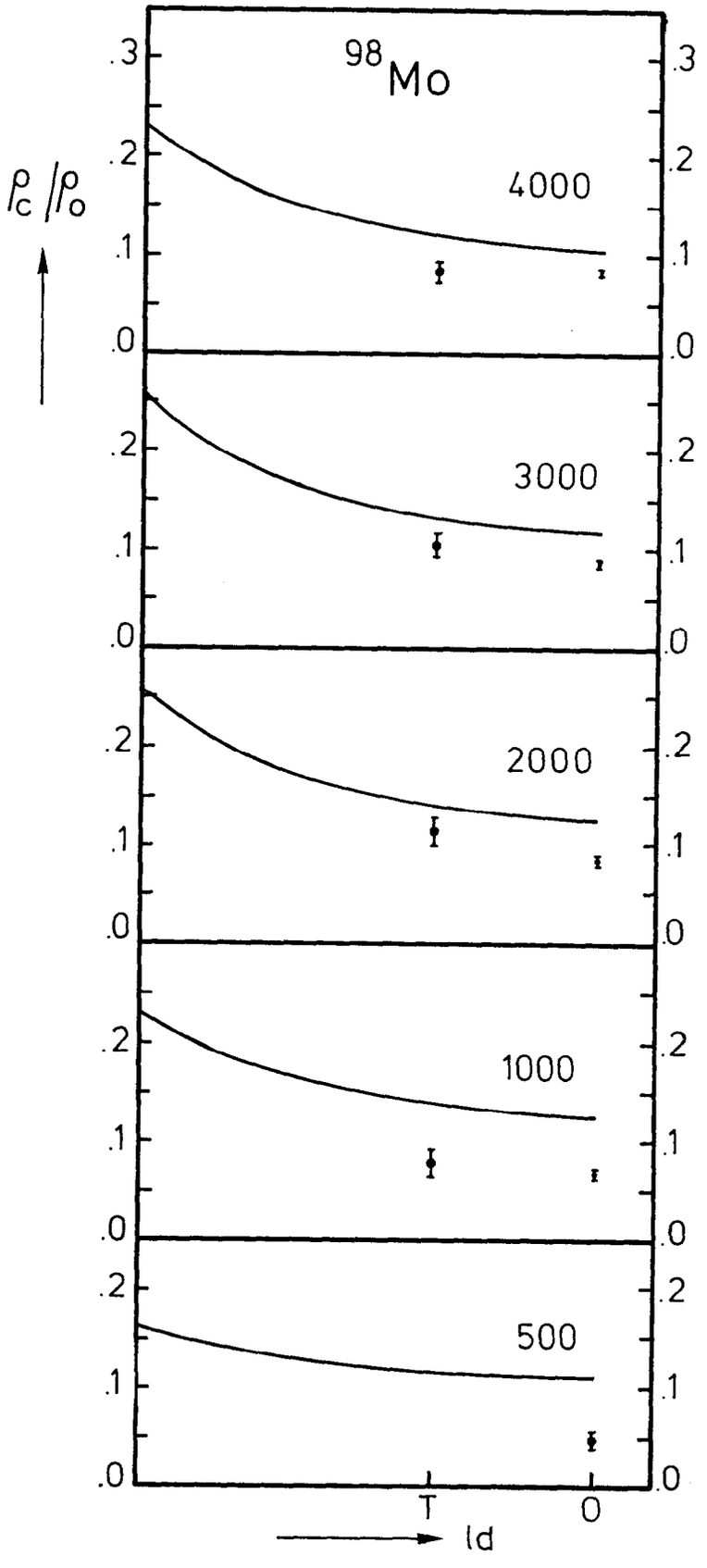

Fig. 12.

Fig. 13.

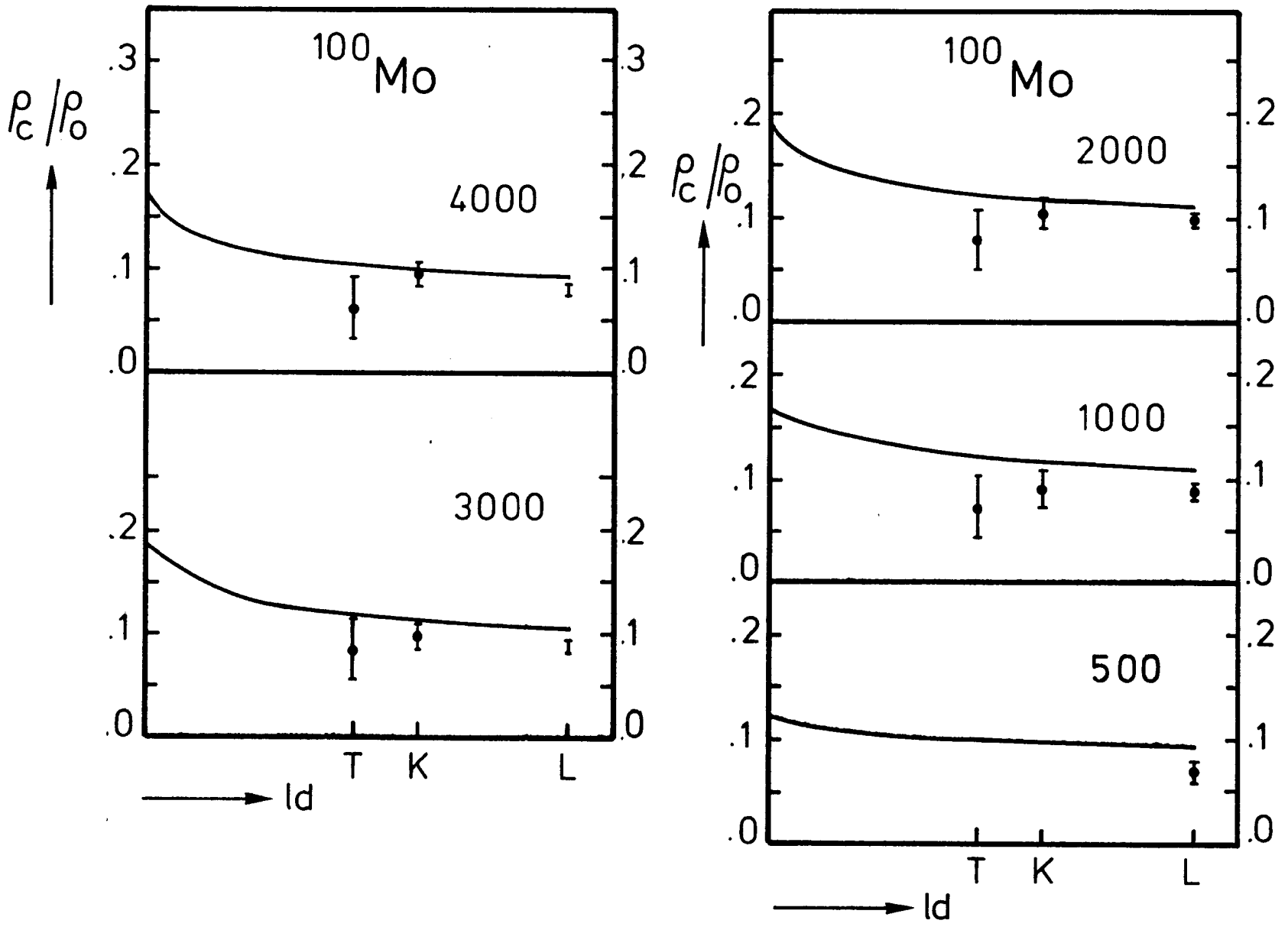
100Mo
ρc/ρo
4000
3000
.3
.2
.1
.0
T K L
ld
100Mo
ρc/ρo
2000
1000
500
.2
.1
.0
T K L
ld

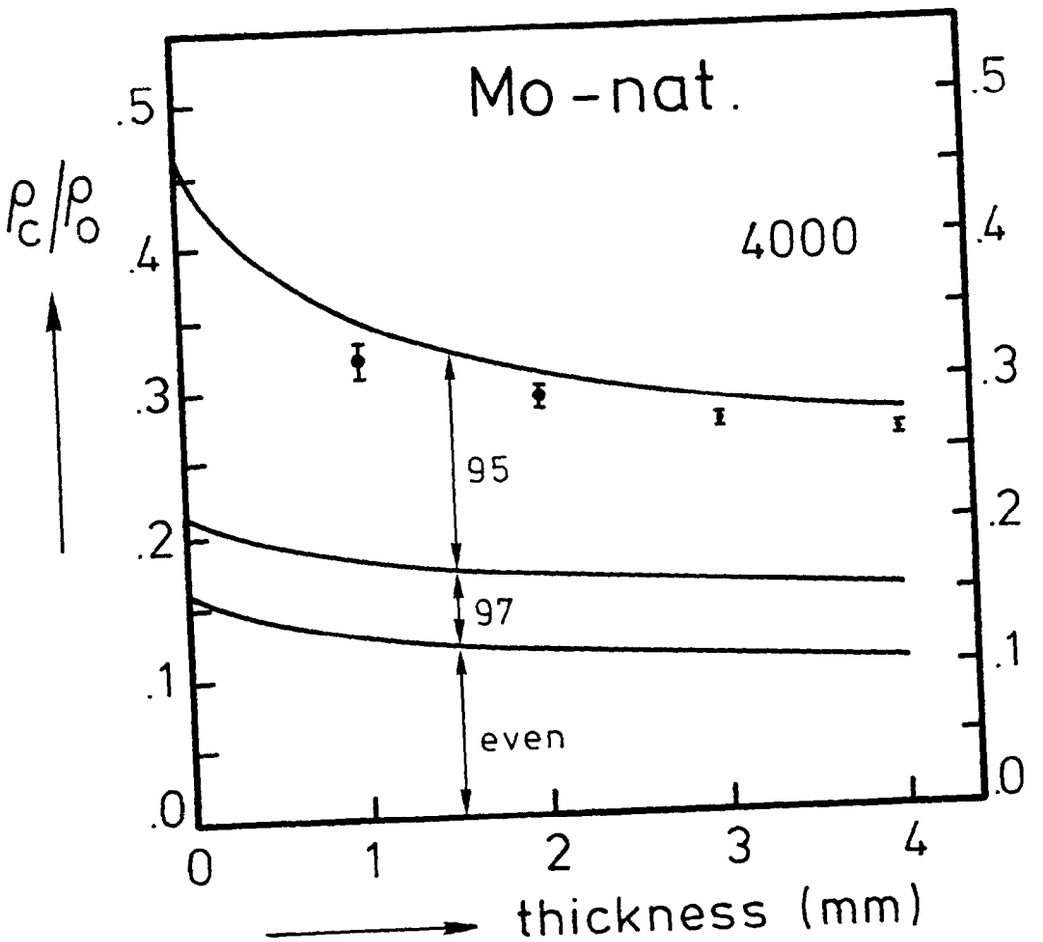
Mo - nat.
4000
ρ_c/ρ_o
95
97
even
0
1
2
3
4
thickness (mm)
.0
.1
.2
.3
.4
.5

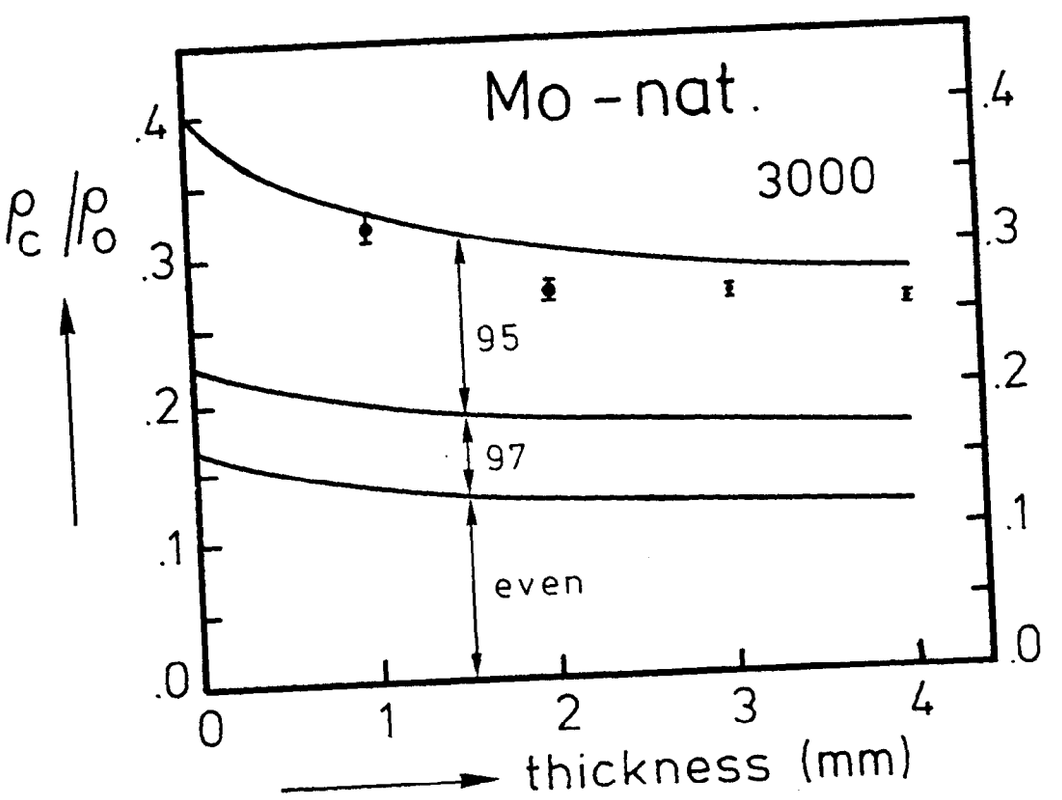
Mo - nat.
3000
ρ_c/ρ_o
95
97
even
0
1
2
3
4
thickness (mm)
.0
.1
.2
.3
.4

Fig. 14a.

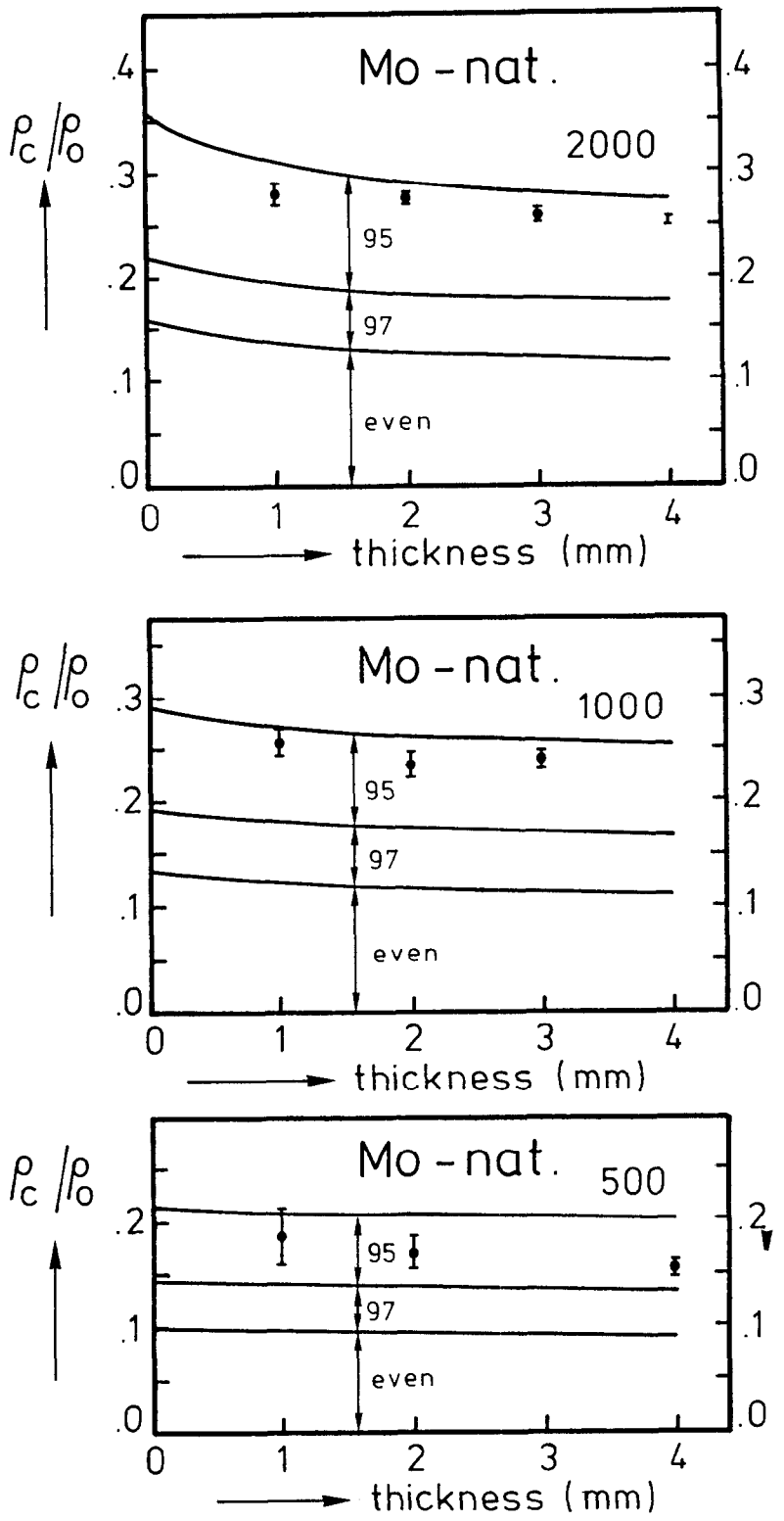
Mo - nat.
2000
95
97
even
ρ_c/ρ_o
thickness (mm)
Mo - nat.
1000
95
97
even
ρ_c/ρ_o
thickness (mm)
Mo - nat.
500
95
97
even
ρ_c/ρ_o
thickness (mm)

Fig. 14b.

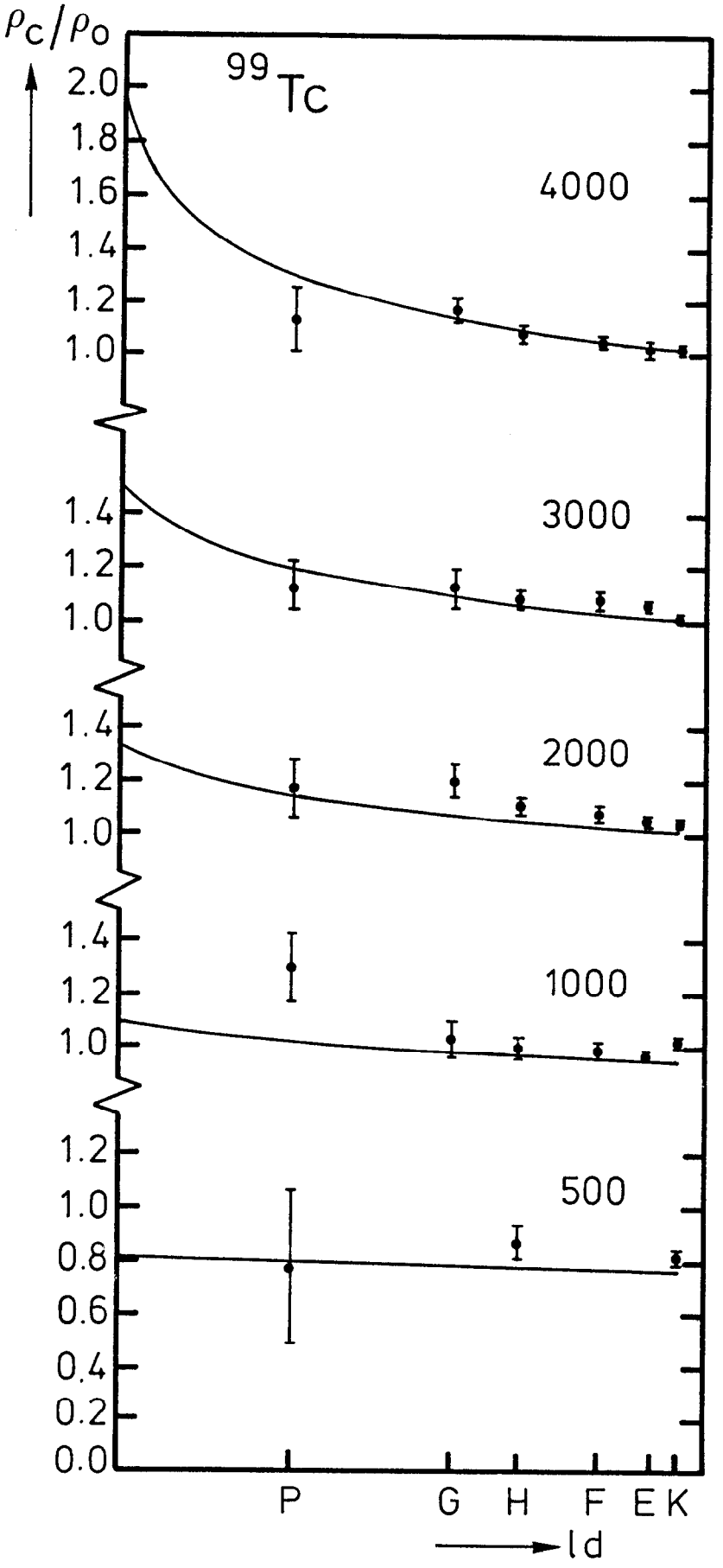
ρc/ρo
99Tc
4000
3000
2000
1000
500
2.0
1.8
1.6
1.4
1.2
1.0
0.8
0.6
0.4
0.2
0.0
P
G
H
F
E
K
ld

Fig. 15.

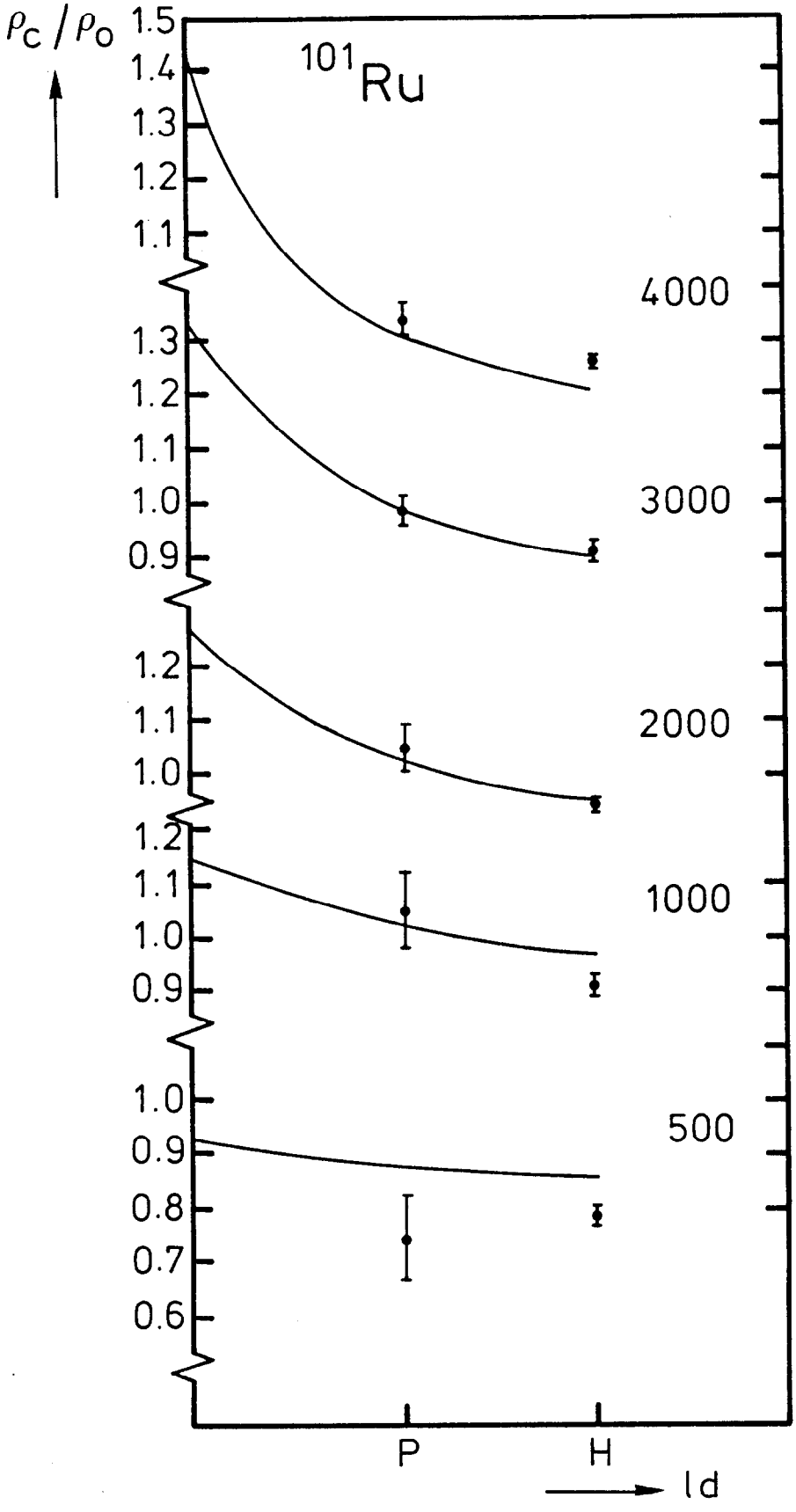
ρc / ρo
101Ru
1.5
1.4
1.3
1.2
1.1
4000
1.3
1.2
1.1
1.0
0.9
3000
1.2
1.1
1.0
2000
1.2
1.1
1.0
0.9
1000
1.0
0.9
0.8
0.7
0.6
500
P
H
ld

Fig. 16.

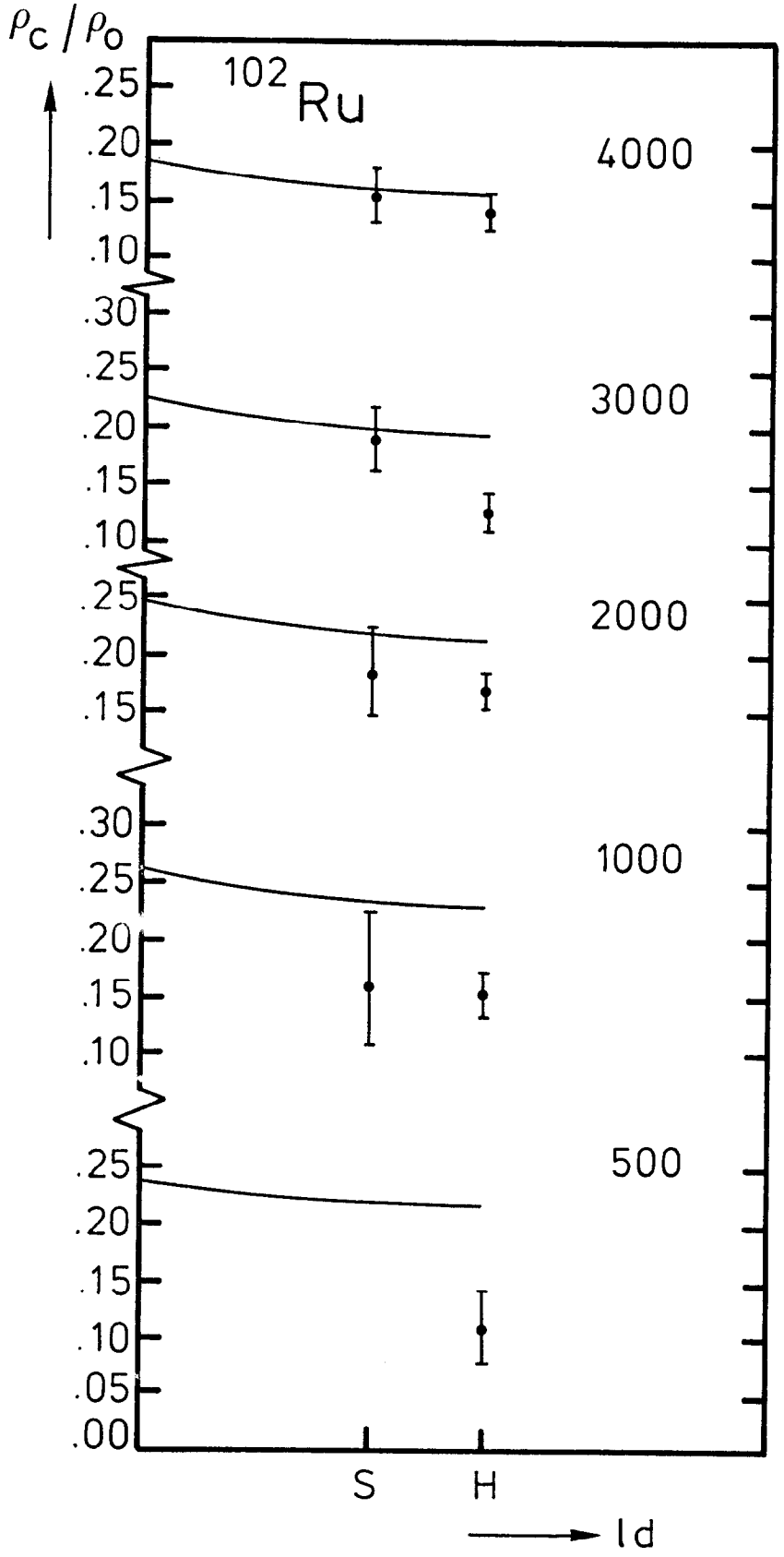
ρc / ρo
102 Ru
4000
3000
2000
1000
500
.25
.20
.15
.10
.30
.25
.20
.15
.10
.25
.20
.15
.30
.25
.20
.15
.10
.25
.20
.15
.10
.05
.00
S
H
Id

Fig. 17.

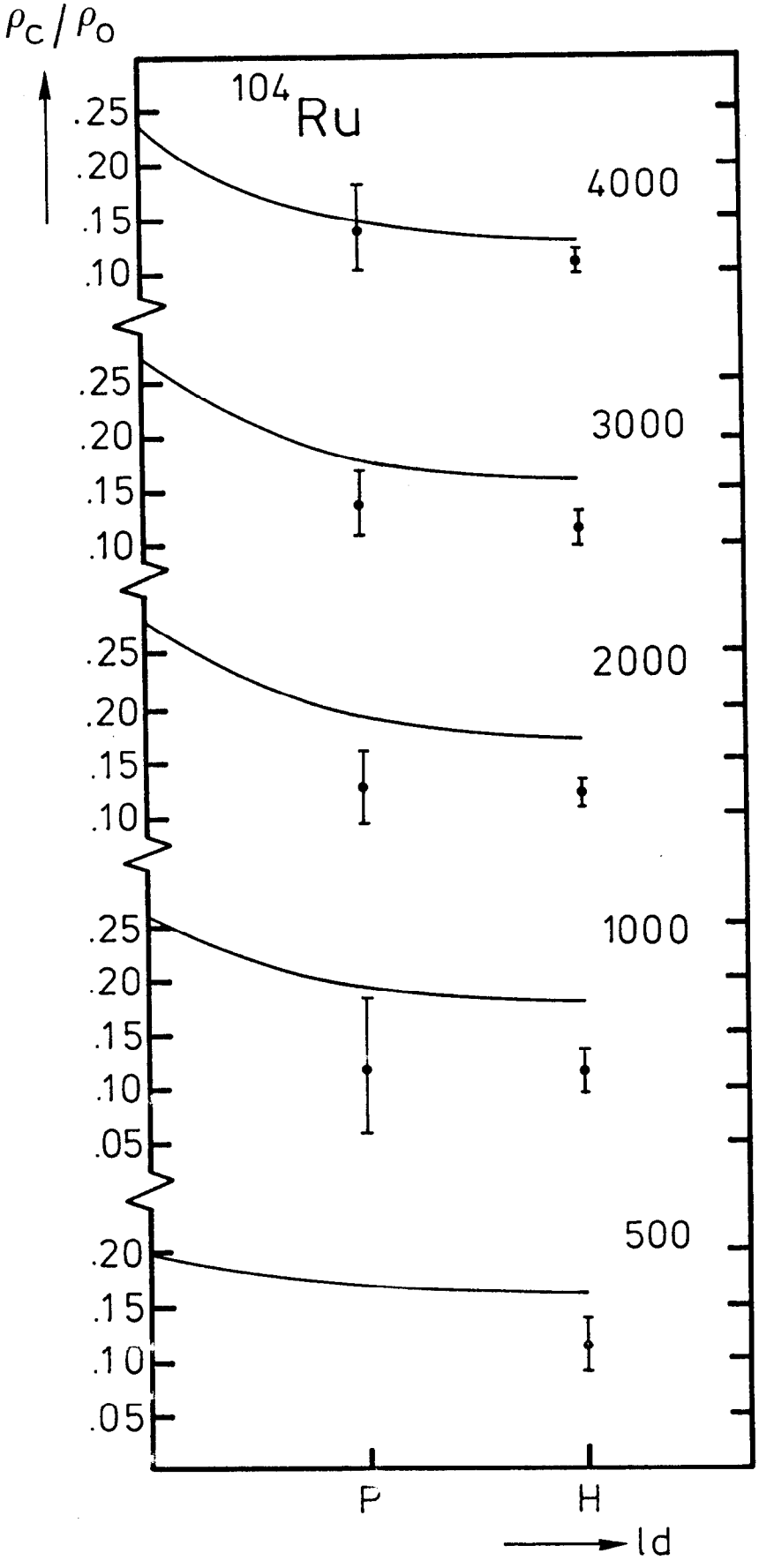

Fig. 18.

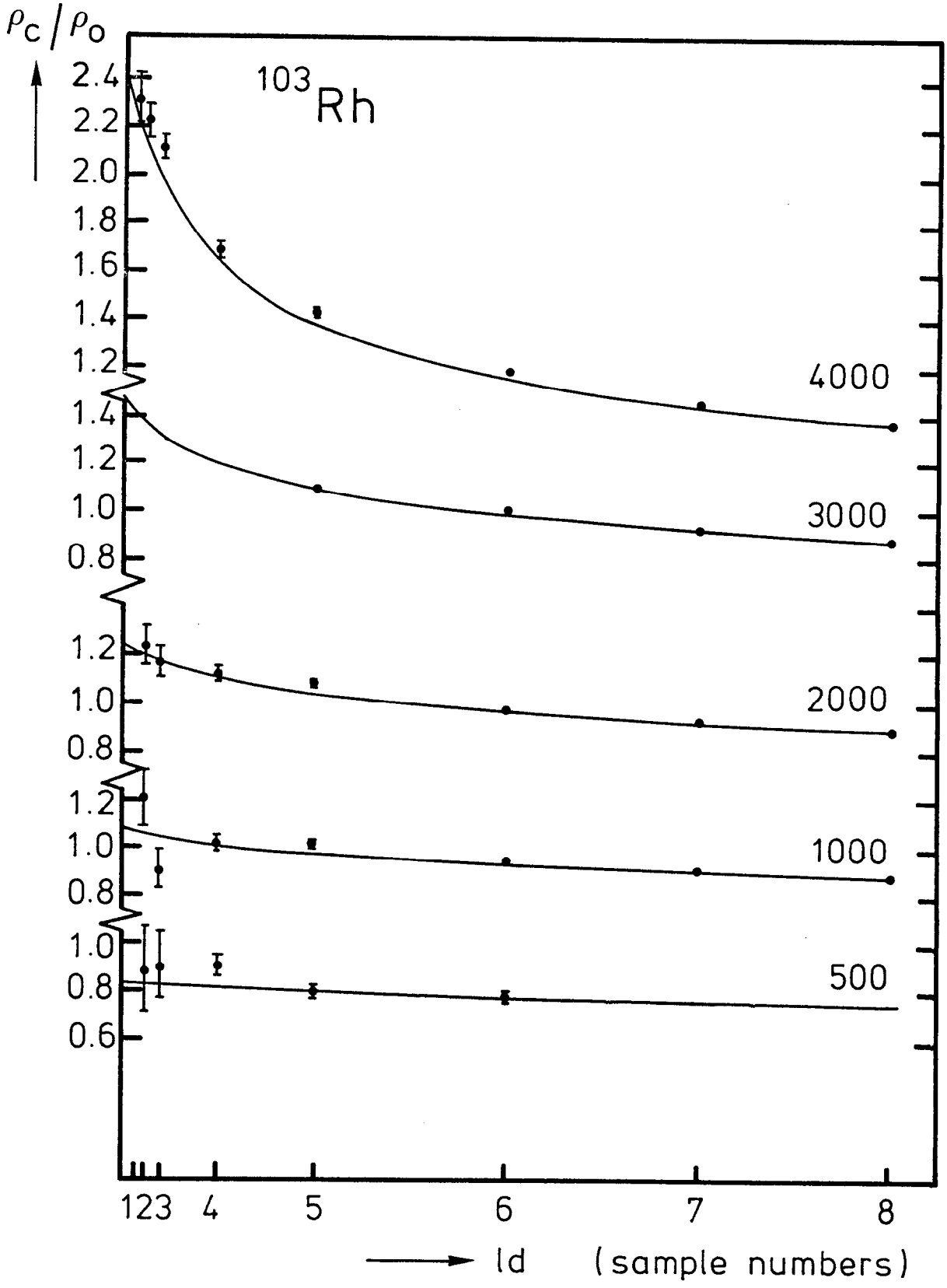
ρc / ρo
103Rh
2.4
2.2
2.0
1.8
1.6
1.4
1.2
1.4
1.2
1.0
0.8
1.2
1.0
0.8
1.2
1.0
0.8
1.0
0.8
0.6
4000
3000
2000
1000
500
123
4
5
6
7
8
Id (sample numbers)

Fig. 19.

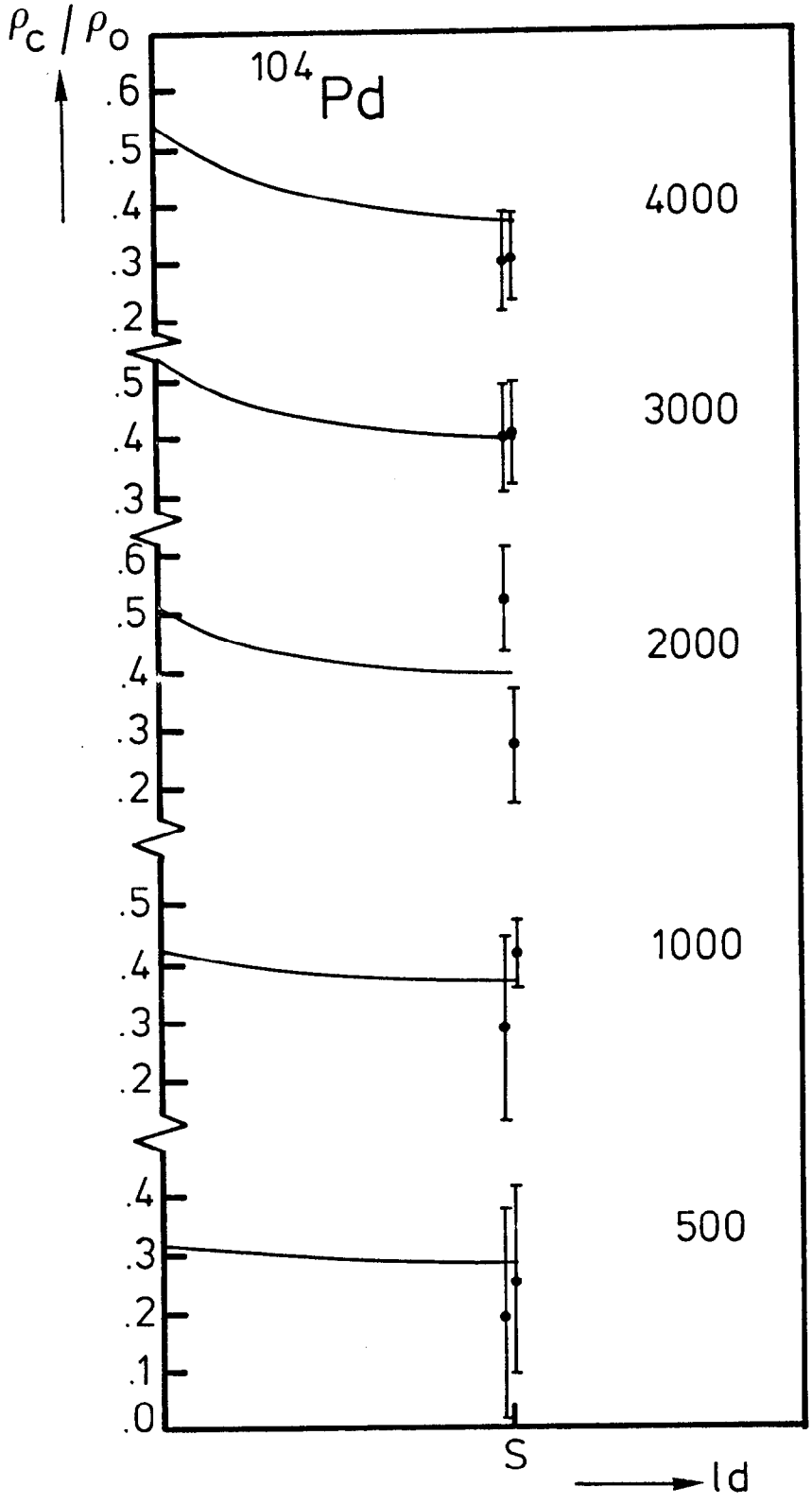
ρc / ρo
104Pd
.6
.5
.4
.3
.2
.5
.4
.3
.6
.5
.4
.3
.2
.5
.4
.3
.2
.4
.3
.2
.1
.0
4000
3000
2000
1000
500
S
ld

Fig. 20.

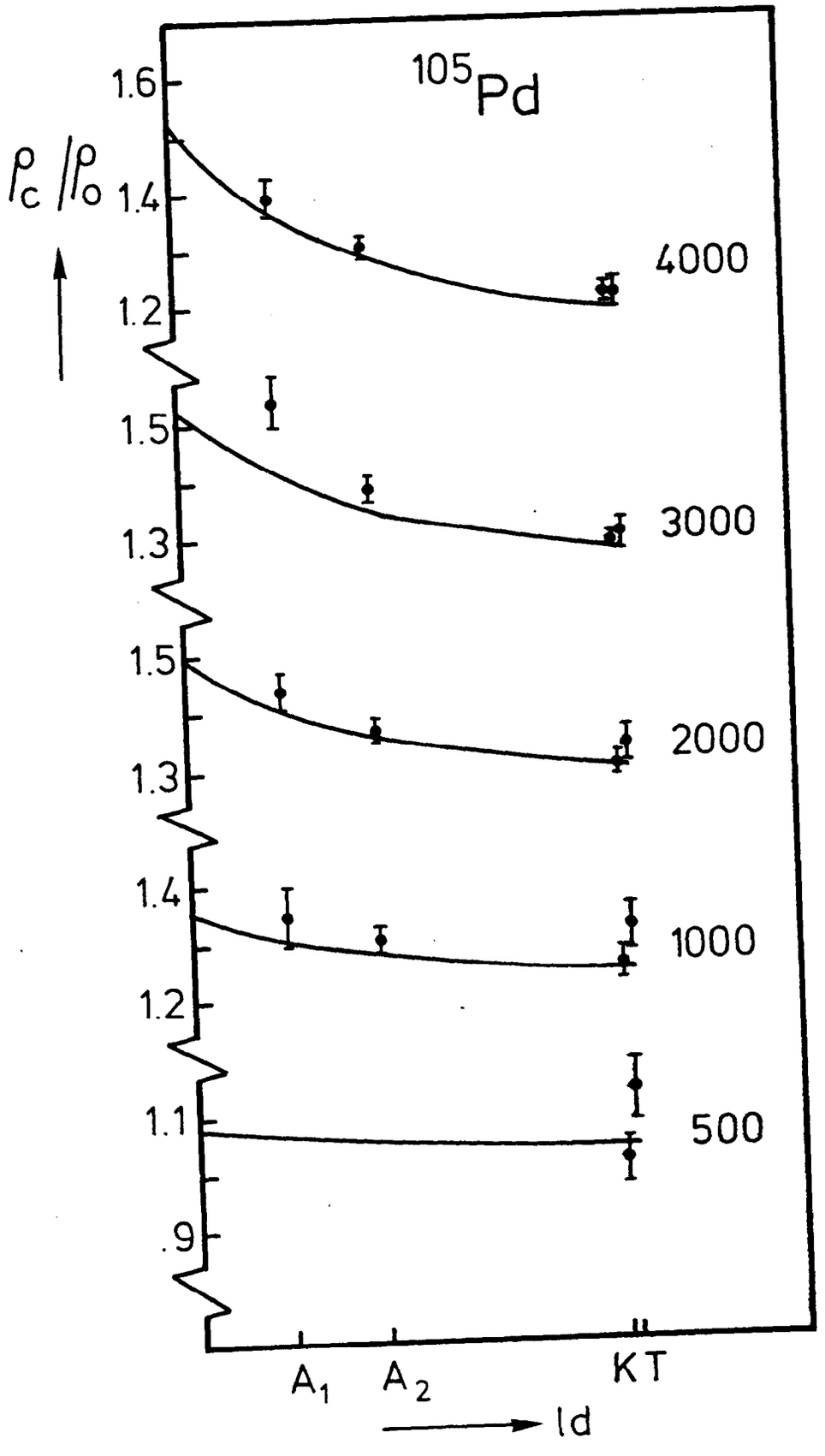
^{105}Pd
ρ_c / ρ_o
1.6
1.4
1.2
1.5
1.3
1.5
1.3
1.4
1.2
1.1
.9
4000
3000
2000
1000
500
A_1
A_2
KT
Id

Fig. 21.

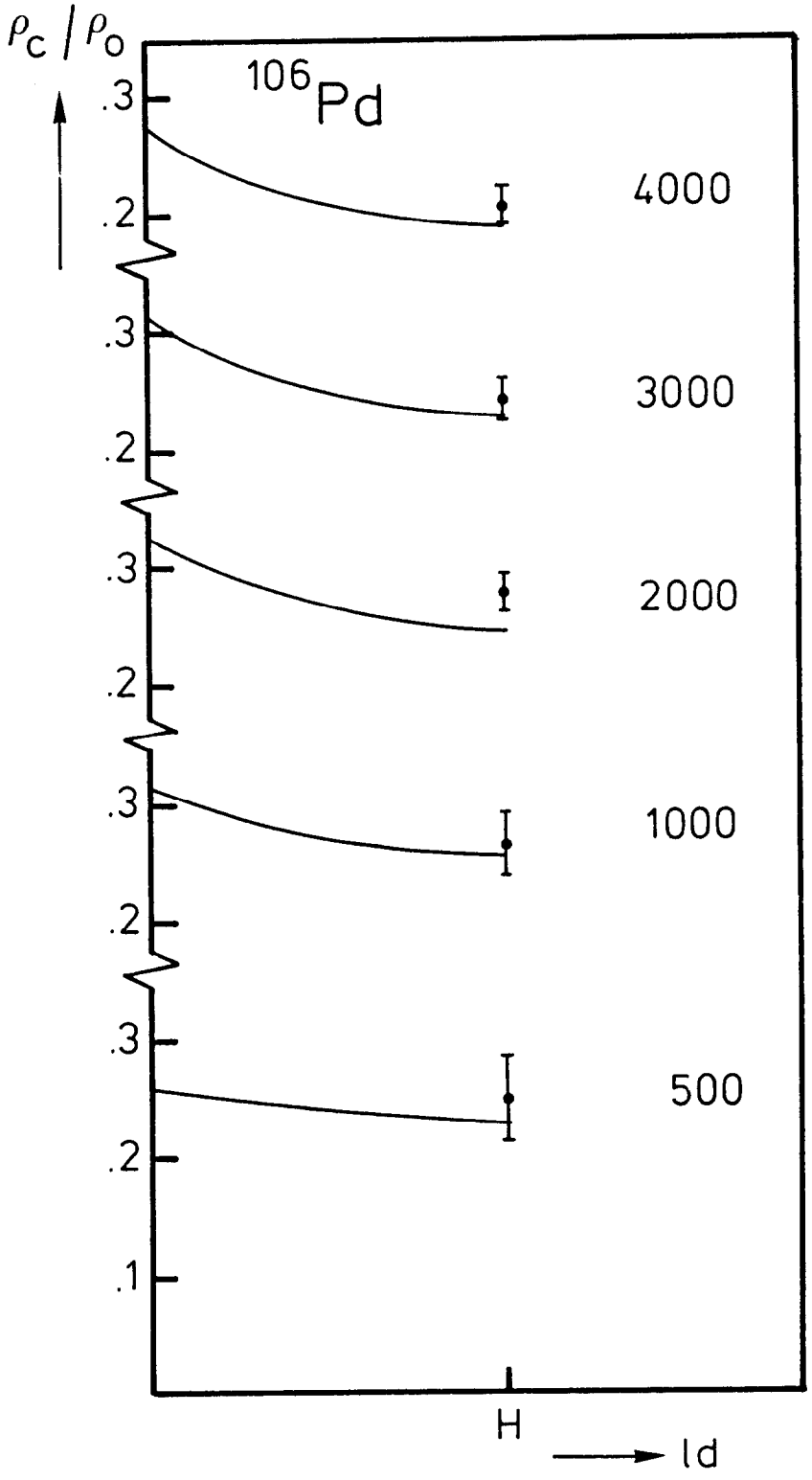

Fig. 22.

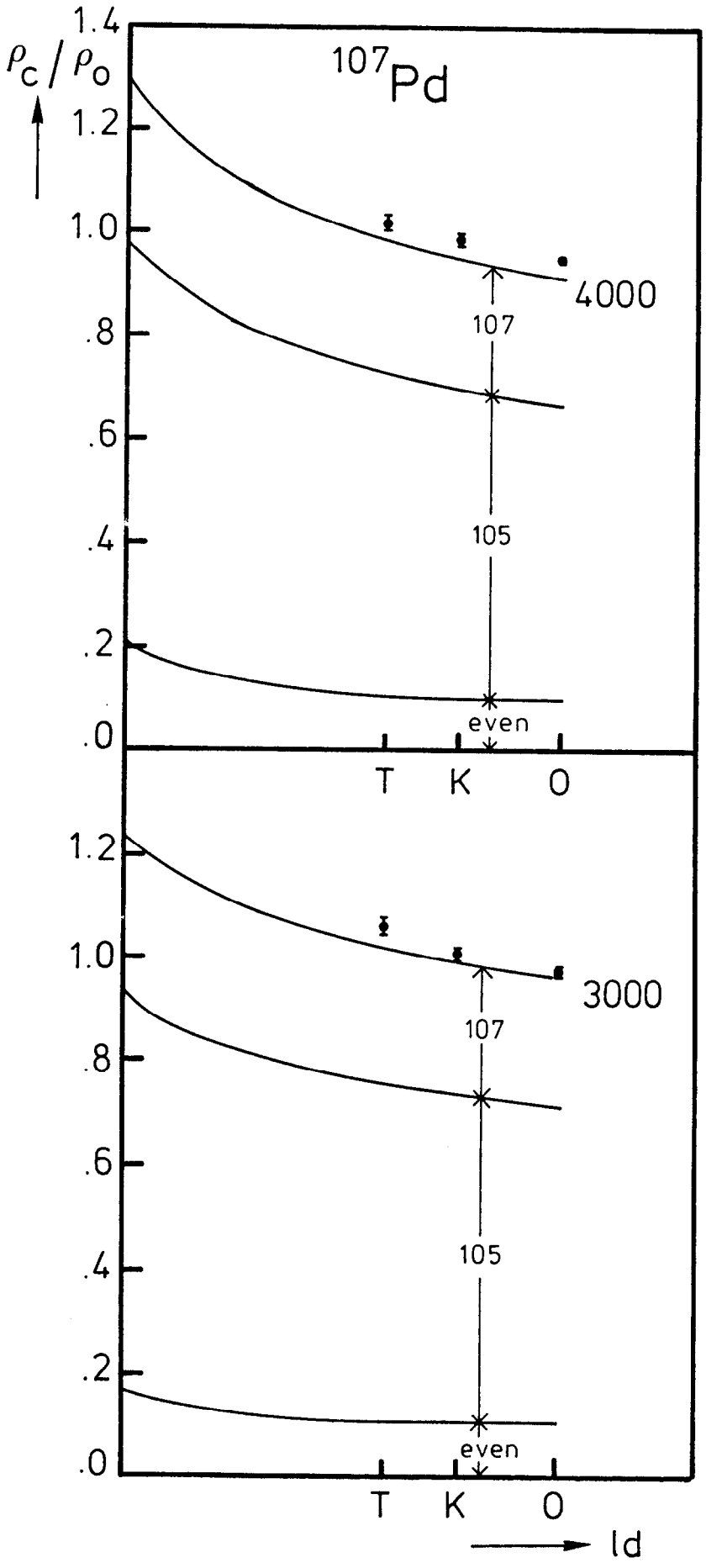
ρ_c / ρ_o
^{107}Pd
1.4
1.2
1.0
.8
.6
.4
.2
.0
4000
107
105
even
T K O
1.2
1.0
.8
.6
.4
.2
.0
3000
107
105
even
T K O
ld

Fig. 23a,b.

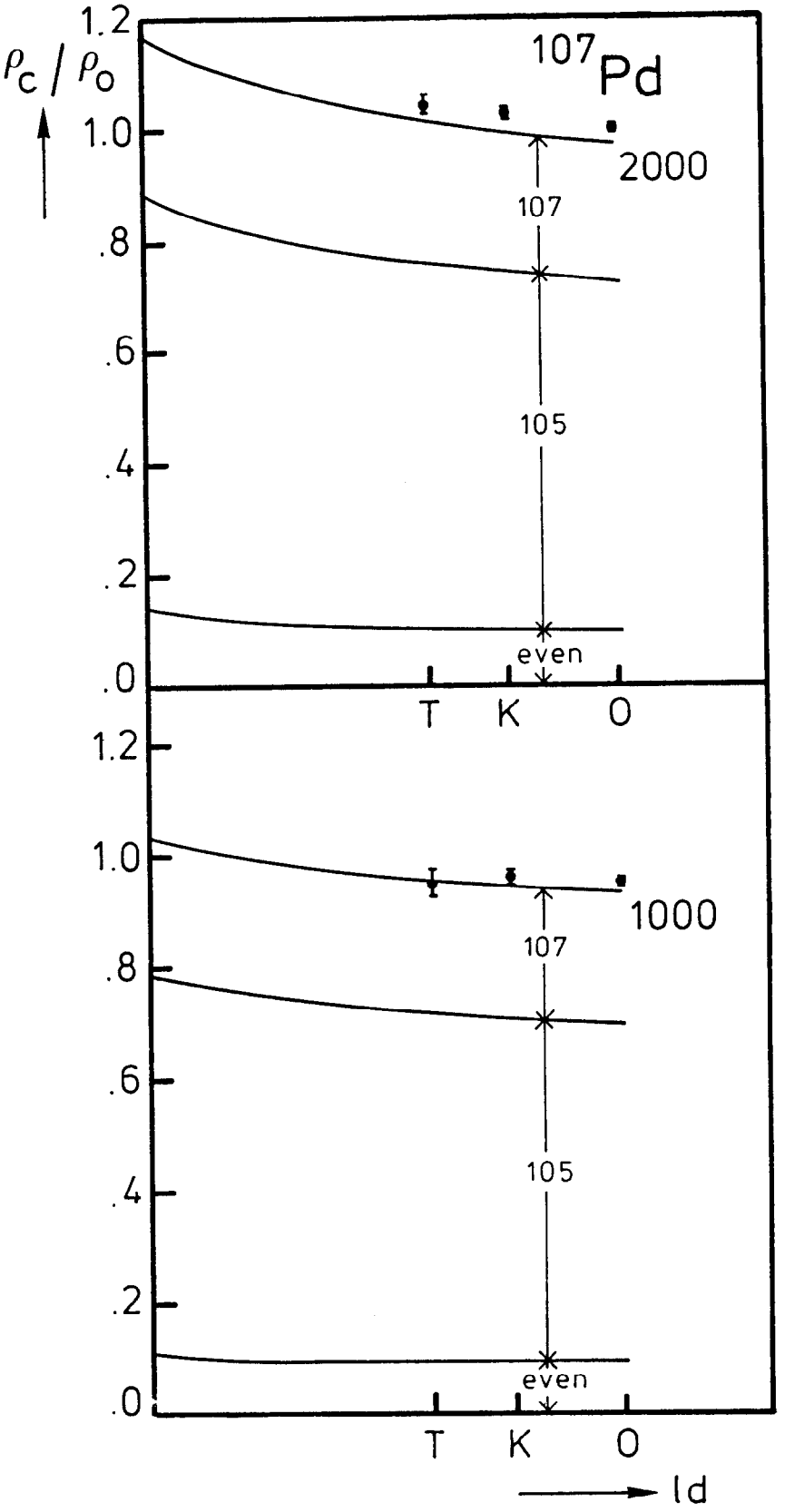

Fig. 23c,d.

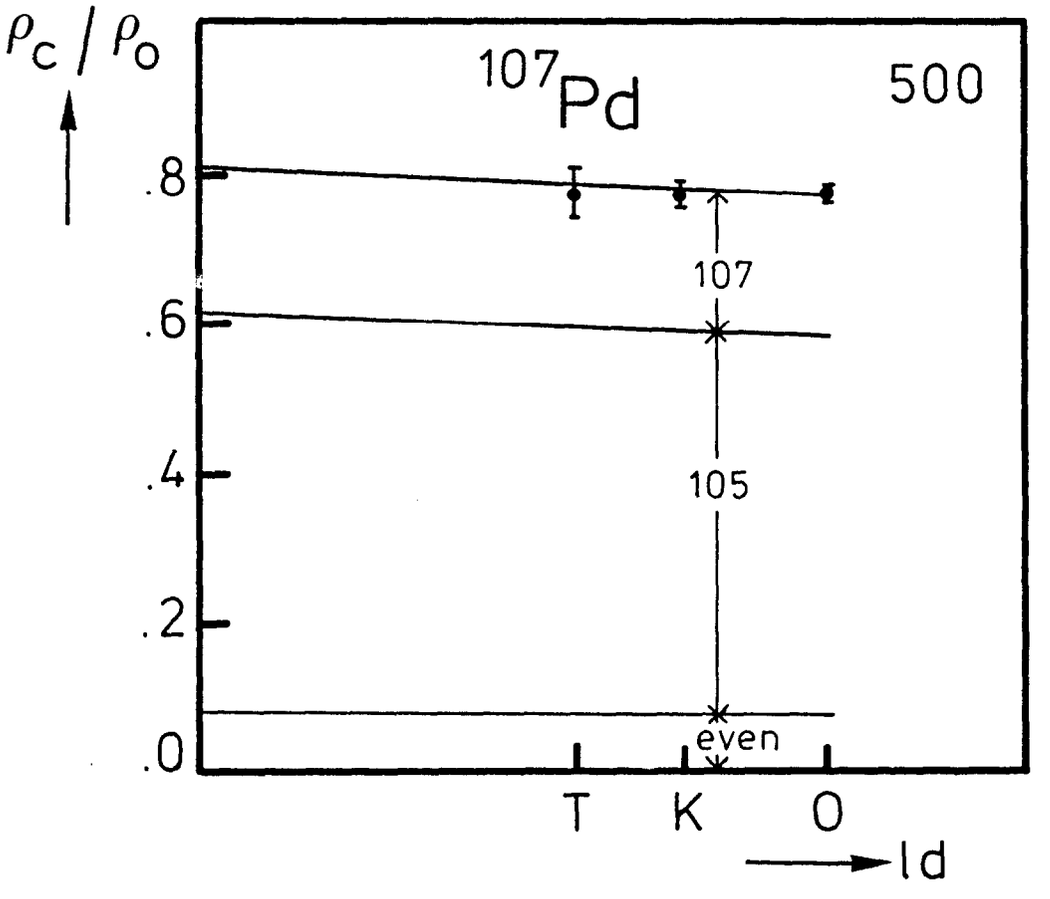

Fig. 23e.

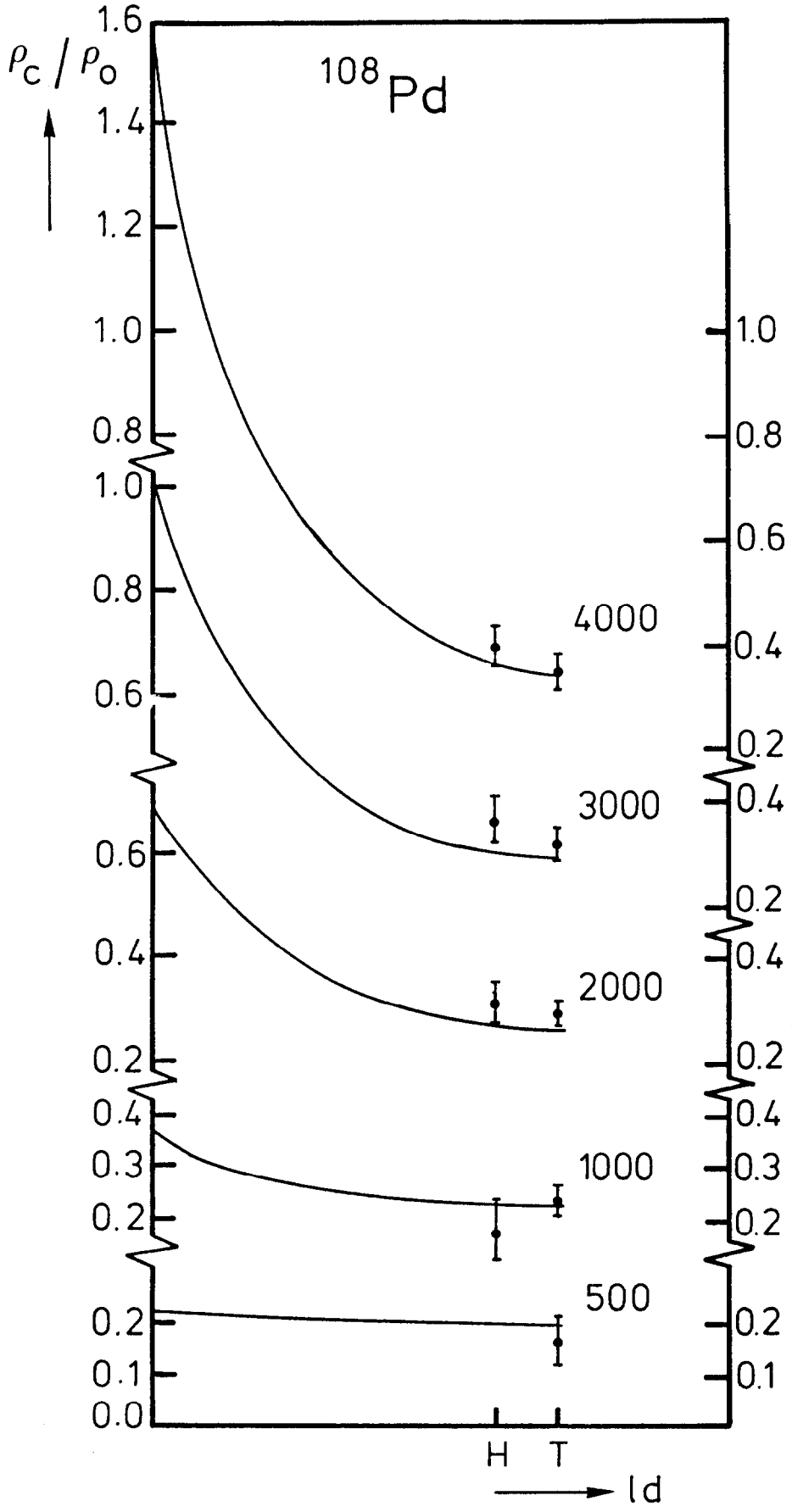

Fig. 24.

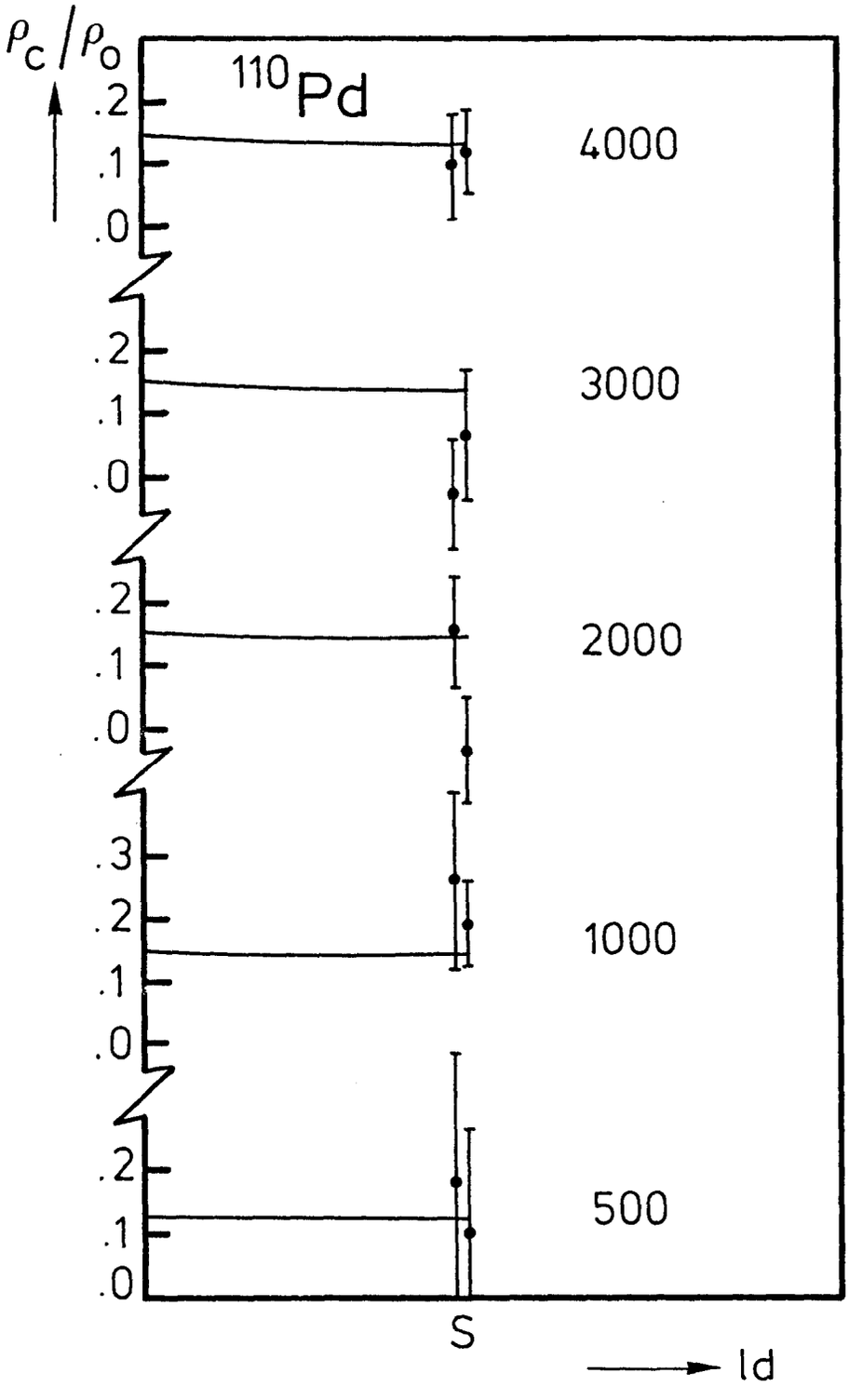

Fig. 25.

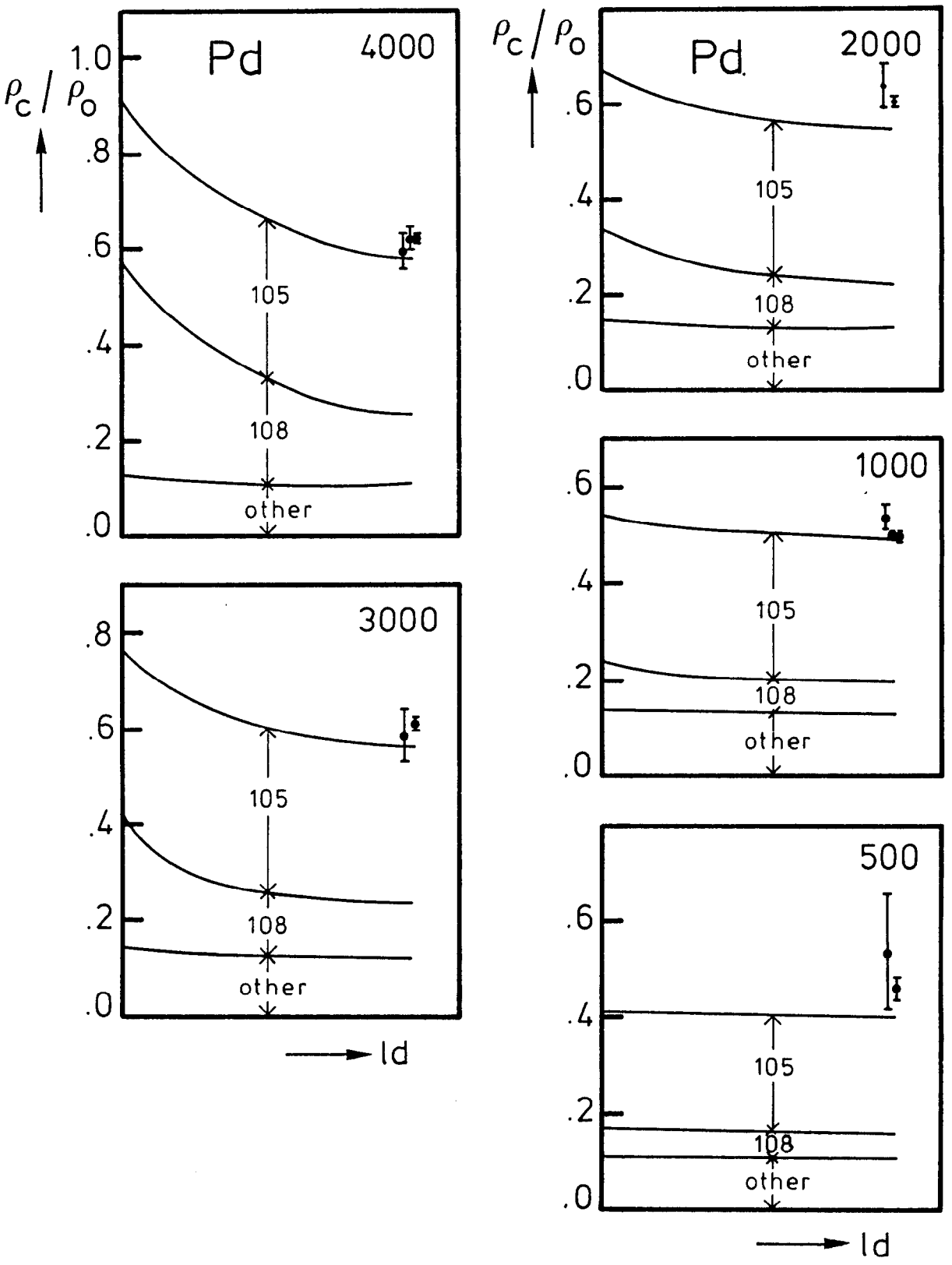

Fig. 26.

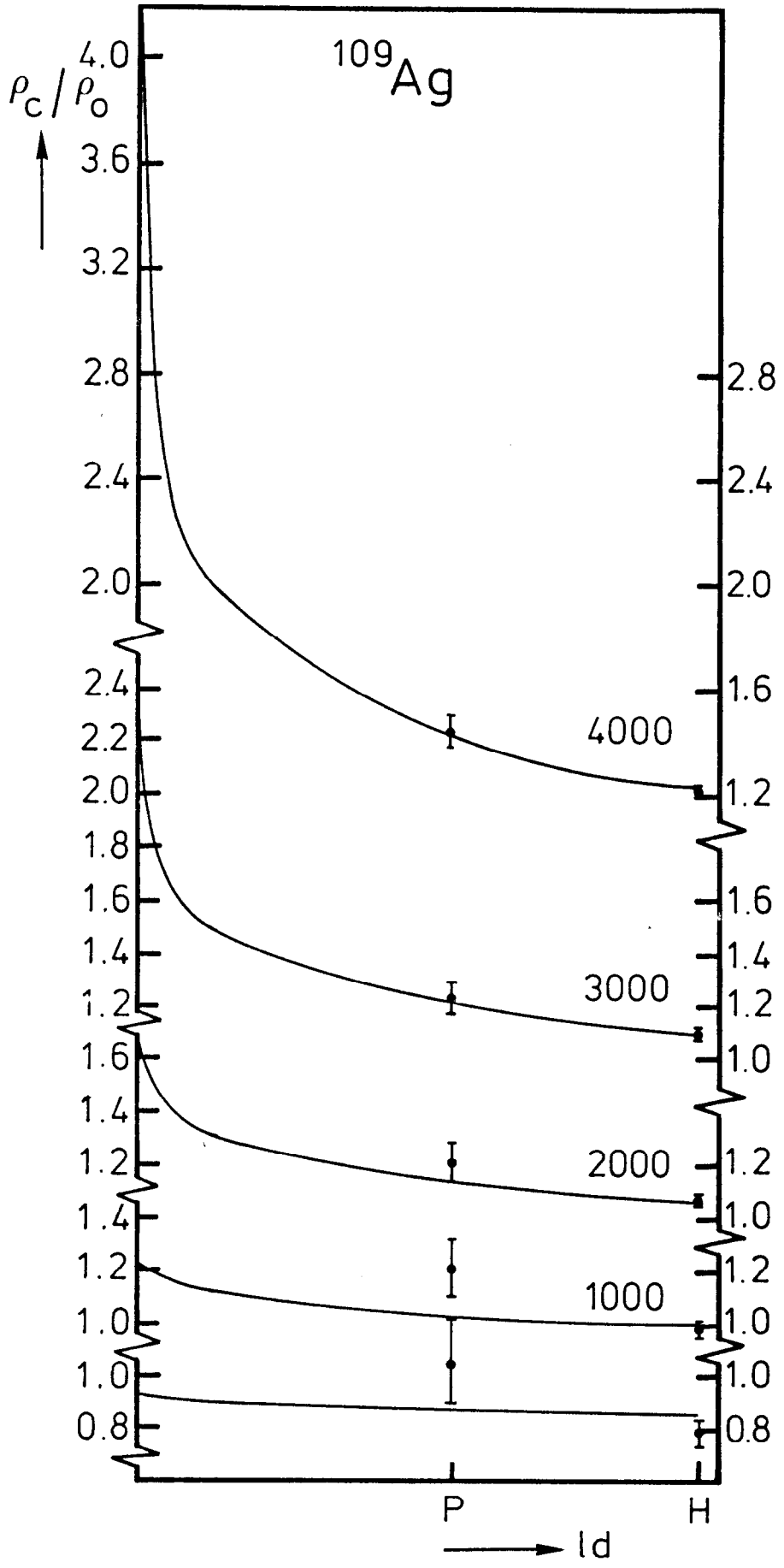
^{109}Ag
ρ_c / ρ_o
4.0
3.6
3.2
2.8
2.4
2.0
2.4
2.2
2.0
1.8
1.6
1.4
1.2
1.6
1.4
1.2
1.4
1.2
1.0
1.0
0.8
2.8
2.4
2.0
1.6
1.2
1.6
1.4
1.2
1.0
1.2
1.0
1.2
1.0
1.0
0.8
4000
3000
2000
1000
P
H
ld

Fig. 27.

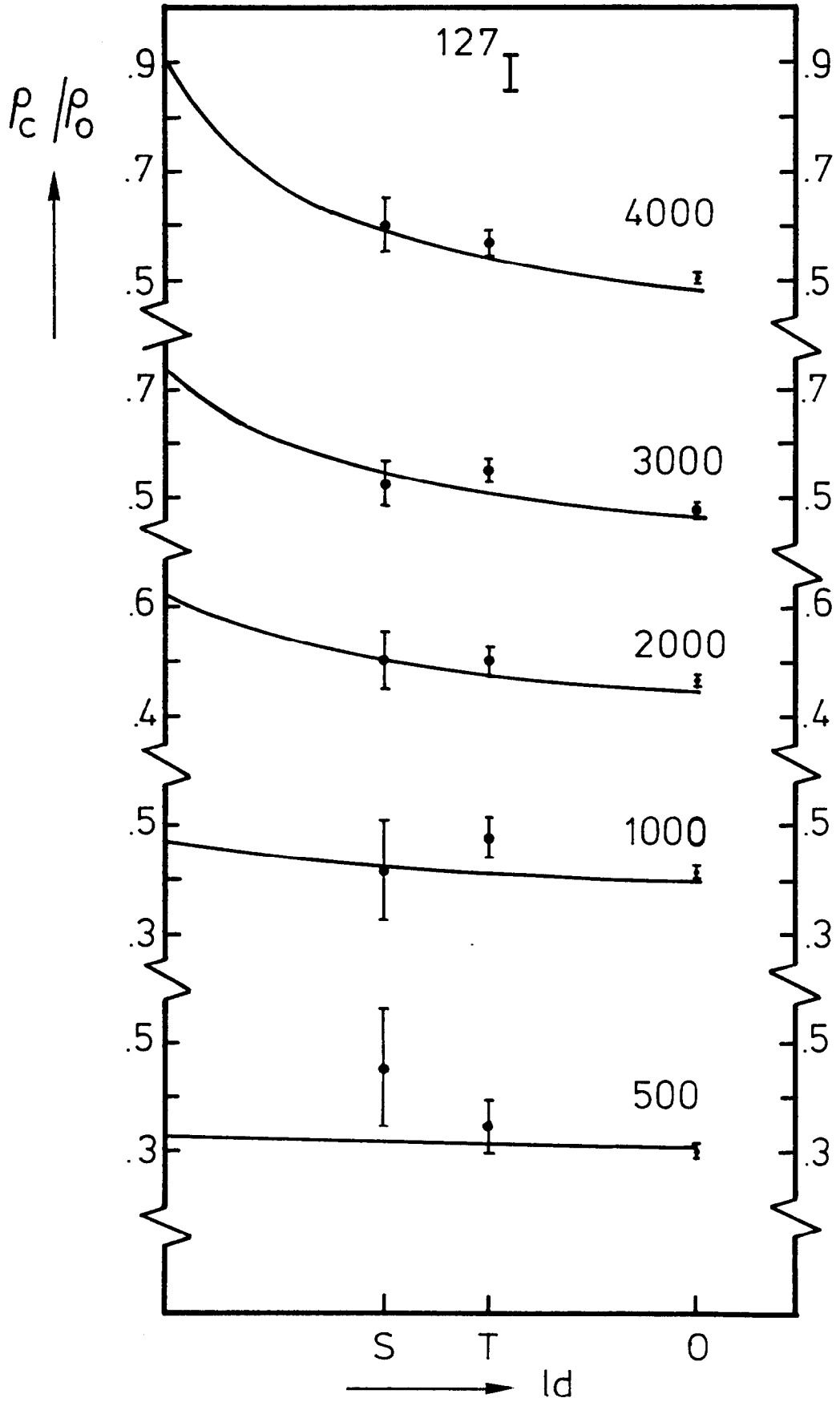

Fig. 28.

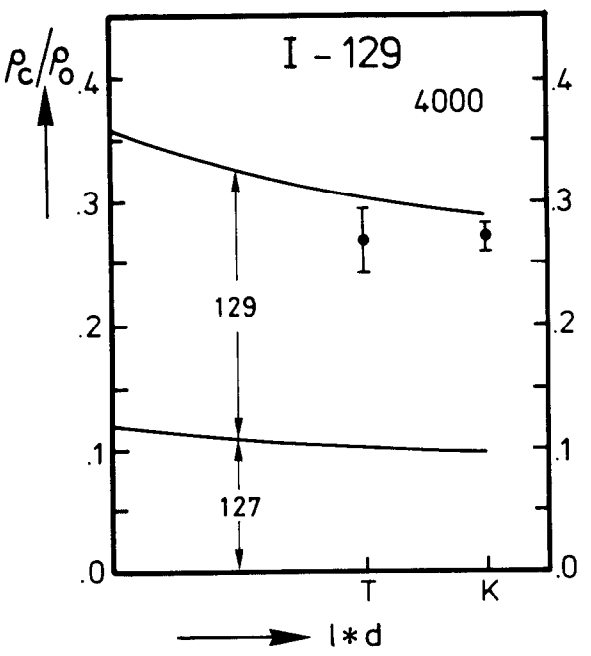
I - 129
4000
ρ_c/ρ_o
129
127
T
K
l*d

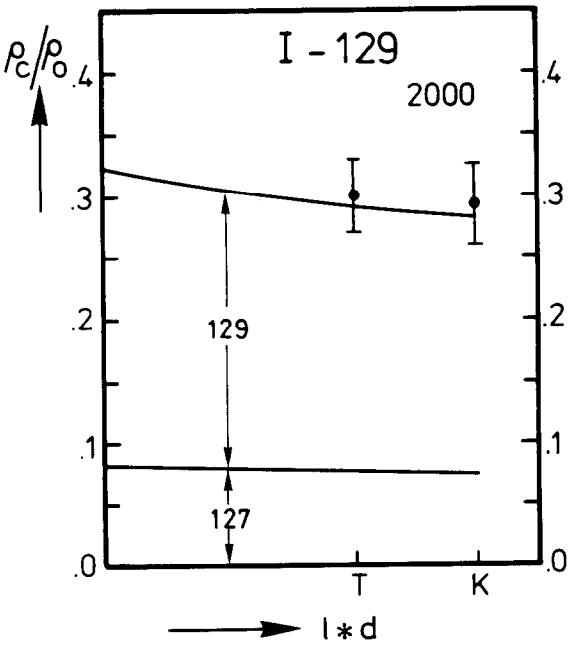
I - 129
2000
ρ_c/ρ_o
129
127
T
K
l*d

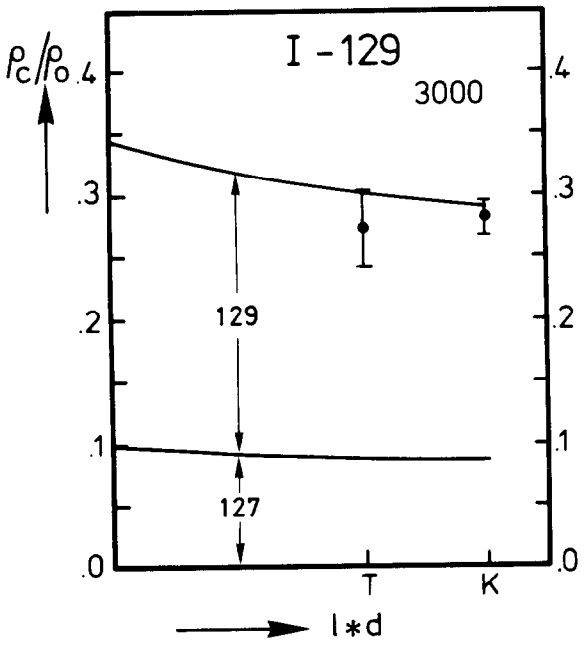
I - 129
3000
ρ_c/ρ_o
129
127
T
K
l*d

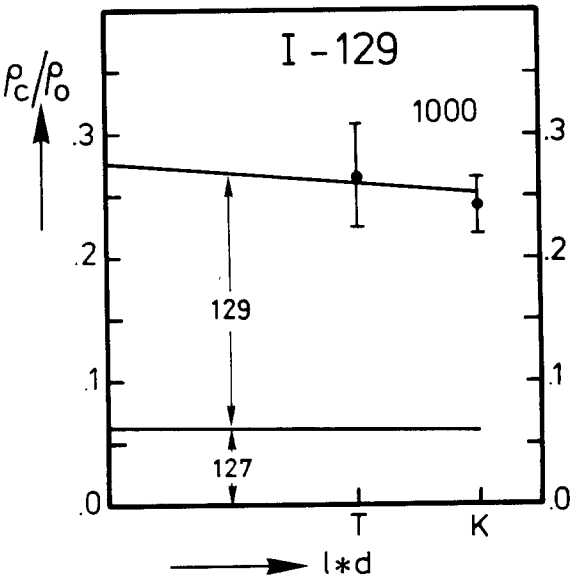
I - 129
1000
ρ_c/ρ_o
129
127
T
K
l*d

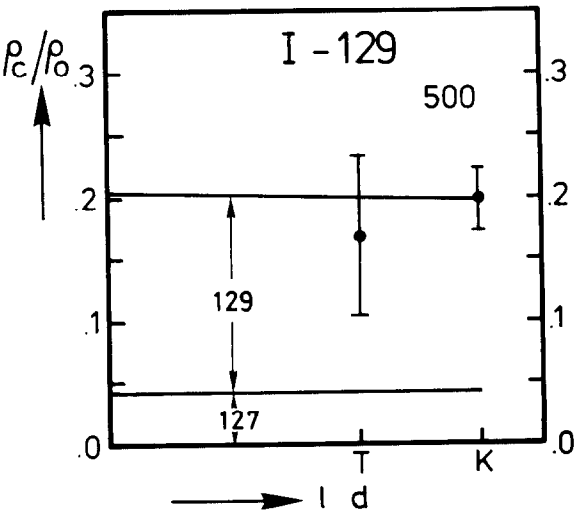
I - 129
500
ρ_c/ρ_o
129
127
T
K
l d

Fig. 29.

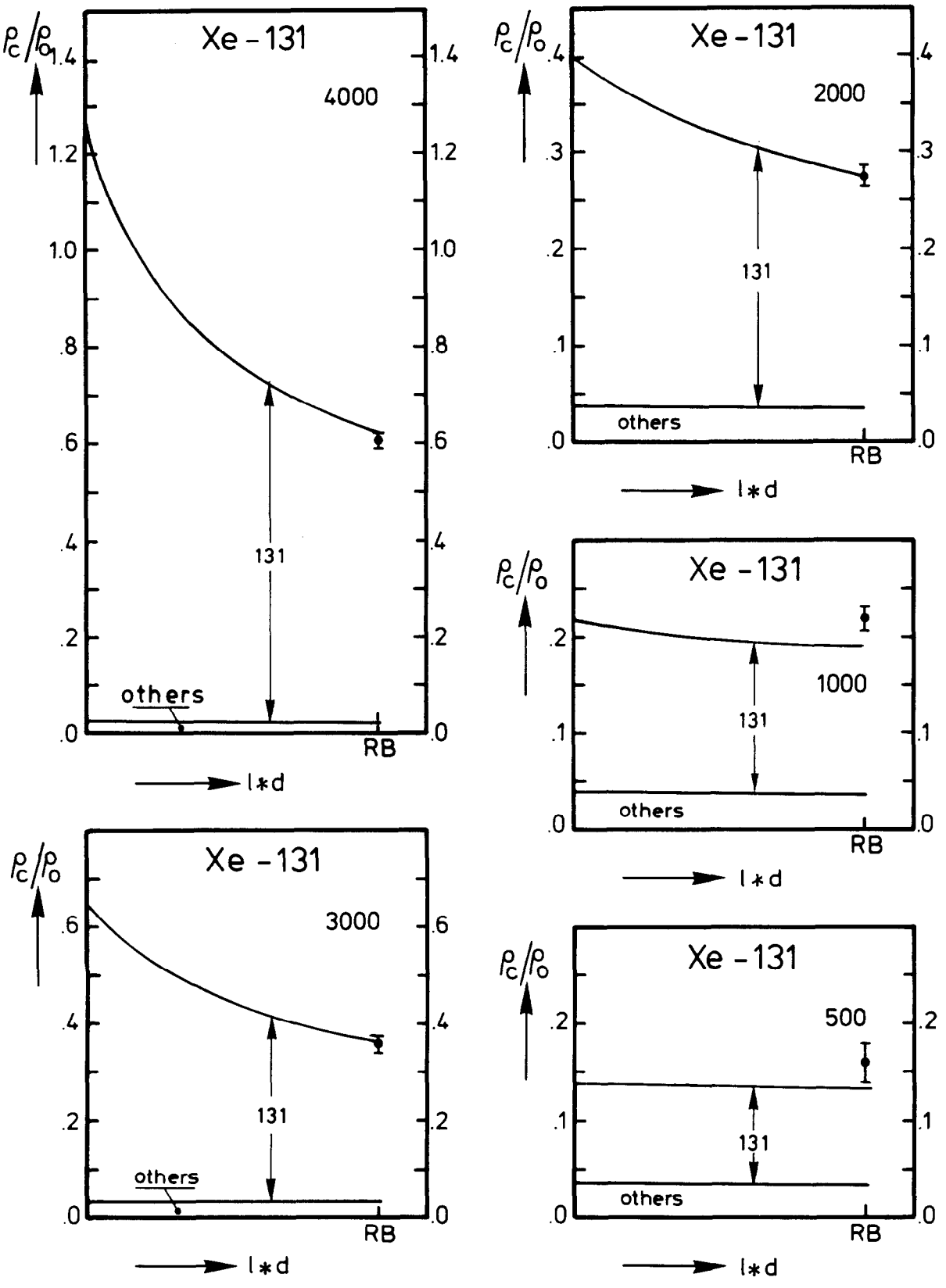
Xe - 131
4000
131
others
RB
l*d
Xe - 131
2000
131
others
RB
l*d
Xe - 131
1000
131
others
RB
l*d
Xe - 131
3000
131
others
RB
l*d
Xe - 131
500
131
others
RB
l*d

Fig. 30.

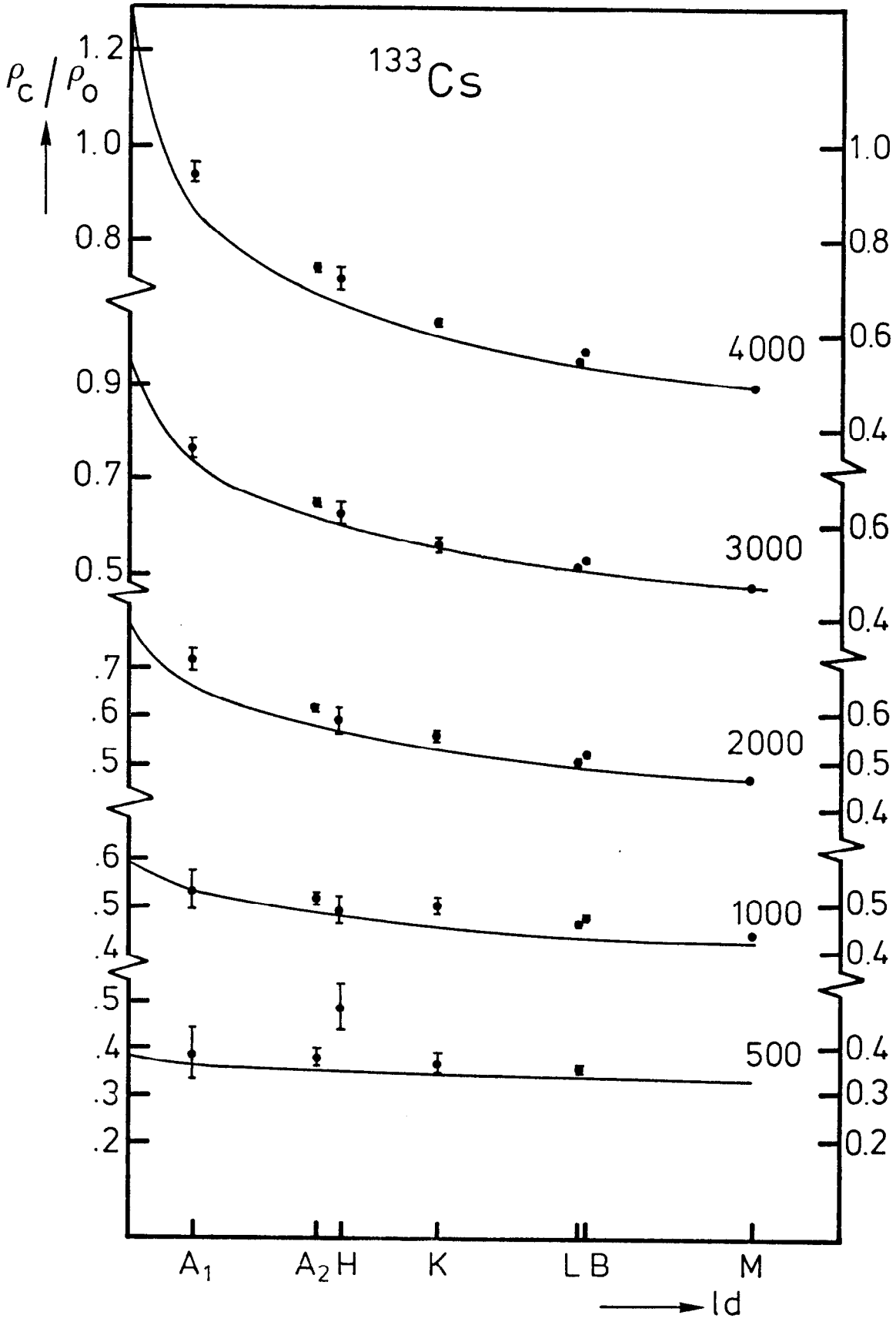

Fig. 31.

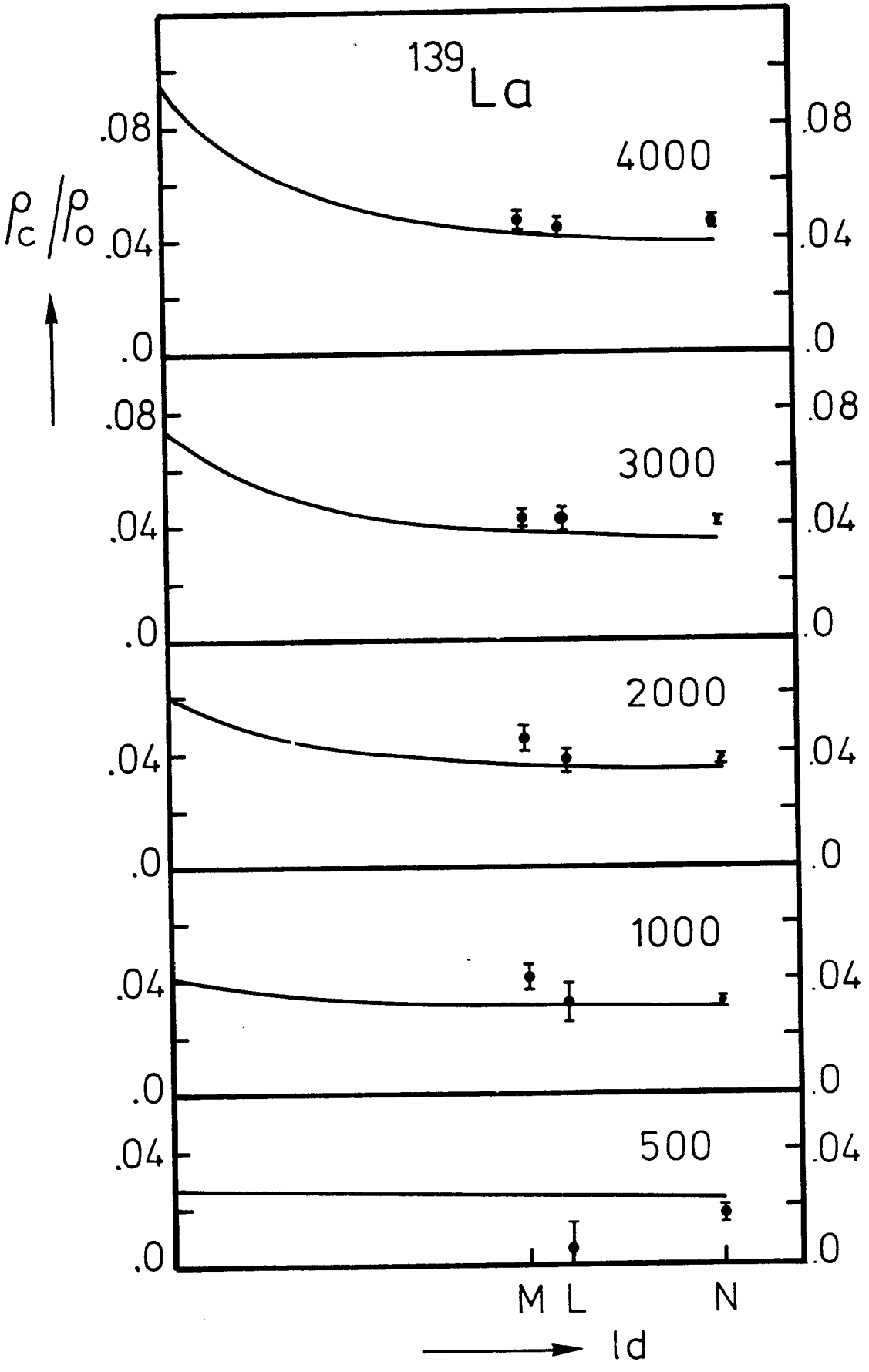

Fig. 32.

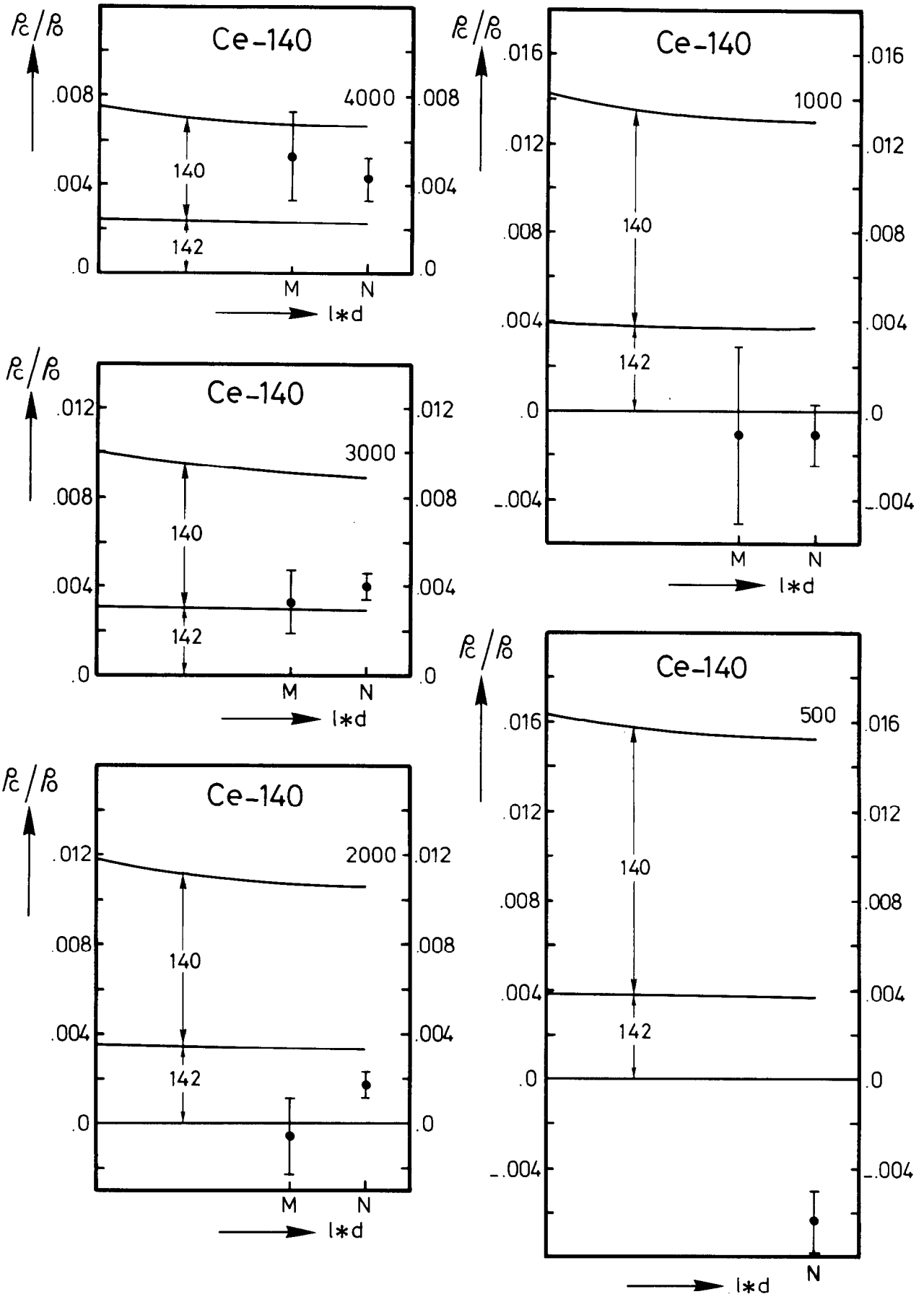
Ce-140
4000
140
142
M
N
l*d
Ce-140
3000
Ce-140
2000
Ce-140
1000
Ce-140
500

Fig. 33.

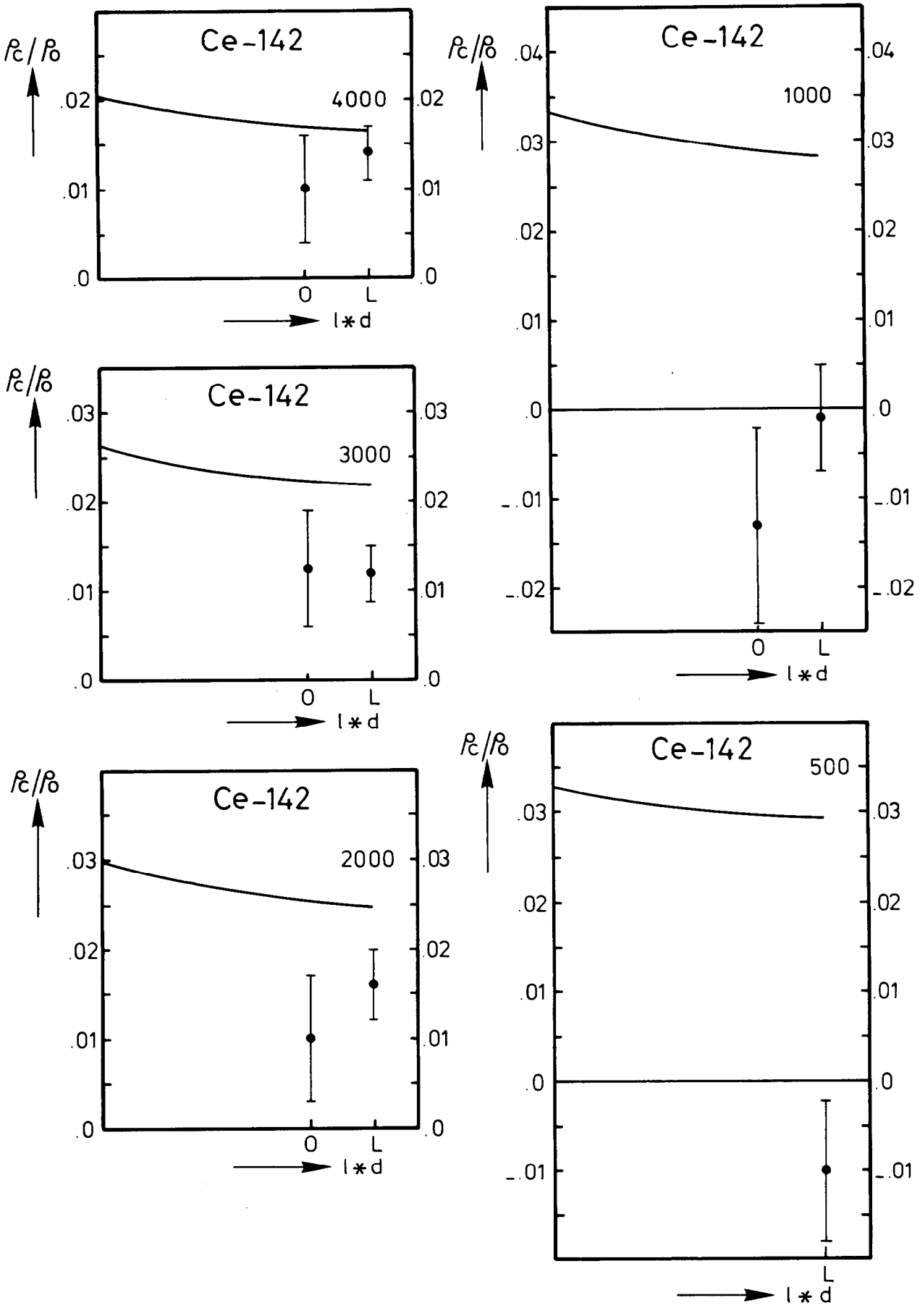
Ce-142
4000
Ce-142
1000
Ce-142
3000
Ce-142
2000
Ce-142
500
Pc/P0
0
L
l*d

Fig. 34.

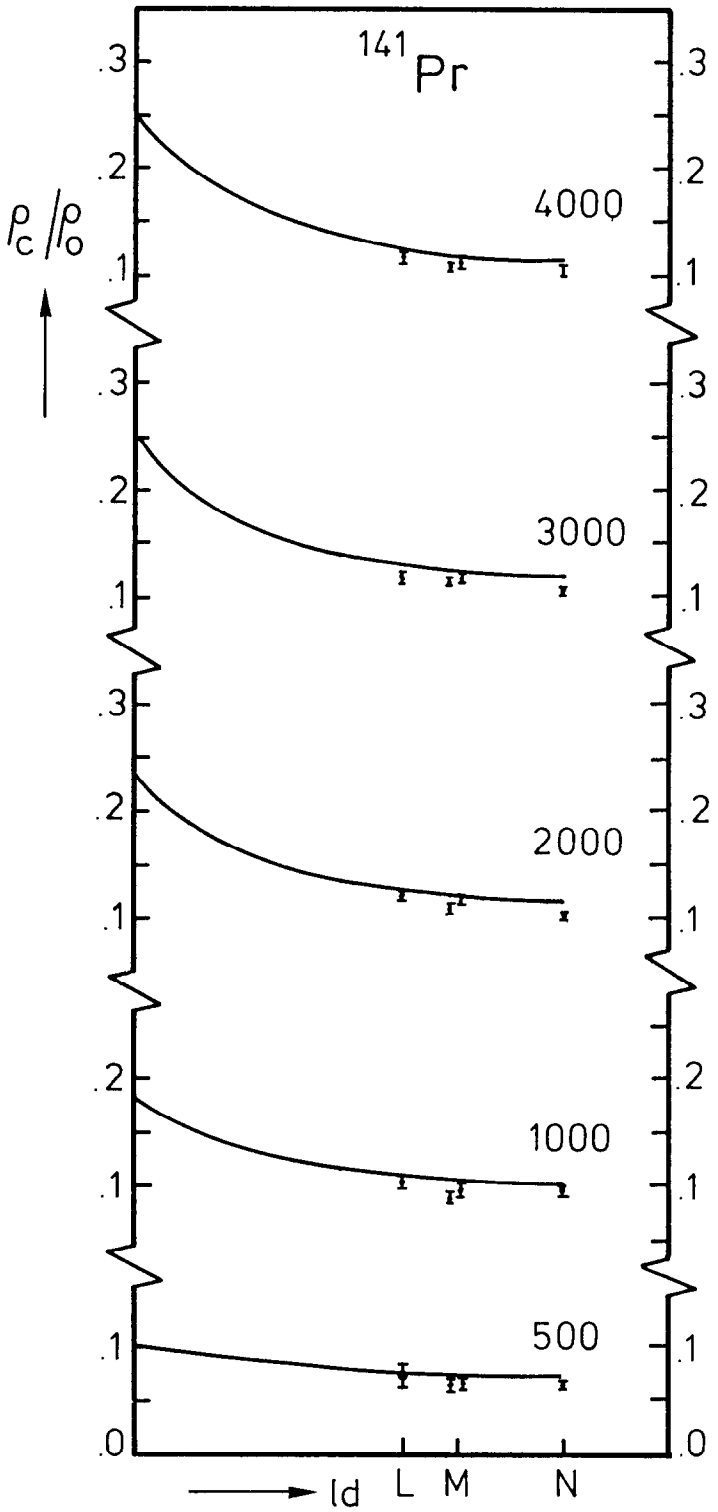

Fig. 35.

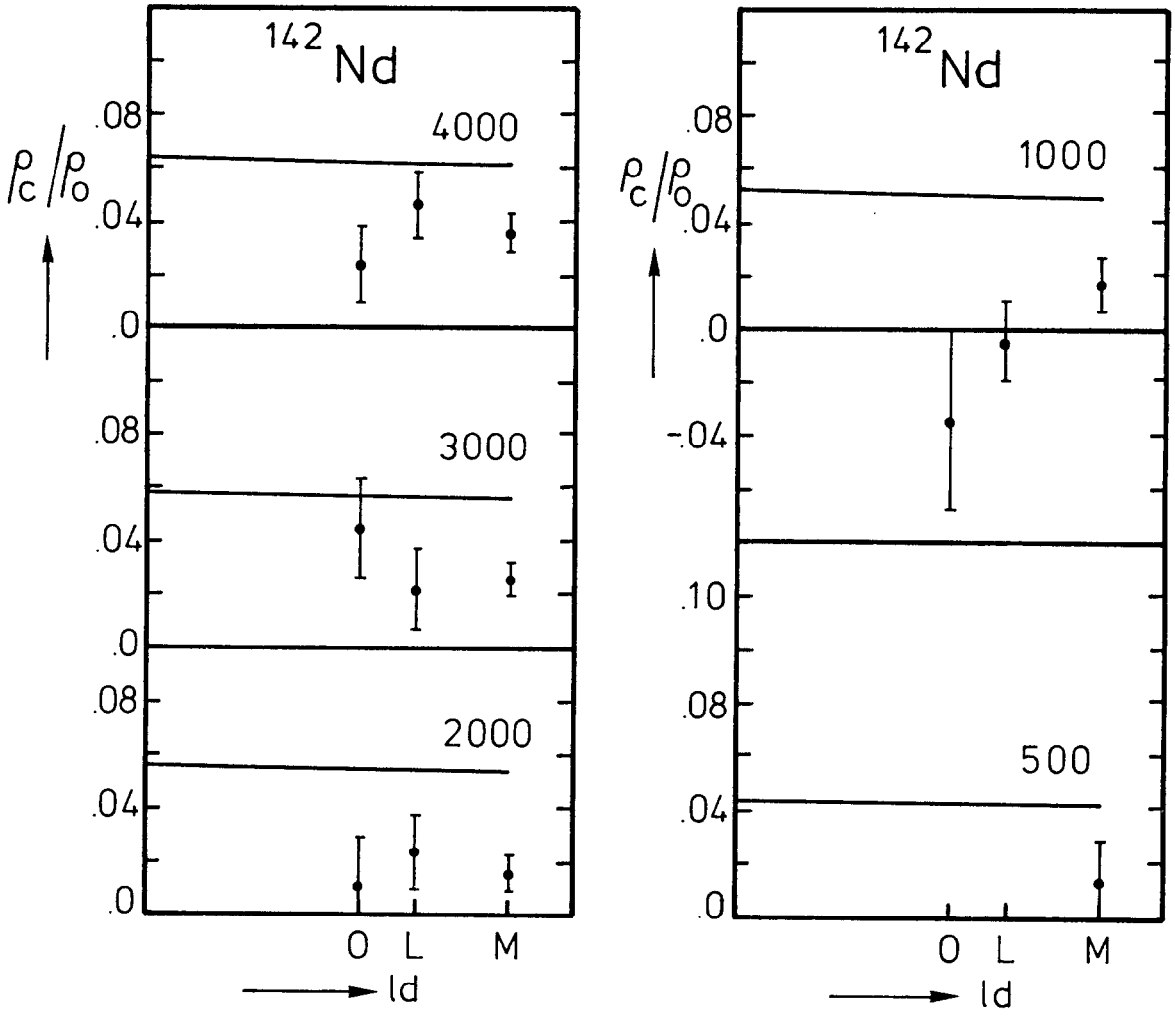
142 Nd
4000
3000
2000
ρ_c/ρ_o
.08
.04
.0
.08
.04
.0
.08
.04
.0
O L M
ld
142 Nd
1000
500
ρ_c/ρ_o
.08
.04
.0
-.04
.10
.08
.04
.0
O L M
ld

Fig. 36.

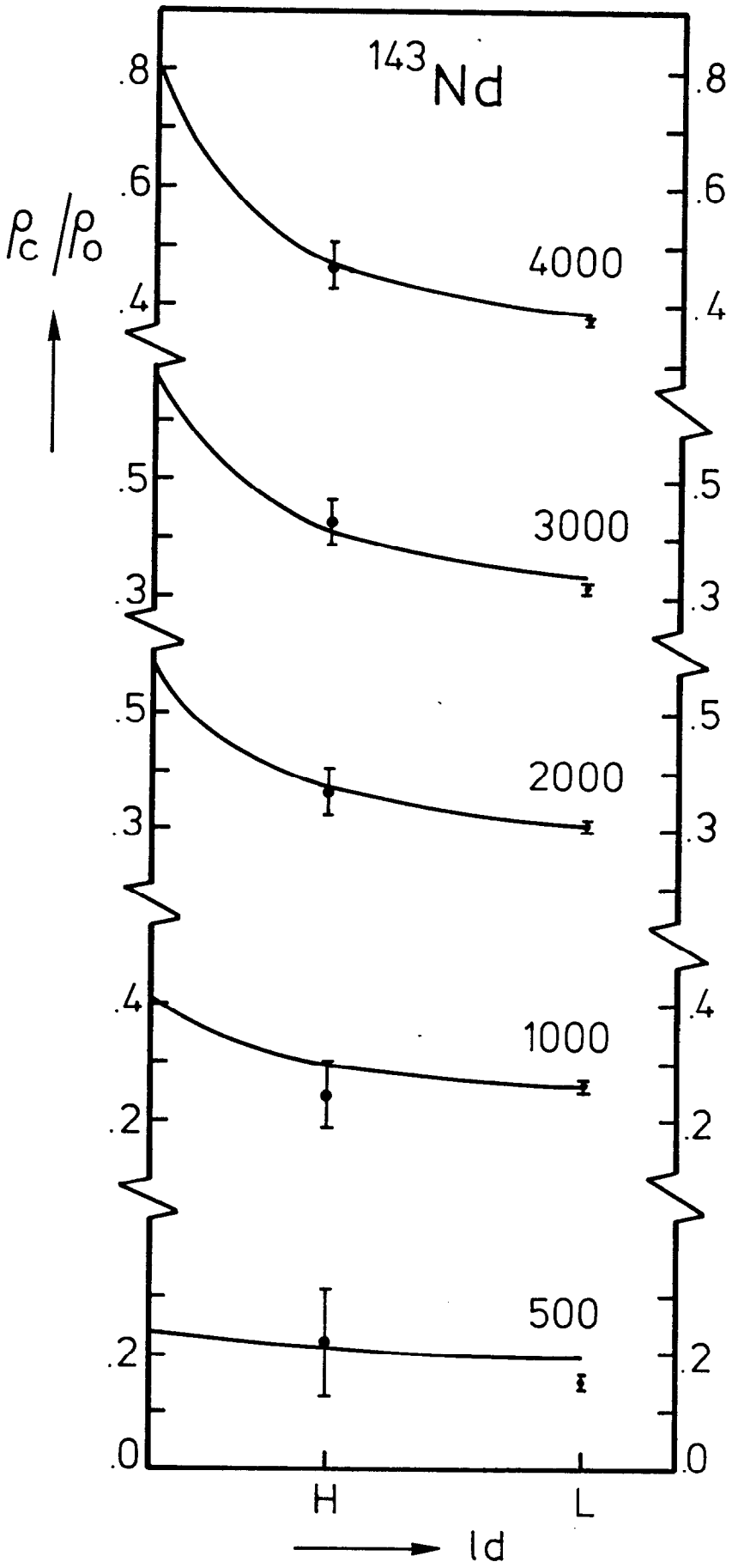

Fig. 37.

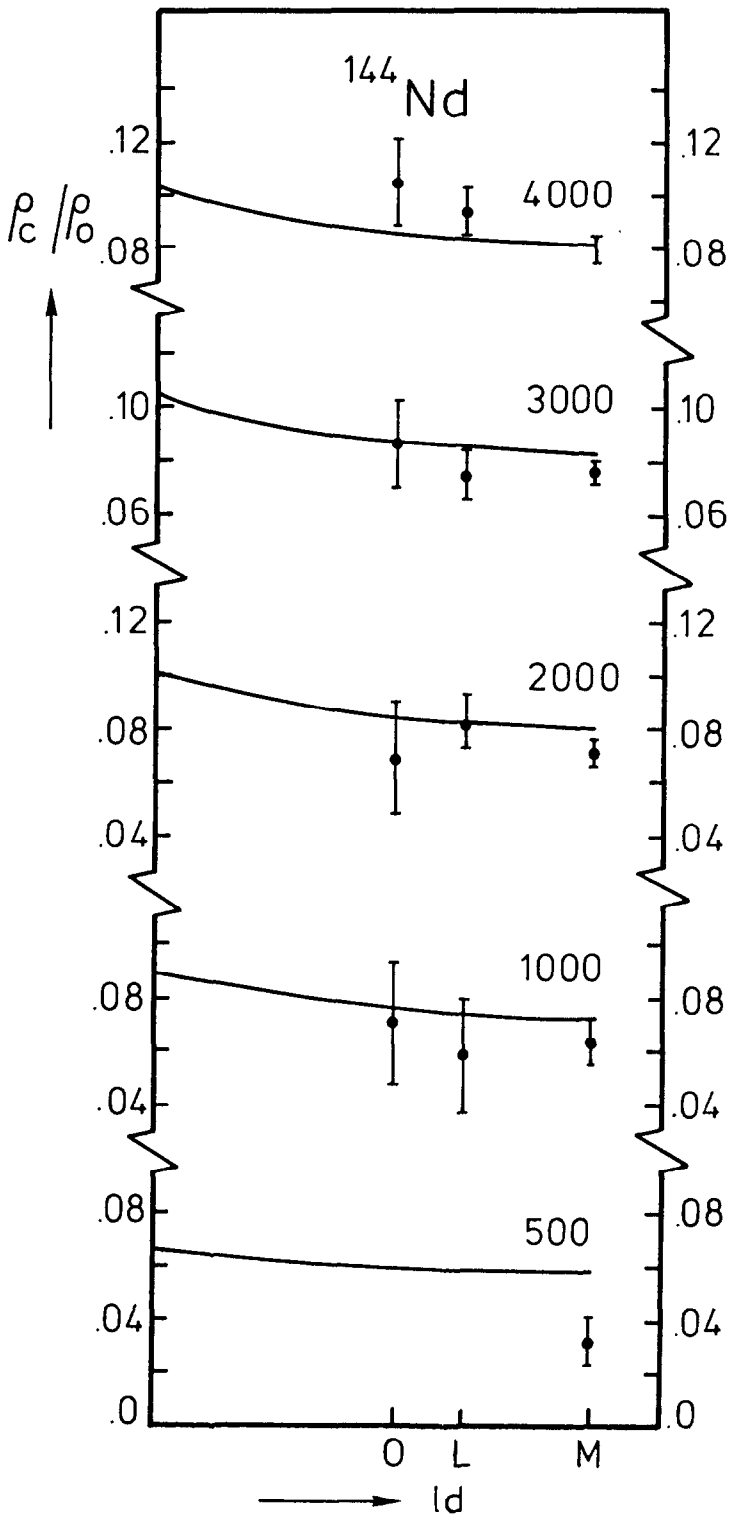

Fig. 38.

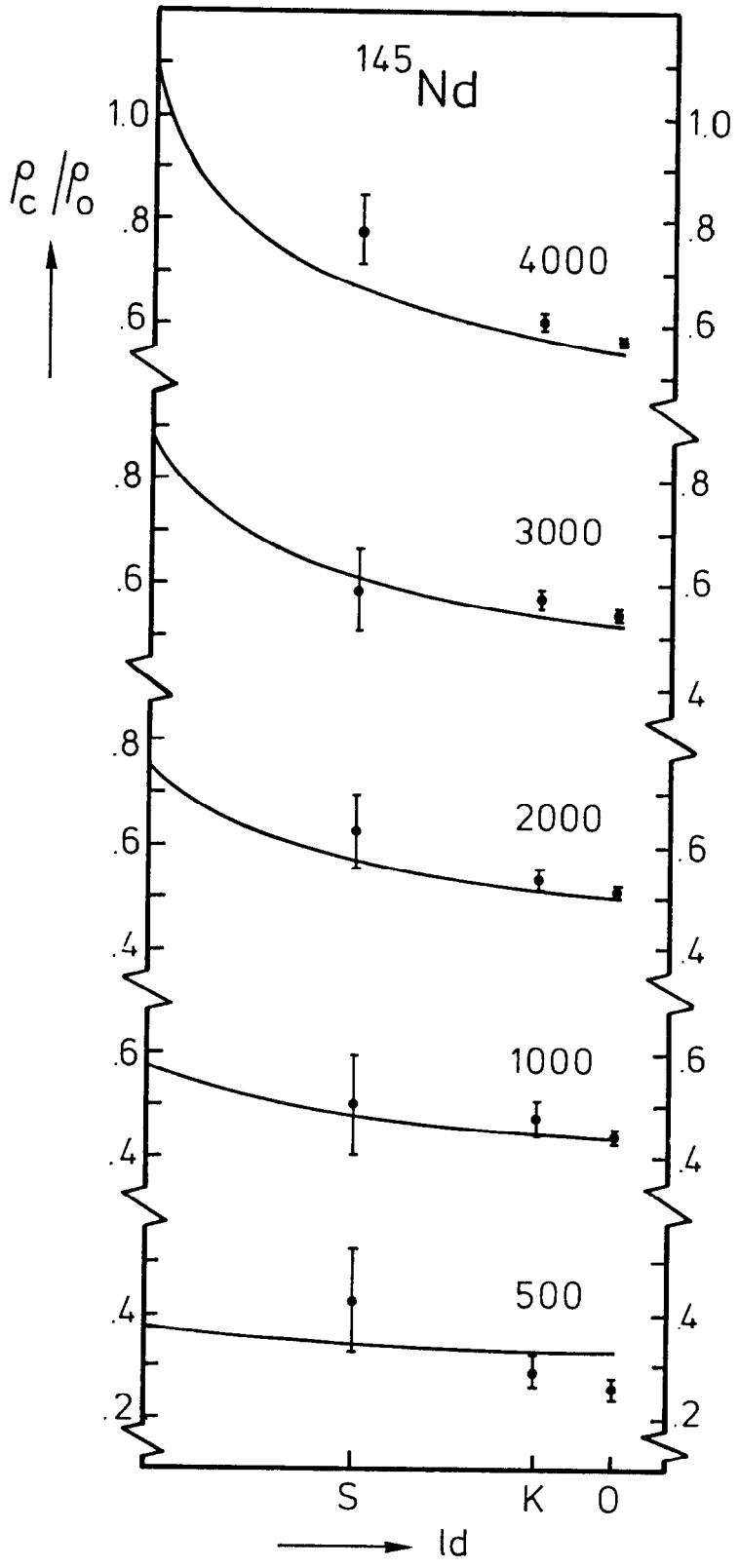

Fig. 39.

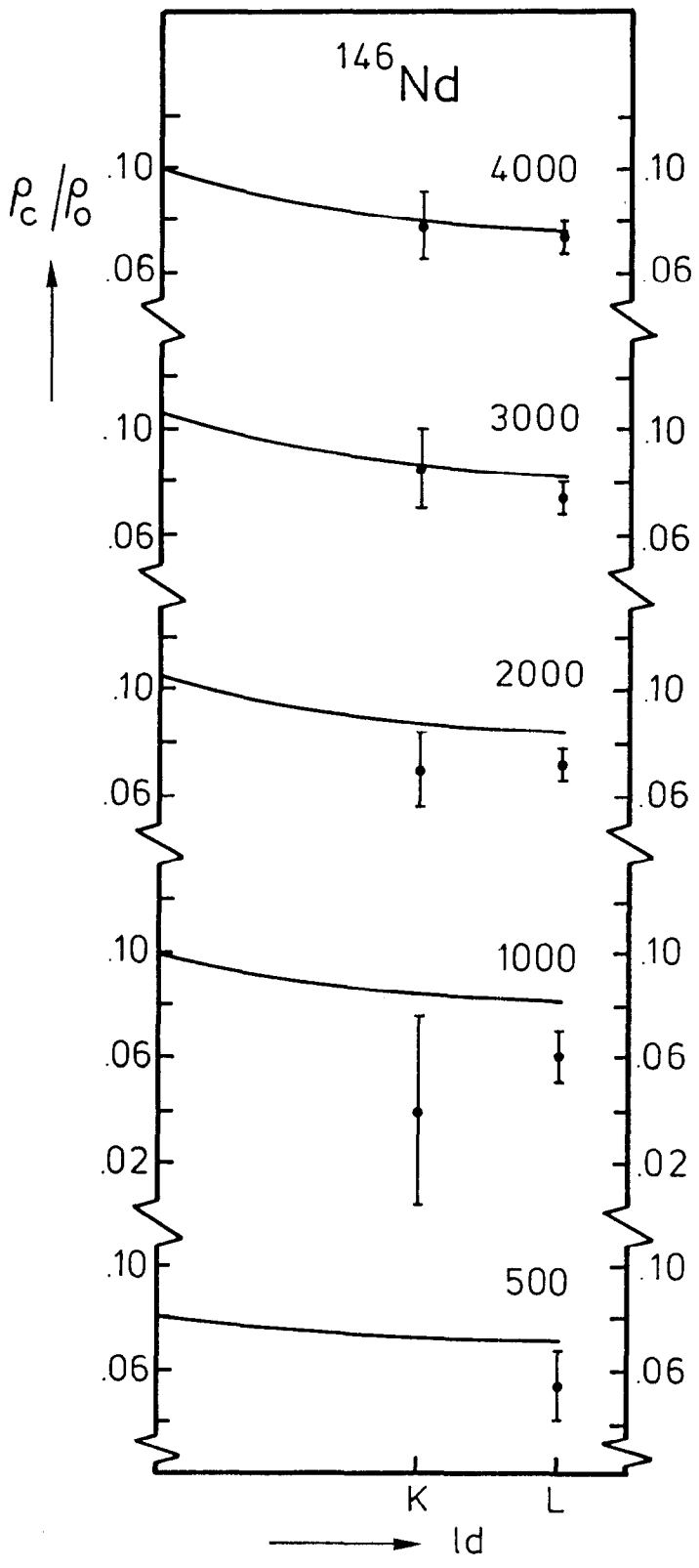

Fig. 40.

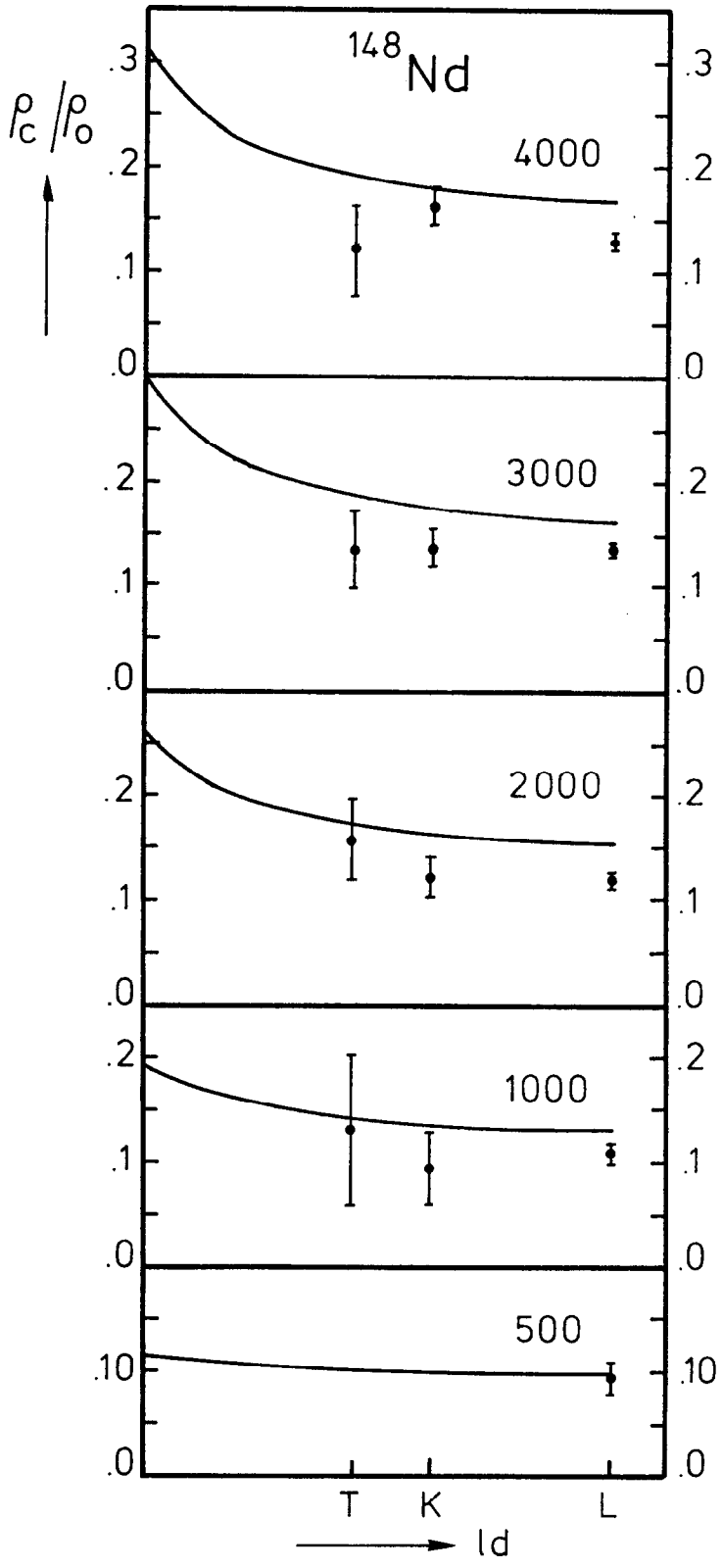

Fig. 41.

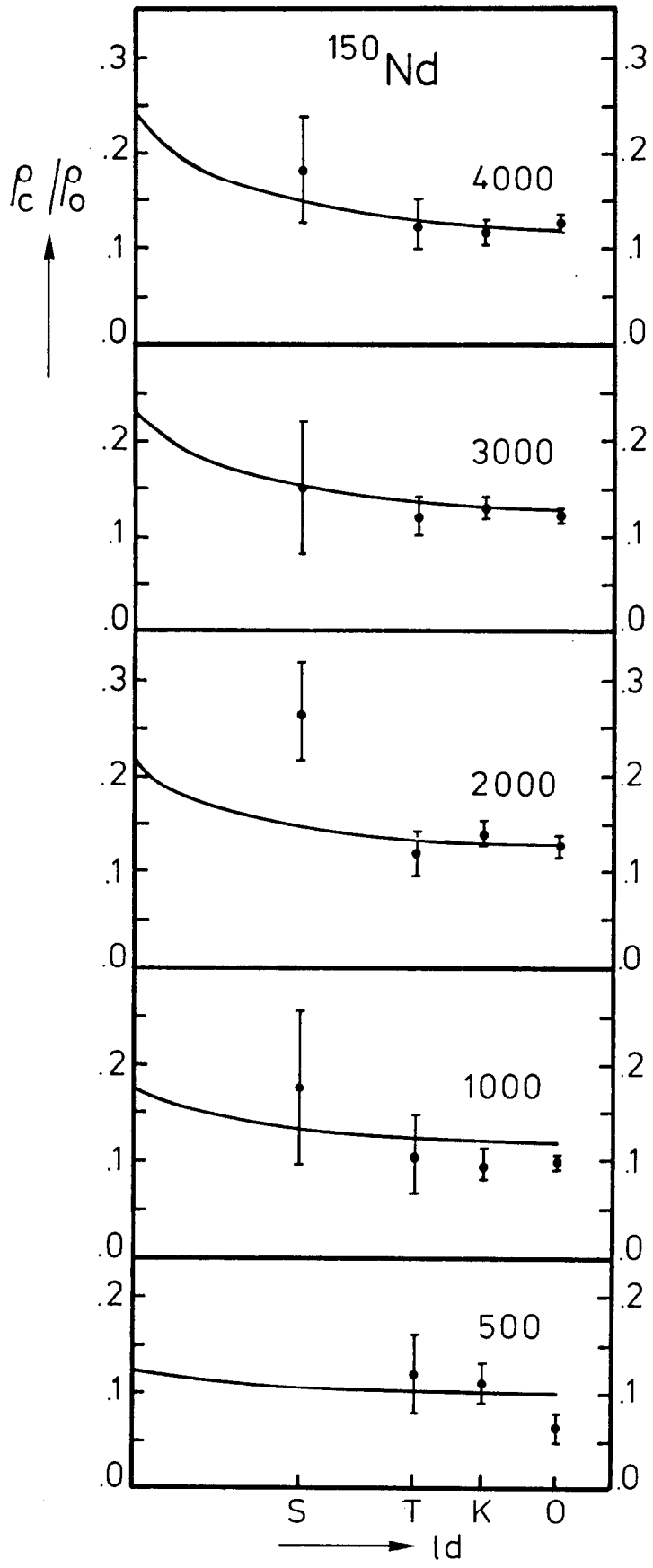

Fig. 42.

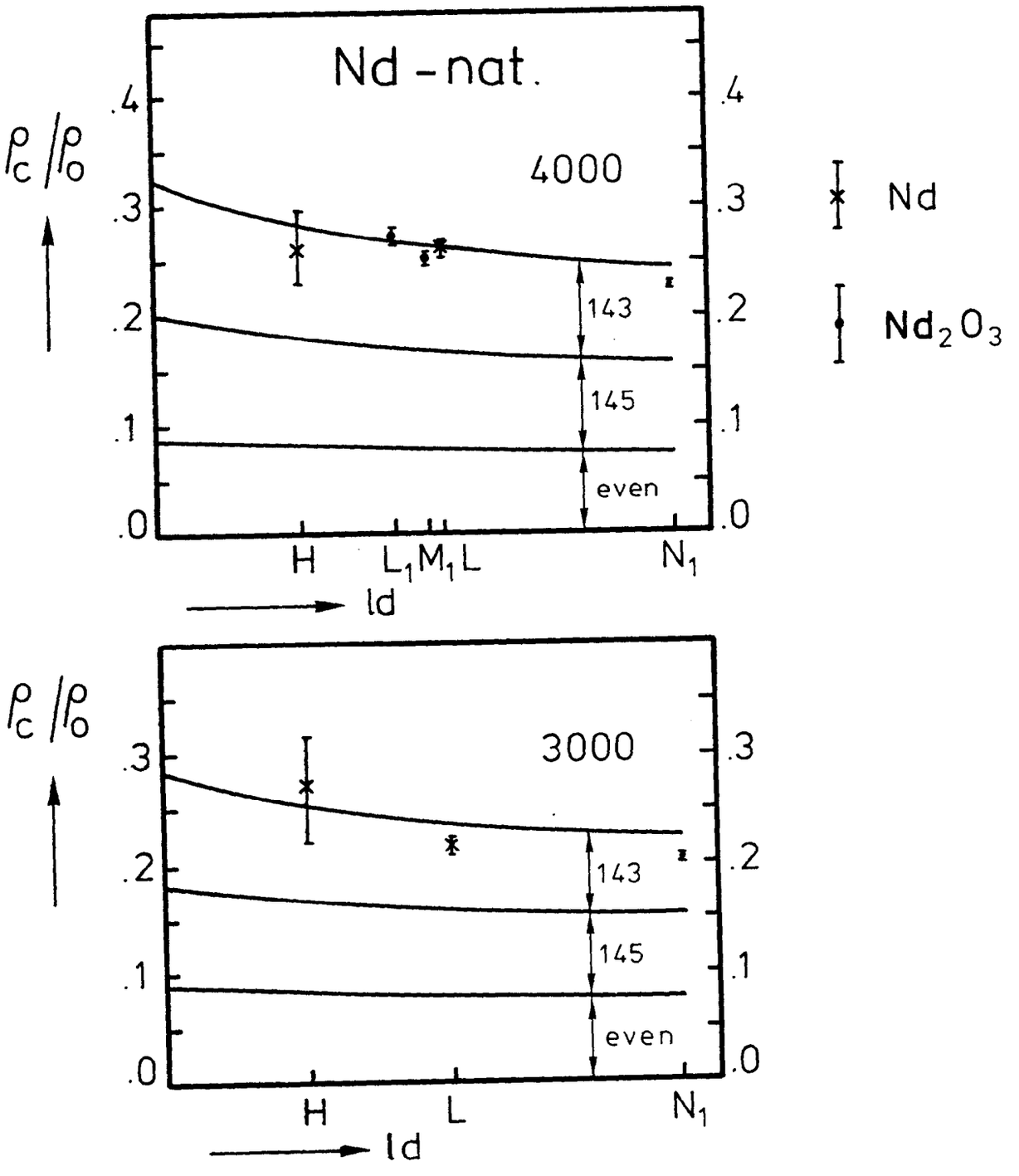
Nd - nat.
4000
143
145
even
H
L1 M1 L
N1
Id
ρc/ρo
3000
143
145
even
H
L
N1
Id
ρc/ρo
Nd
Nd2O3

Fig. 43a.

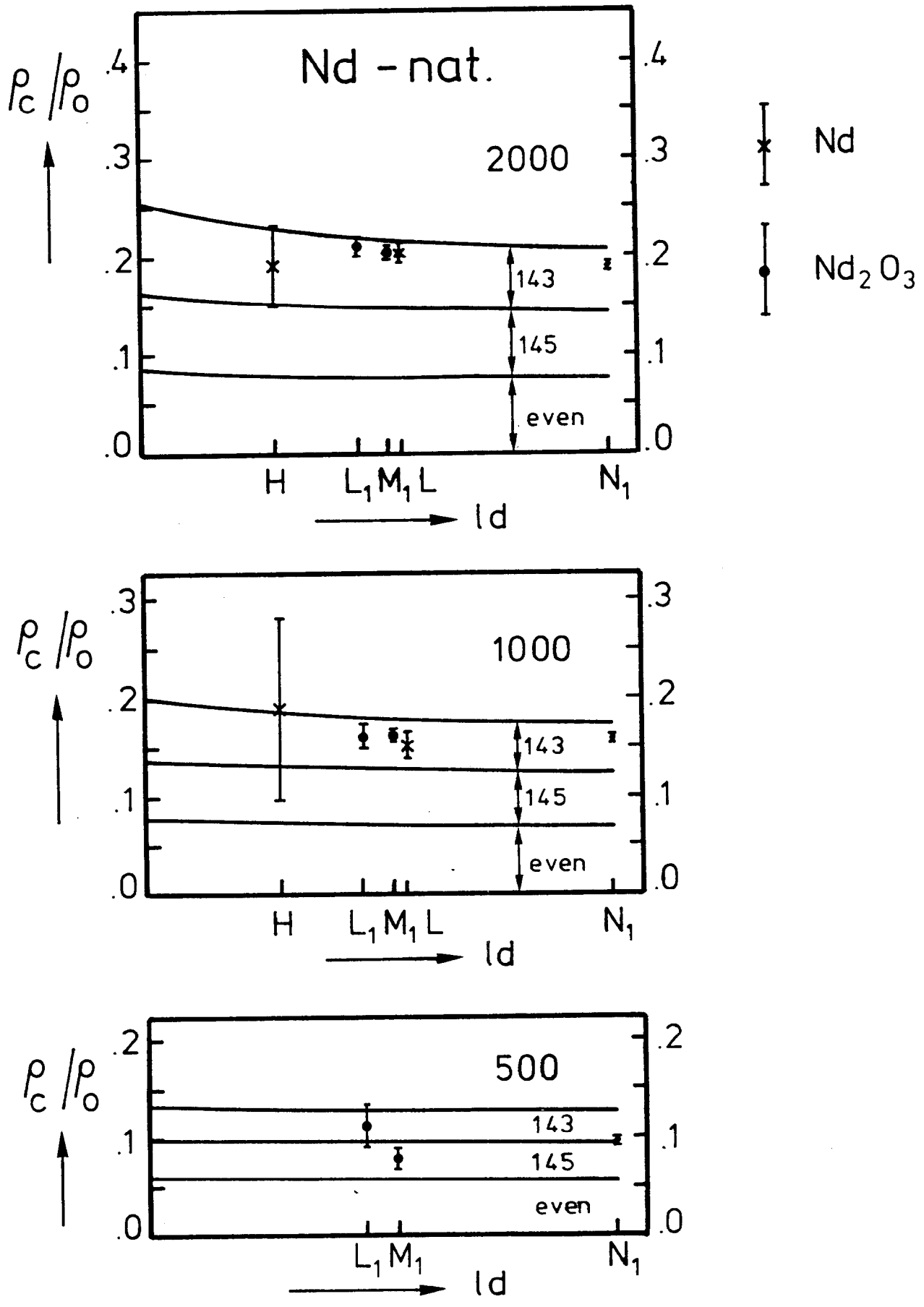

Fig. 43b.

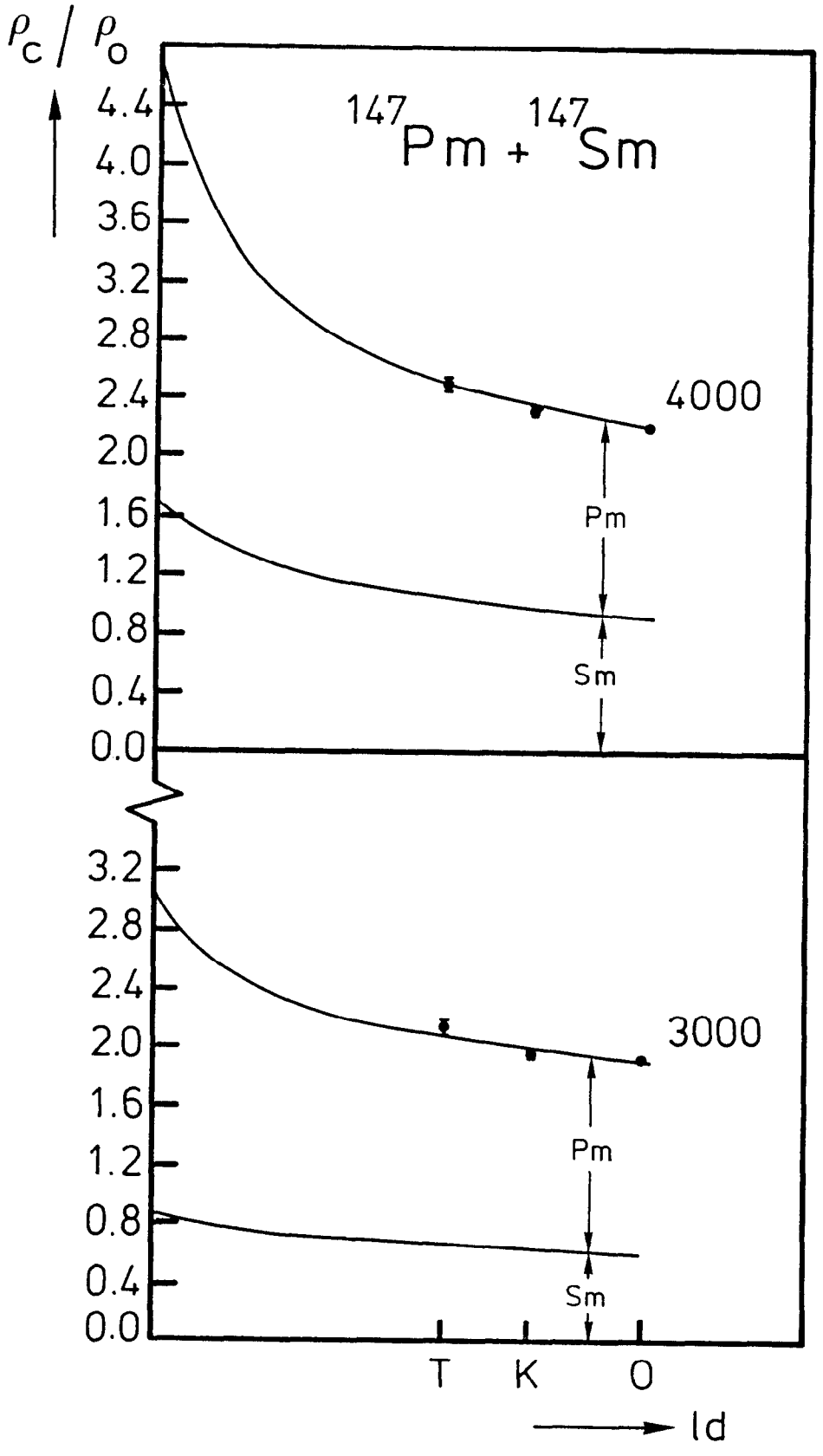
ρc / ρo
147Pm + 147Sm
4.4
4.0
3.6
3.2
2.8
2.4
2.0
1.6
1.2
0.8
0.4
0.0
4000
Pm
Sm
3.2
2.8
2.4
2.0
1.6
1.2
0.8
0.4
0.0
3000
Pm
Sm
T K O
ld

Fig. 44a.

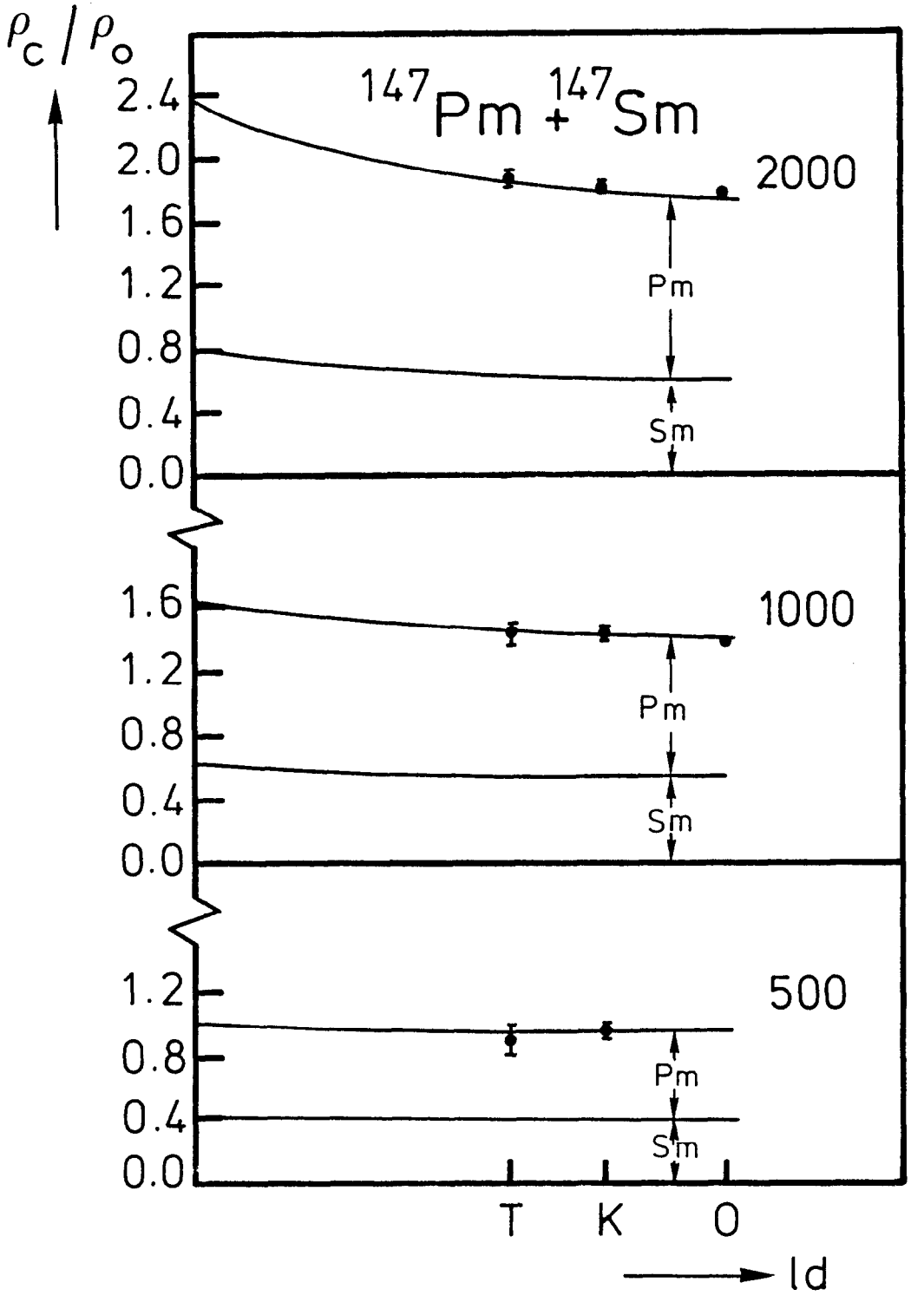

Fig. 44b.

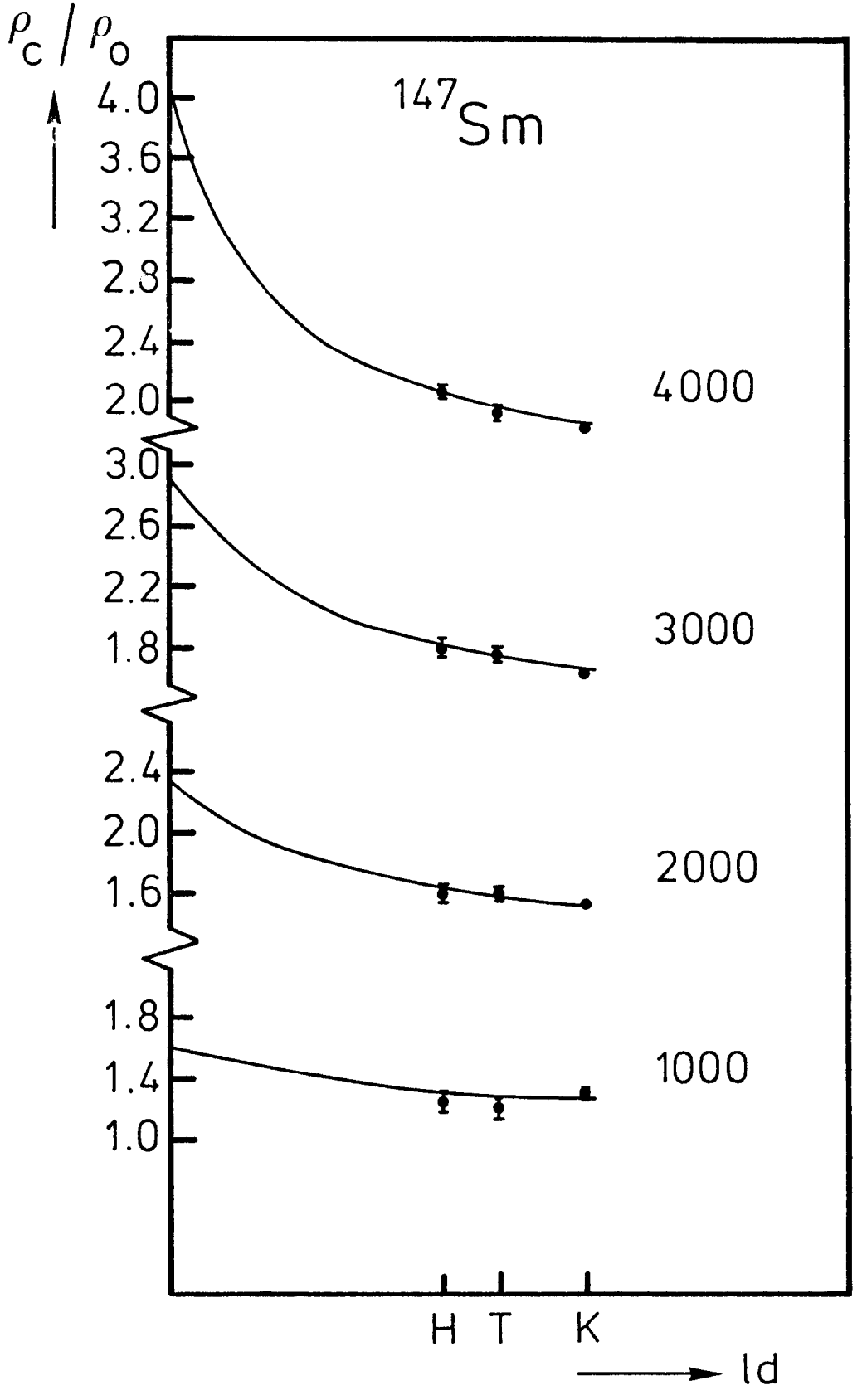
ρc / ρo
147Sm
4.0
3.6
3.2
2.8
2.4
2.0
3.0
2.6
2.2
1.8
2.4
2.0
1.6
1.8
1.4
1.0
4000
3000
2000
1000
H T K
ld

Fig. 45.

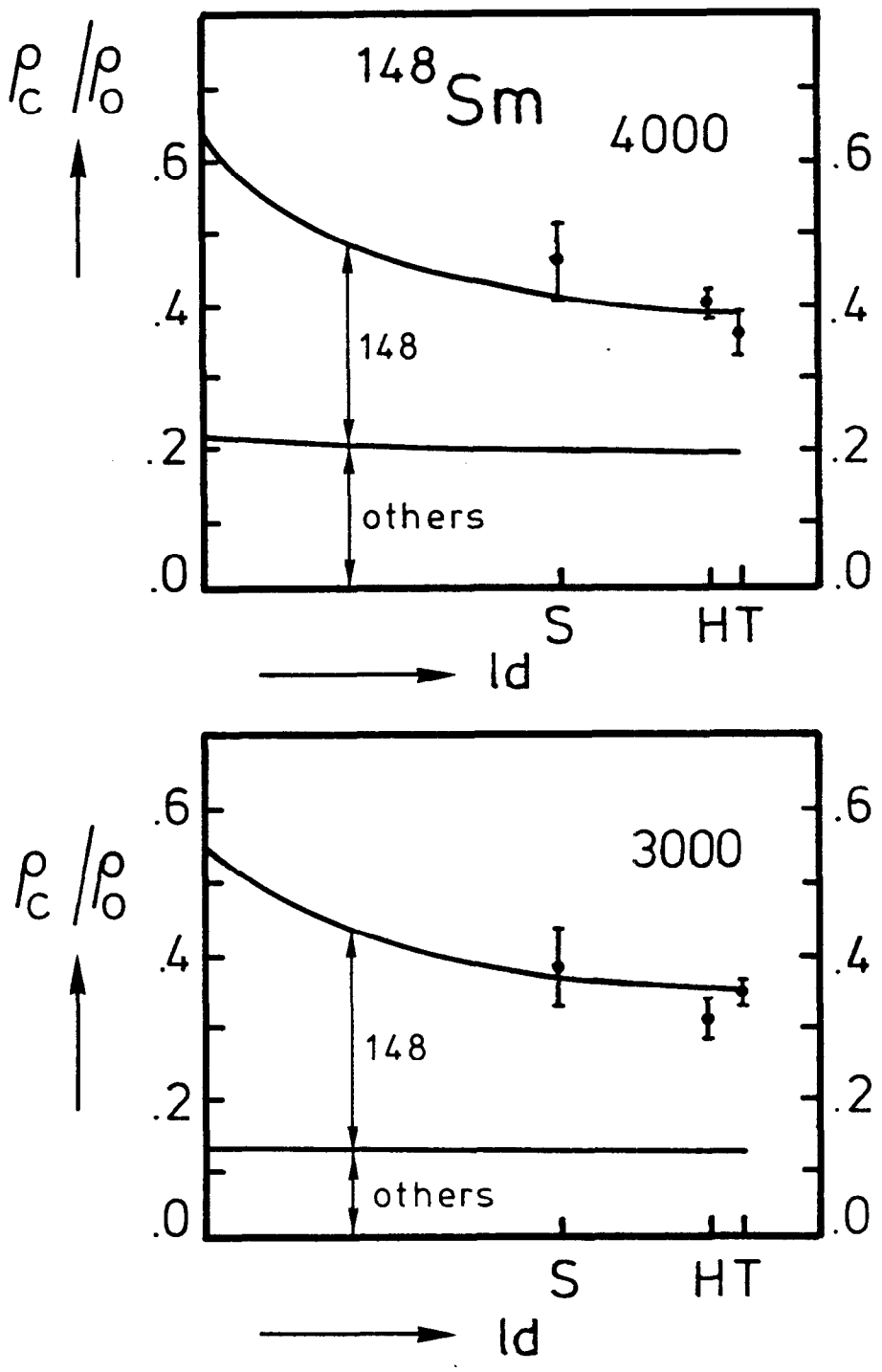
ρ_c/ρ_o
^{148}Sm
4000
.6
.4
.2
.0
148
others
S
HT
Id
ρ_c/ρ_o
3000
.6
.4
.2
.0
148
others
S
HT
Id

Fig. 46a.

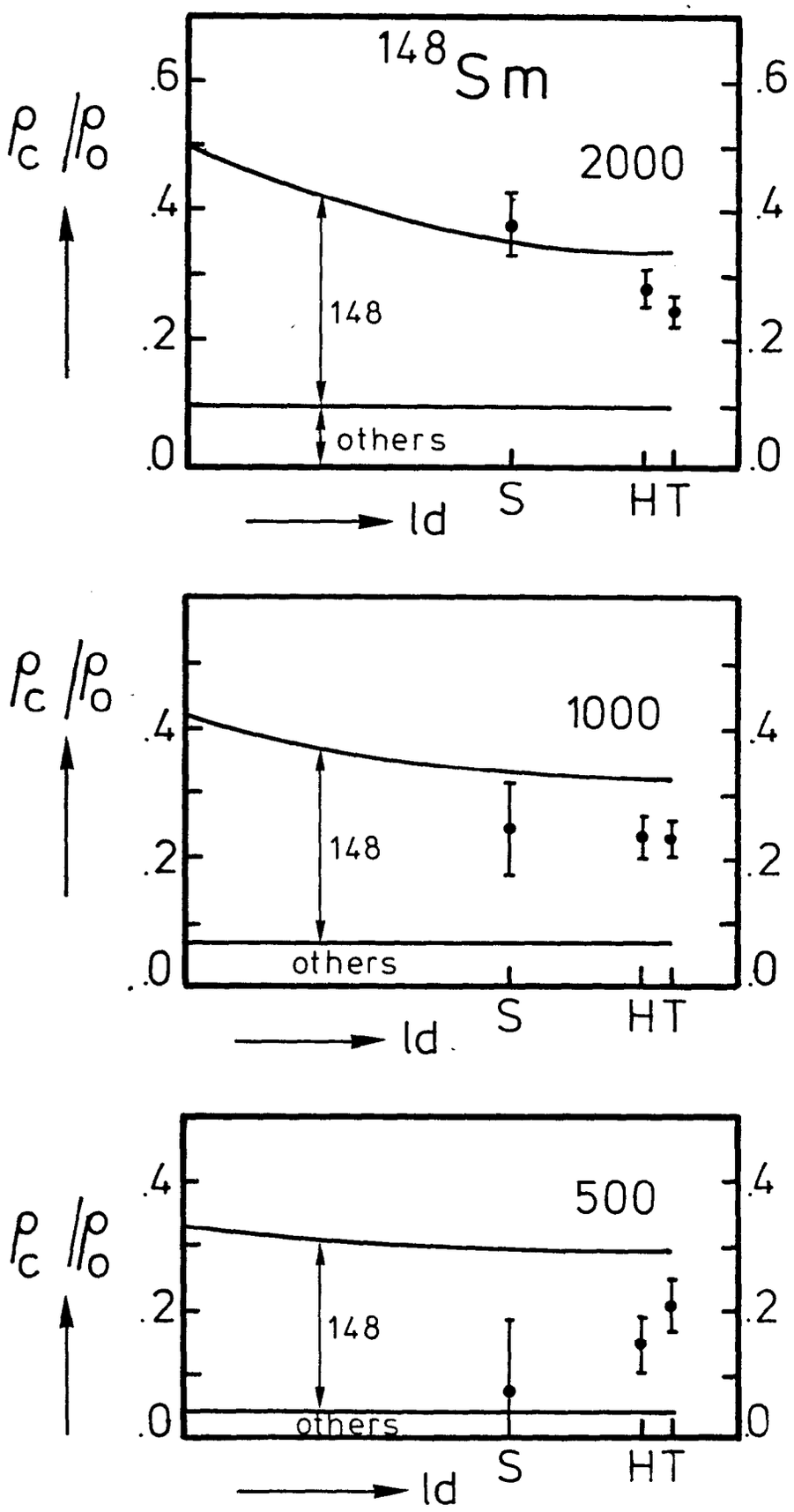

Fig. 46b.

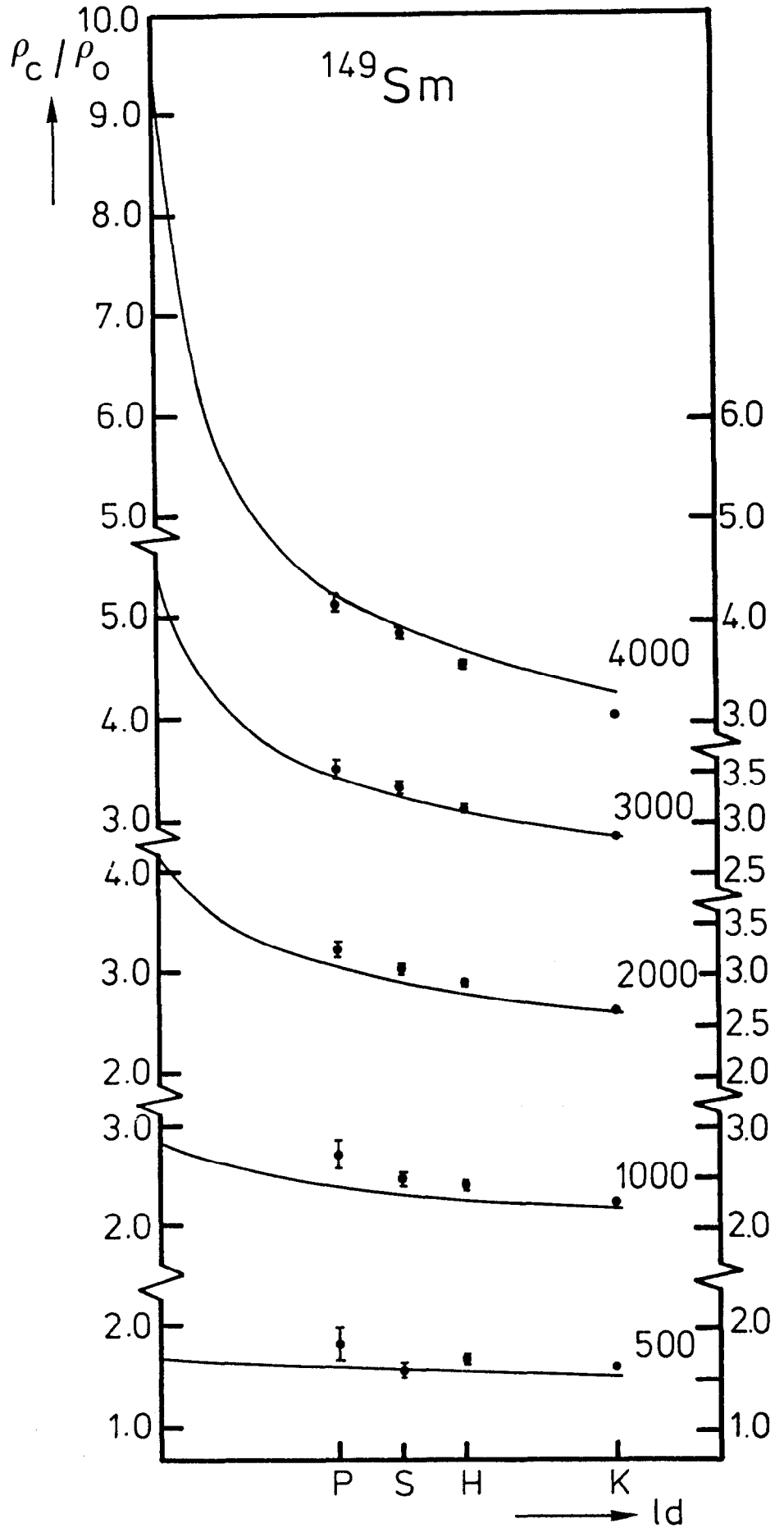
ρ_c / ρ_o
^{149}Sm
10.0
9.0
8.0
7.0
6.0
5.0
5.0
4.0
3.0
4.0
3.0
2.0
3.0
2.0
2.0
1.0
6.0
5.0
4.0
3.0
3.5
3.0
2.5
3.5
3.0
2.5
2.0
3.0
2.0
2.0
1.0
4000
3000
2000
1000
500
P
S
H
K
ld

Fig. 47.

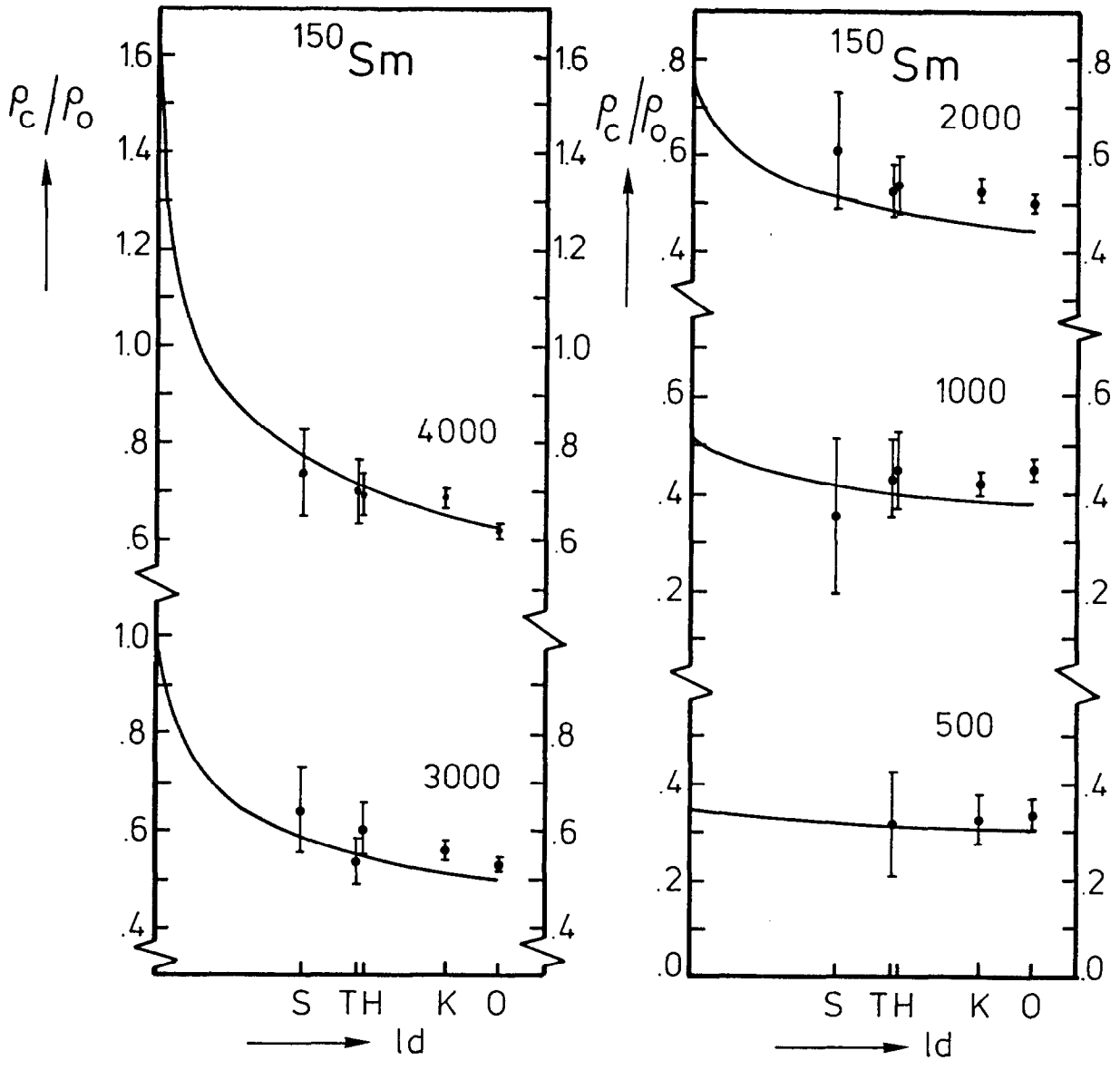

Fig. 48.

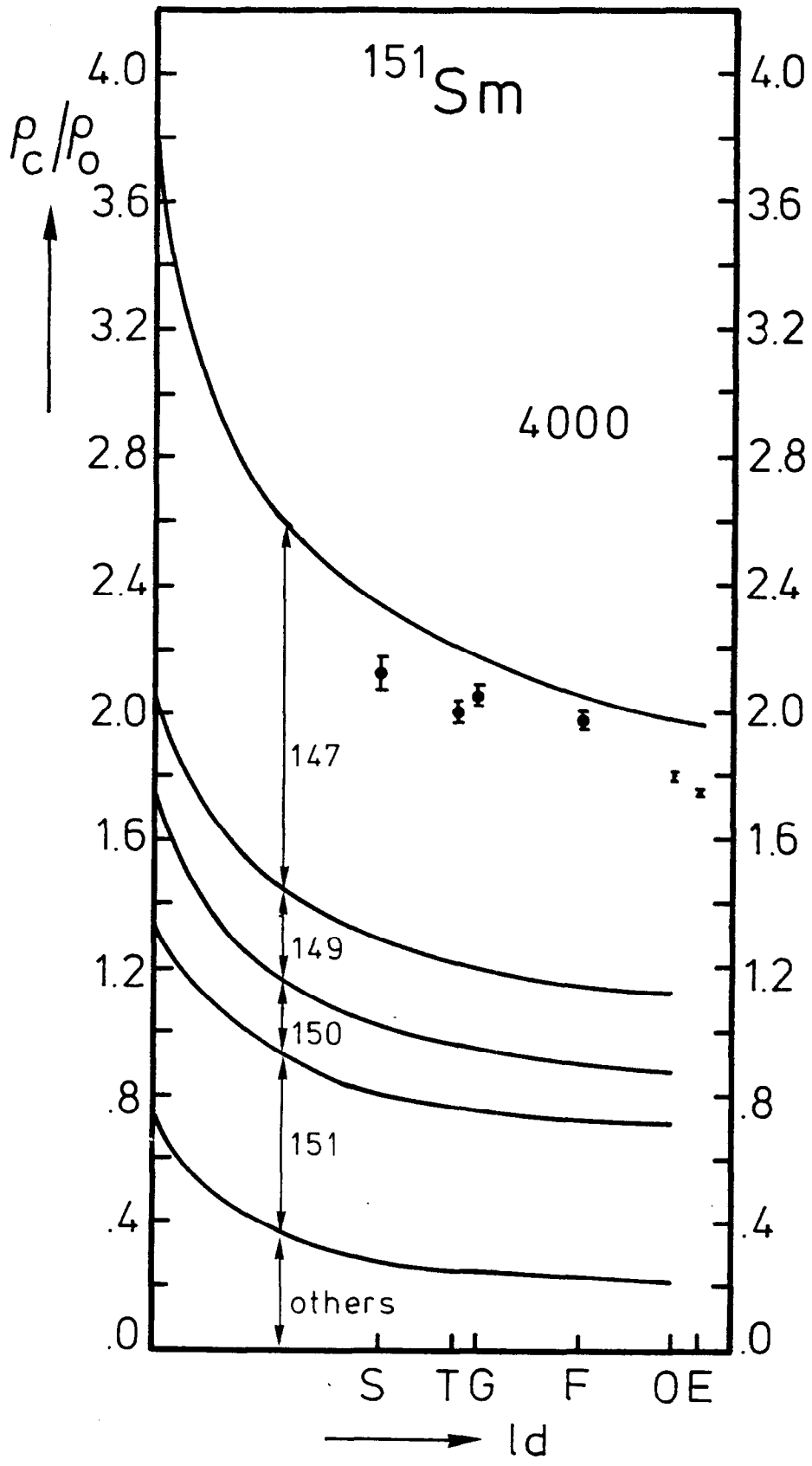
^{151}Sm
ρ_c/ρ_o
4.0
3.6
3.2
2.8
2.4
2.0
1.6
1.2
.8
.4
.0
4000
147
149
150
151
others
S
TG
F
OE
ld

Fig. 49a.

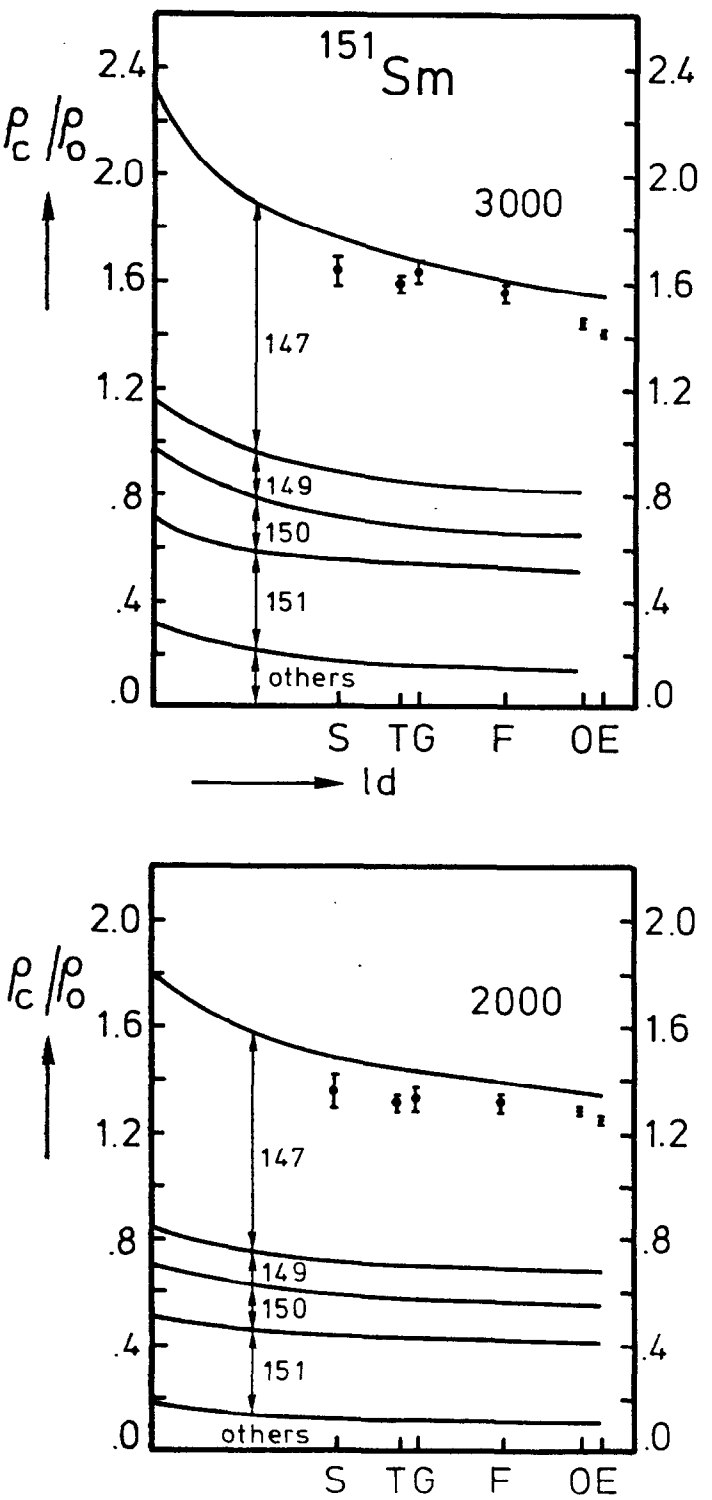
151Sm
3000
2000
147
149
150
151
others
ρ_c/ρ_o
2.4
2.0
1.6
1.2
.8
.4
.0
S TG F OE
ld

Fig. 49b.

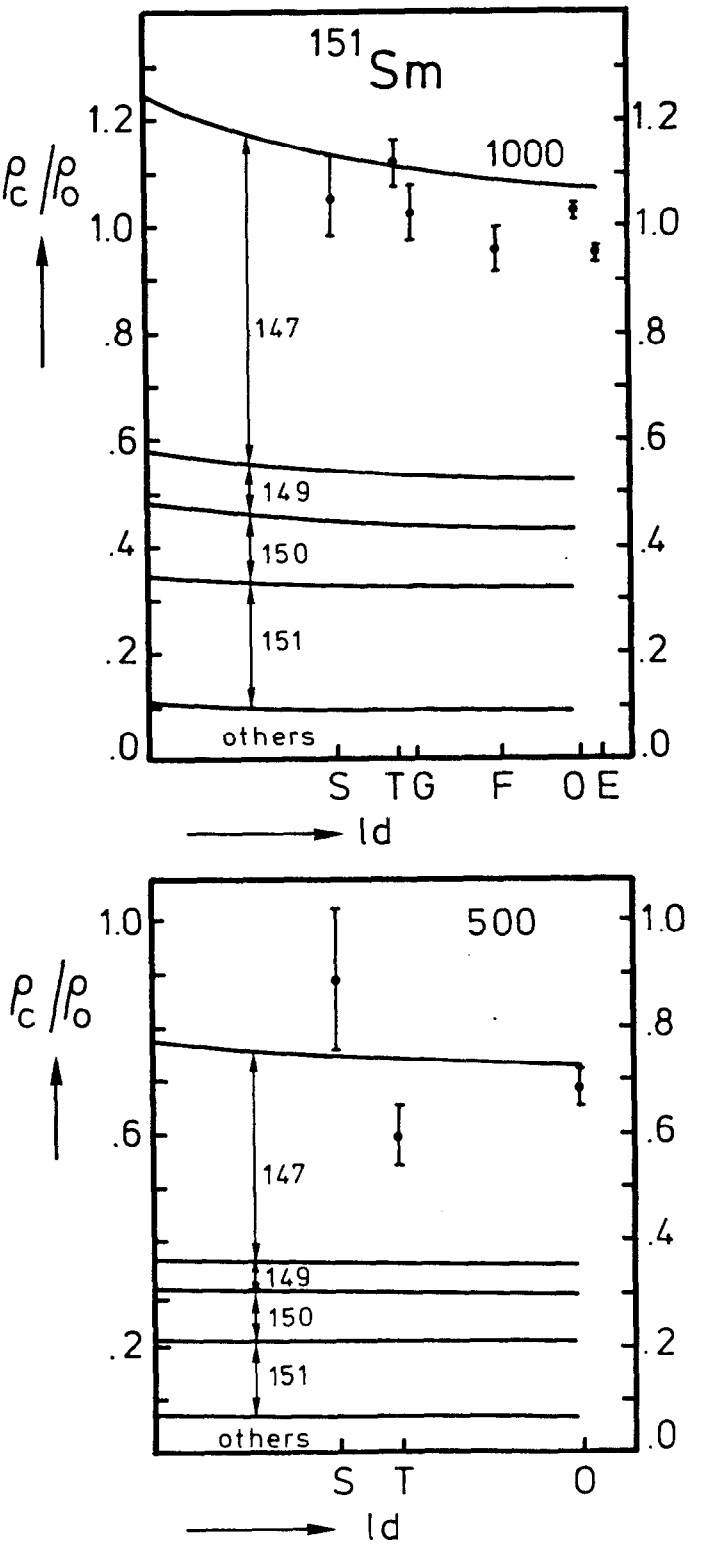
151Sm
1000
147
149
150
151
others
S TG F OE
ld
500
147
149
150
151
others
S T O
ld
ρc/ρo
1.2
1.0
.8
.6
.4
.2
.0

Fig. 49c.

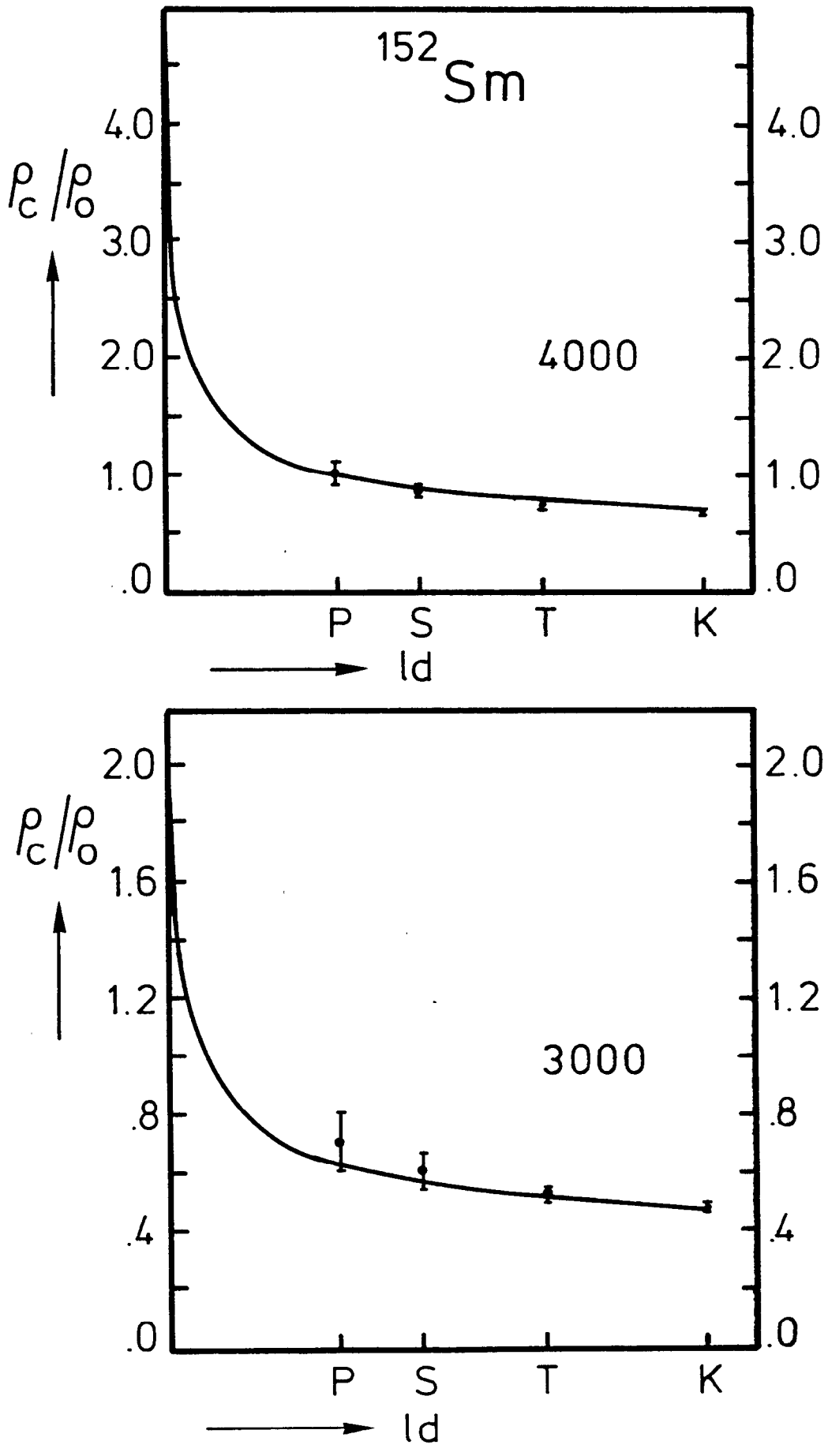
152Sm
4.0
3.0
2.0
1.0
.0
ρc/ρo
4000
P
S
T
K
ld
2.0
1.6
1.2
.8
.4
.0
ρc/ρo
3000
P
S
T
K
ld

Fig. 50a.

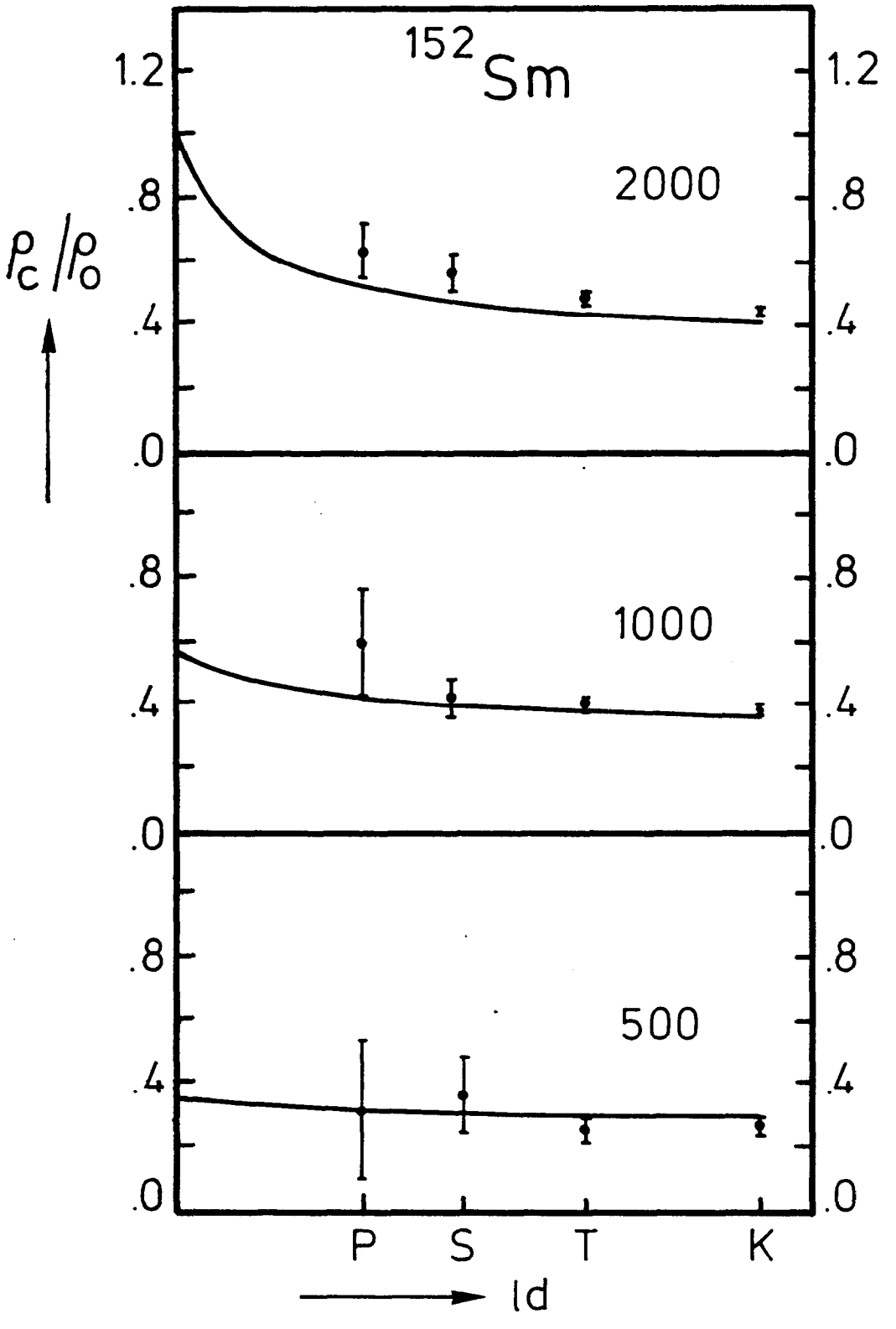

Fig. 50b.

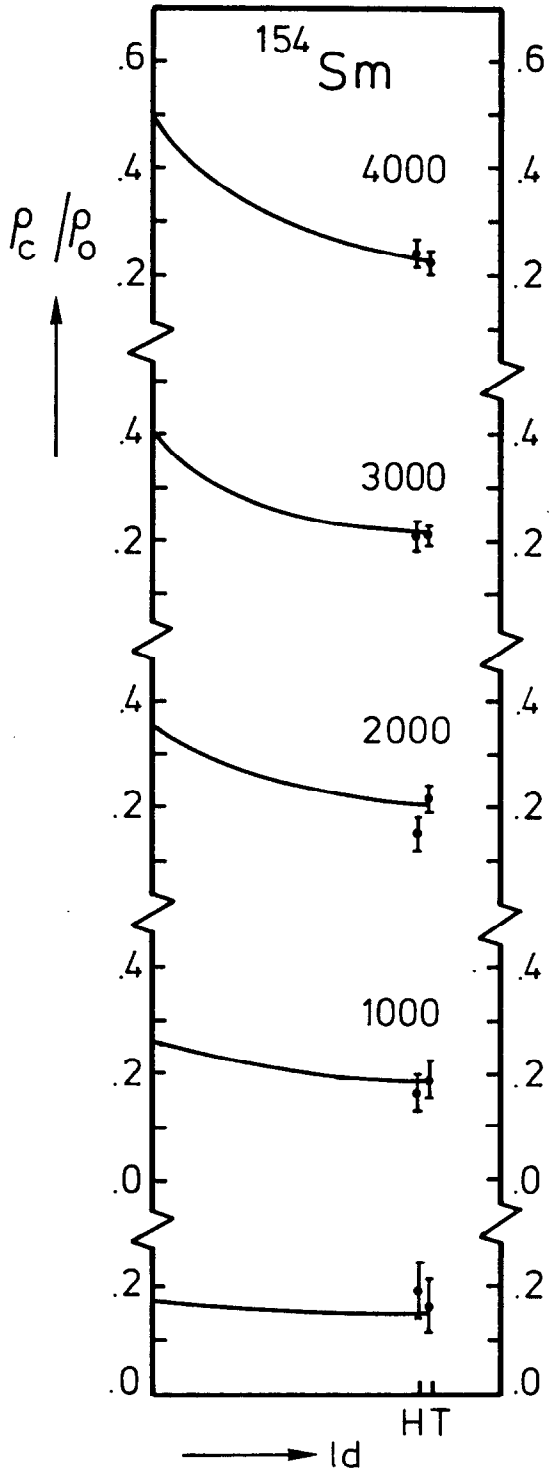

Fig. 51.